DISSERTATION

FAMILIAL VARIATION IN PERSONAL $PM_{2.5}$ EXPOSURE WITHIN A RURAL RWANDAN COMMUNITY PRE AND POST CLEAN ENERGY INTERVENTION

Submitted by

Ky Tanner

Department of Mechanical Engineering

In partial fulfillment of the requirements

For the Degree of Doctor of Philosophy

Colorado State University

Fort Collins, Colorado

Summer 2025

Doctoral Committee:

Advisor: John Volckens

Ellison Carter
Maggie Clark
Shantanu Jathar
Christian L'Orange

ABSTRACT

FAMILIAL VARIATION IN PERSONAL $PM_{2.5}$ EXPOSURE WITHIN A RURAL RWANDAN COMMUNITY PRE AND POST CLEAN ENERGY INTERVENTION

Exposure to fine particulate matter ($PM_{2.5}$) from solid fuel combustion is a major determinant of global morbidity and mortality. However, demographic variations in personal exposure remain uncertain across many high-risk populations. Liquefied petroleum gas (LPG) stoves have been proven to emit far less $PM_{2.5}$ than traditional biomass burning stoves and significantly reduce personal exposures in randomized control trials. However, there is uncertainty surrounding the difference in exposure reductions produced by LPG stove interventions among men, women, and children. This work describes personal $PM_{2.5}$ exposures and exposure reductions among household members (adult men, adult women, and children) in rural sub-Saharan Africa, where biomass fuel was the primary household energy source, before and during a whole-household energy intervention. LPG stoves were used to replace traditional biomass burning stoves, and solar-based electric lighting replaced traditional kerosene lamps. Personal $PM_{2.5}$ exposures were assessed using wearable monitors that combined real-time sensing, time-integrated (gravimetric filter) sampling, and continuous location-activity tracking over 48-hr sampling periods.

First, the baseline variation in $PM_{2.5}$ exposures among adults (men and women) and adolescent/pre-adolescent children within two rural Rwandan villages was assessed prior to the introduction of clean energy technology, when all participants still relied on their traditional forms of household energy. Linear mixed models, controlling for household, were used to

examine the variation in baseline exposures among family members. A spaciotemporal analysis was also employed to apportion personal $PM_{2.5}$ exposures into unique time-activity patterns, revealing previously unknown behavioral patterns between the demographics.

For the intervention phase of the study, an intent-to-treat (ITT) framework was used to examine the variation in personal $PM_{2.5}$ exposure reductions achieved by the whole-household energy intervention among men, women, and children within the community. Results from this analysis indicate that interventions for household energy systems, in conjunction with familial lifestyle and behavior modifications, are necessary to reduce personal $PM_{2.5}$ exposures in rural sub-Saharan African communities.

ACKNOWLEDGEMENTS

Being a part of the SHEAR research team has been a hugely impactful chapter in my life. From learning about the complex protocols associated with collecting and maintaining such a massive digital (and physical) body of data with Christian, to exploring the exciting and often harsh reality of gathering data in the field with Bonnie, this work has truly expanded on all aspects of my being. However, the most impactful lesson I've taken away from this experience is the scale of complexity and beauty that creates our reality, and how much of its mystery we still don't understand.

I came into the Volckens group straight out of NC State with a bachelor's degree in environmental engineering. At the time I thought I was incredibly special and that I could easily do anything I set my mind to. I believe Dr. Volckens recognized this ambition and therefore provided an ample opportunity to push my limits. My trip to Rwanda in the summer of 2022 was the first real test. I had never been to Africa before, let alone a last-mile community on the edge of the Tanzanian savanna. I was initially accompanied by Bonnie Young for the first week of the trip, a seasoned researcher with years of field experience in Latin America. However, once Bonnie left I got to experience, for the first time in my life, being truly alone.

The remaining 30 days of the trip were transformative. Being alone in a small rural town where no one understood English and few had ever interacted with a foreigner, gave me a lot of time to ponder the great questions of life. I grappled with the current state of the world, what my purpose on the planet was, and the many different lifestyle changes I needed to implement before becoming the most inspired version of myself. It was a transcendental and incredibly

illuminating experience. I have so many stories from this period and the following trip in 2023 that greatly shaped my character and perspective on life, these lessons will stick with me forever.

Words cannot encapsulate how valuable this experience was, I am very grateful to Dr. Volckens for entrusting me with the role of training the SHEAR field team on UPAS/AMOD protocols and helping to set up logistics for the study. I am also extremely grateful for the friendships I made in the community. From driving around the countryside with Cleophas scouting residences for rent, to being an honorary member of the Ndego community soccer team with Felician and The Rhinos, I felt incredibly welcomed by everyone I met and I cherished every interaction with the Rwandan SHEAR team and staff.

I also need to express a huge thanks to Dr. Christian L'Orange, who has been an invaluable mentor for me over the years. Christian has an unparalleled understanding of seemingly everything tech/engineering, and was always open to discuss and share his knowledge with me. I found it particularly venerable when he would send out mass emails to everyone in the group letting us know when he'd be setting up a new server, or updating the breaker system for the rooftop power supply, just in case anyone wanted to come along and learn more about these systems. Christian has taught me so much about data management, both common and niche engineering tools/systems, and has been the cornerstone of my knowledgebase for server navigation/utilization. I'm incredibly thankful for all the time I've spent learning from him.

Dr. Bonnie Young has also been an invaluable mentor for me. She was there for my introduction to field work, and has since continued being a positive, encouraging presence anytime challenges arose or when work seemed overwhelming. Bonnie taught me how to retain rigor in data collection/interpretation, while also understanding the reality that real-world data will never be perfect. She also helped me understand that we must learn (as best we can) the

unwritten norms and behaviors underpinning the societies we gather data from, and how recognizing those cultural caveats is often foundational to the interpretation of results.

I also need to thank my family and friends for all their support during this endeavor. Y'all have been there for me through it all, and some of you even came out to visit during my last week in Rwanda. Your unwavering support has been incredibly important to me. All the hours we spent chatting on the phone or hanging out in person gave me the motivation I needed to keep pushing through the minefield of the challenges (academic and otherwise) I encountered over these past five years. I wish I had the space to acknowledge each of you individually, but as a collective, thank you all so much for the love, support and guidance. I could not have done this without you!

To my peers Emilio Molina Rueda and Jacob Fontenot, you guys were there for me at the beginning of this journey and have seen me at some of my lowest points. While you faced many of the same challenges and were undoubtedly overwhelmed at times with your own circumstances, you never failed to show up when I needed it most. I will always remember and appreciate the kindness you shared in some of my darkest moments. I'm sad our time together is ending, but I hope you know you'll always have a friend in me, whenever you need it.

Finally, I want to acknowledge my committee at large. All of you have been fundamental to my development as a scientist. Two of the most influential courses I took during my time at CSU were the Aerosol Physics class in the Spring of 2021 with Dr. Santanu Jathar, and the Environmental Statistics class in the Fall of 2021 with Dr. Ellison Carter. The passion for research and science you displayed truly inspired me. I would be so grateful to attain even just a fraction of the impact you have both made on the world.

Maggie Clark and John Volckens were the co-principal investigators for the SHEAR project. It has been incredibly humbling to watch how they navigated the management of such a large-scale, international, interdisciplinary, and groundbreaking research project with an endless stream of moving parts, in the midst of one of the most contentious periods for federal research funding our nation has ever seen. They remained optimistic and committed to the project and the people, no matter how bleak the situation appeared. Somehow, they always pulled the ship together, even when all hope seemed lost. I am sincerely impressed with the grace and fortitude you both displayed managing this project, and hope to one day have the strength to pull off such a great endeavor myself.

Overall, I am incredibly grateful for all the experiences and all the support I've received throughout this PhD process. I have learned so much about myself, air pollution science, the Rwandan people, and what it means to be successful in life. I will remember my time with the Volckens group and the SHEAR team fondly, and I'll always be open to helping if called upon. The following dissertation discusses my contribution to the SHEAR project in great, technical detail, I hope you enjoy it.

PREFACE

A standard dissertation is typically drawn from three unique bodies of work. However, I begin my time at CSU during the summer of 2020, right as the COVID-19 pandemic began taking full effect. Because of this, the SHEAR study was delayed and new funding came in to support work mitigating the spread of airborne diseases. Therefore, my initial PhD work consisted of characterizing the emission rates and size distributions of large salivary (spit) particles produced by humans during the acts of talking, singing, and playing woodwind instruments. While my committee found this work novel and of value to the scientific community, we decided there was no feasible way to bridge the gap between it and my SHEAR study work. So, my COVID music study work will not be included as a chapter in my general dissertation. However, we added the manuscript produced from this work as Appendix D at the end of this dissertation document for anyone interested.

The manuscript describes emission rates and size distributions from large salivary particles (d_p > 35 μm in aerodynamic diameter) produced by 70 volunteers of varying age and sex while vocalizing and playing woodwind instruments. Mitigation efficacies for face masks (while singing) and bell covers (while playing instruments) were also examined. We did not include any supplementary material for this work as a fifth appendix. But, for anyone wanting that information, the full article and associated SI can be found here. All the figures, tables, equations, and literature citation numbers (including ones referencing the SI document) use their original manuscript numeration. Appendix D has a numeration coding completely independent from the rest of the document.

TABLE OF CONTENTS

CHAPTER 1: BACKGROUND AND INTRODUCTION

1.1 Health Effects of $PM_{2.5}$ Exposure

Exposure to $PM_{2.5}$ (particulate matter with an aerodynamic diameter less than 2.5 μm) was responsible for an estimated 7.8 million premature deaths and 231 million disability-adjusted life years (DALYs) lost globally in 2021.[1,2] Health outcomes attributed to $PM_{2.5}$ exposure include incidence and exacerbation of chronic obstructive pulmonary disease, asthma, ischemic heart disease, acute lower respiratory tract infections, stroke, and lung cancer, among others.[3–7] Black carbon (BC) a fractional component of $PM_{2.5}$ often associated with PM produced from combustion, has also been implicated in the contribution to many adverse health effects including stroke, cardiopulmonary morbidity, and premature mortality.[8–11]

1.2 Discrepancies in Personal Exposure Monitoring by Region and Demographic

The $PM_{2.5}$ exposure burden remains uncertain for many demographic groups and across various geographic regions due to a lack of collected personal $PM_{2.5}$ exposure data. For example, a recent review of 140 personal exposure studies that met established quality-control criteria (having at least 10 unique participants, a minimum of 20 hours of continuous monitoring, and the use of the same type of monitoring equipment throughout the duration of the study) found that none of these studies compared personal $PM_{2.5}$ exposure among men, women, and children in either low-income or low-middle-income countries (LICs and LMICs).[12] Another recent review article comparing the methodologies used to asses household $PM_{2.5}$ pollution in sub-Saharan Africa concluded a considerable lack of research on household pollution measurements of any kind in this region, with an increasing population using unclean fuels.[13]

1.3 $PM_{2.5}$ Emissions from Daily Energy Needs

Unfortunately, it is often these same regions where the highest rates of biomass burning for daily cooking and heating needs are experienced.[14–16] Traditional cooking with biomass fuel is often carried out with inefficient cookstoves and in poorly ventilated spaces, producing dangerously high concentrations of $PM_{2.5}$ and associated BC.[17] As of 2020, it was estimated that 84% (CI: 82, 86%) of people in sub-Saharan Africa relied on biomass fuel for daily cooking, and this percentage was projected to decrease only to 81% (CI: 76-85%) by 2030.[15] Further, in most rural regions of sub-Saharan Africa, traditional cooking using biomass fuel remains ubiquitous, with the rate estimated to be >99% in rural Rwanda.[16] Access to clean energy has been proposed as a basic human right and liquefied petroleum gas (LPG) is a promising, often feasible alternative to traditional biomass fuel stoves.[18,19] Laboratory tests have suggested LPG stoves can produce 99% lower $PM_{2.5}$ emissions than a traditional biomass burning three-stone fire.[20,21]

Much of sub-Saharan Africa also relies on kerosene burning lamps to provide lighting. This style of lighting has been shown to produce high concentrations of $PM_{2.5}$ on its own (10x WHO guidelines), however when combined with the emissions from biomass burning cookstoves, these lamps further exacerbate personal $PM_{2.5}$ exposure.[22–25] Kerosene lamps are often overlooked due to their relatively smaller emissions factors than biomass burning cookstoves, but self-reported use of kerosene lamps in the SHEAR pilot study was associated with an 80% increase in personal $PM_{2.5}$ exposures ($p<0.001$). Integrated exposure curves have been developed for describing the non-linear relationships between personal $PM_{2.5}$ exposures and various associated health risks (COPD, ischemic heart disease, etc.).[6] These curves indicate that the reductions in personal $PM_{2.5}$ exposures associated with LPG interventions may be enough to mitigate some health risks; however, it is unclear whether they are enough to mitigate the risk for more sensitive conditions, like stroke incidence. Therefore addressing PM emissions from all forms of household energy has been proposed as a way to lower personal exposures to a level that mitigates all associated health risks.[23]

1.4 Demographic Diversity in Previous Personal Exposure Studies

Prior LPG intervention personal exposure studies have shown switching participants' fuel source from biomass to LPG can significantly reduce personal $PM_{2.5}$ and BC exposures.[26–30] However, these studies were usually limited to examining only the exposure change of adult females in the population, and only addressed emissions associated with traditional cooking (not whole-household energy). Similarly, most of the non-intervention personal PM exposure studies conducted in sub-Saharan Africa have mainly just focused on women and/or young children (0 to 5 years).[31–35] The rationale behind this focus is that women are the primary cooks for the vast majority of homes in these study regions, and are therefore assumed to be at greatest risk for health complications attributed to household air pollution exposure. However, higher background rates of major air pollution related diseases have been observed for men, leading some researches to question the validity of these assumptions.[36]

Children are a particularly vulnerable demographic to the adverse health effects of air pollution due to their heightened breathing rate, developing respiratory system, and immature immune system.[37–41] Children are often assumed to have identical exposures to their primary guardian (usually their mother) due to perceived similarity in daily activities and exposure patterns.[42] These types of assumptions for relative demographic exposures to $PM_{2.5}$ are referred to as equivalent exposure ratios, and they are used in the mortality and morbidity calculations made by the global burden of disease study.[43] Some researchers have argued that these type of assumptions may contribute to underpredicting premature deaths by as much as 220%, especially in geographic locations with sparse data on personal exposure.[44] Overall, the lack of exposure data for men and children (5 to 17 years) in sub-Saharan Africa limits our understanding of the nature of the exposure burden for this understudied region of the world, and in turn also limits efforts to mitigate this risk.[43,45]

1.5 Personal Exposure Monitoring: The 'Gold Standard'

Personal exposure (i.e., data collected from within one's breathing zone) is considered the "gold standard" for estimating individual risks because it accounts for variations in exposure that occur as a function of time, location, activity, and behavior. Personal exposure data are especially important for risk assessment differentiation between various demographic groups within the same geographical region.[12,45,46] Understanding individual $PM_{2.5}$ exposure patterns in sub-Saharan Africa is especially crucial since this region accounts for an estimated 31% of global deaths related to household air pollution, despite having only 15% of the global population in 2021.[1,47]

Personal $PM_{2.5}$ exposure studies in this region have been limited due to a lack of wearable, robust, accurate and scalable (i.e. quickly deployable with standardized quality assurance measures) $PM_{2.5}$ monitoring technology. This technical limitation has been a defining reason for the lack of exposure data on men and older children in previous studies.[45] However, recent improvements in personal $PM_{2.5}$ monitoring technology have increased our ability to track exposures in space and time with less disruption to individual's daily routines.[26,48–56] This work utilized one such technology to monitor the personal $PM_{2.5}$ exposure levels of individuals in a rural Rwandan community over a 3 year period, both before (15-months) and during (17-months) a whole-household energy randomized control intervention.

1.6 Overview and Objectives of this Work

This work provides two novel contributions illuminating the nature of personal $PM_{2.5}$ exposure in rural Rwanda: a baseline analysis of the demographic variation in $PM_{2.5}$ exposure within a rural Rwandan community, and an intent-to-treat (ITT) analysis examining the effect of a combined LPG/solar-based electric lighting intervention within the community. Chapter 2 introduces the SHEAR (Sustainable Household Energy Adoption in Rwanda) project, a clean energy intervention project (where LPG replaces biomass burning stoves, and solar-based electric lighting replaces kerosene burning lamps) that provided the framework for all the data presented here. This chapter discusses the sampling and analysis methods common between the baseline and intervention phases of the study. Chapter 3 analyzes the baseline variation in $PM_{2.5}$ exposures among adults (both men and women) and adolescent/pre-adolescent children (aged between 8 and 17 at the time of enrollment, hereafter referred to as “child” or “children”) within the two SHEAR villages prior to the clean energy technology introduction, when all participants still relied on solid biomass fuel as their sole form of household cooking energy, and most relied on kerosene lamps for additional lighting. Space-and-time-resolved personal exposure data are combined with a machine-learning cluster analysis and geocoded land-use feature data to apportion personal $PM_{2.5}$ exposures into unique time-activity patterns. Chapter 4 employs an ITT framework to examine the reductions in personal $PM_{2.5}$ and BC exposure achieved during the fully subsidized clean energy intervention among men, women, and children within the same community. This analysis employes linear mixed effect models to determine the variation in exposure reductions between men, women and children at both the household and community levels.

CHAPTER 2: THE SHEAR STUDY

2.1 Study Setting

The SHEAR project (Sustainable Household Energy Adoption in Rwanda) is a 3-year randomized control trial (2022-2025; US ID: NCT05668624) located in the communities of Karambi and Isangano within the Eastern Province of Rwanda. Figure 2.1 provides a map of the study region.

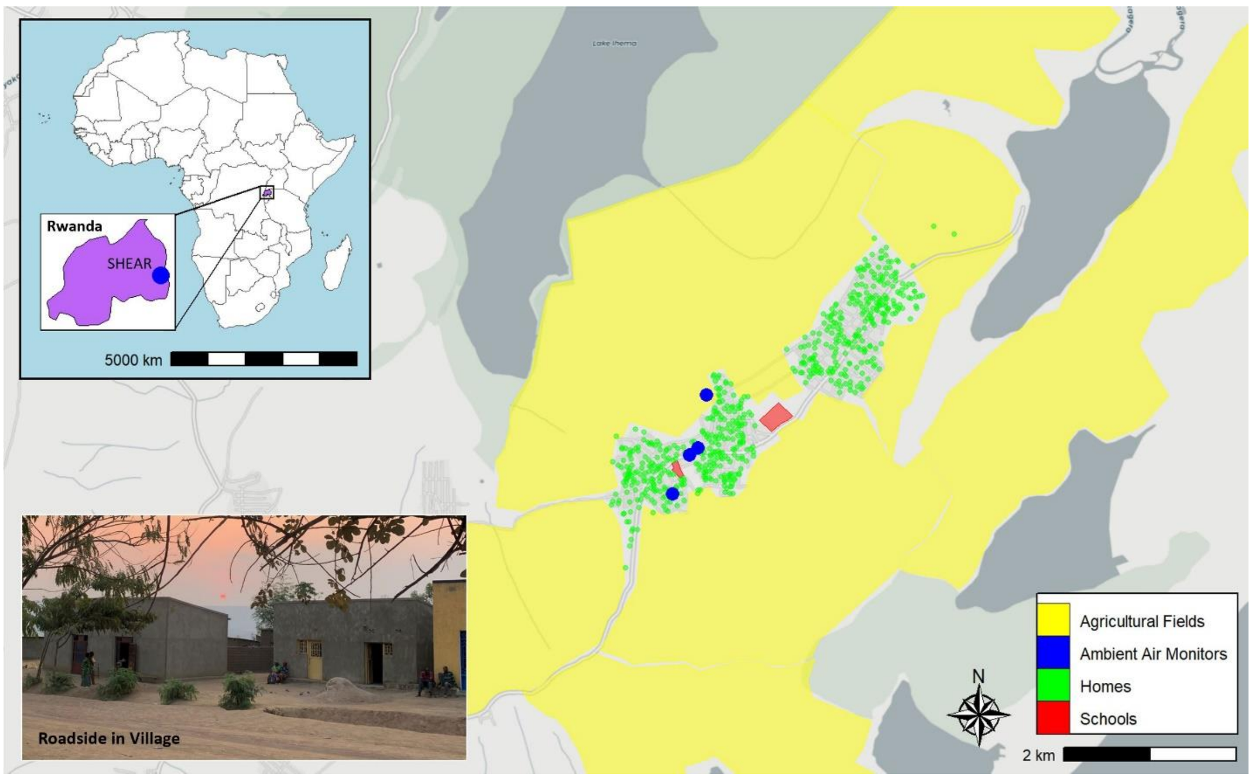

Figure 2.1: Map of the Study region. Green dots represent the locations of SHEAR study households (n = 579), blue dots depict the AMOD deployment locations (ambient air monitoring sensors n = 4), the yellow polygons are various fields participants conduct agricultural work in, and the red polygons show the school boundaries. The inset map of Africa in the top left corner of the figure highlights Rwanda, the country where this study is located and the blue dot within this inset map shows the exact location of the SHEAR study. The bottom left insert image depicts a typical roadside in one of the study villages.

The villages were chosen because they will not be receiving distributed electricity during the study period (there is a plan to connect them to the national grid eventually) and traditional energy sources for cooking and lighting were used nearly universally amongst the households in the region, prior to the energy intervention. These villages typify rural sub-Saharan African subsistence farming communities with limited resources and virtually no access to modern forms of household energy (e.g. grid electricity or pumped natural gas).

2.2 Experimental Design

The SHEAR project introduced a clean household energy intervention to homes within the community, employing LPG to replace biomass fuel for cooking and solar-based electric lamps to replace kerosene burning lamps for lighting. Households were randomized into three study arms: 248 into the full subsidy arm receiving clean energy (and the associated technology) free of charge, 141 into the random subsidy arm having to pay for the clean energy at various discounted rates, and 235 into the control arm not receiving any clean energy (until the end of the study, as an incentive). Participants were visited up to seven times over the course of the 3-year study for responding to surveys, gathering data on health metrics, and monitoring their personal $PM_{2.5}$ exposures. Regardless of which study arm households were assigned, no household received any clean energy technology during the first visit. This visit was used to establish participants' baseline health measures and $PM_{2.5}$ exposure levels prior to the intervention.

The personal $PM_{2.5}$ exposure data collected during the initial baseline visit are the focus of Chapter 3, while the exposure data collected from households within the full subsidy (treatment) and control arms during the intervention phase of the study are the focus of Chapter 4. Other aspects of the SHEAR project not described in this work include the characterization of associations between $PM_{2.5}$ exposure and indicators of morbidity (e.g. blood pressure, lung function), and for the random subsidy arm an investigation into the causal relationship between the randomized cost of LPG/solar electricity, the measured use of the LPG/solar electricity, and personal $PM_{2.5}$ exposures.

2.3 Study Enrollment Eligibility Criteria

To be eligible for participation in the study, households must have conformed to following inclusion criteria: (1) located in the study area of Isangano and Karambi; (2) had an adult male and female, or a single adult, head of household over 18 years, and at least one child 8 to 17 years of age; (3) non-smoking; (4) primarily used an open fire or wood/charcoal stove; (5) did not do any commercial cooking; (6) were not currently pregnant (women); and (7) did not plan to move within the next 3 years. Participants provided informed consent approved by the Rwanda National Ethics Committee (# 00001497) and by the Institutional Review Board at Colorado State University (IRB # 3946).

2.4 Household Characteristics

At the time of enrollment, participants completed an initial baseline household survey providing information on each participating family member's gender, age, and occupation, along with other household details like who is the primary cook, how many stoves are in the home, etc.

Households in the study region were predominantly constructed of locally produced mud bricks with metal roofs. Floors in houses varied from packed dirt to poured concrete pads. Tiled or painted concrete floors were present in higher income homes. Houses ranged from one to five bedrooms, often adjoining a large multipurpose communal room. Smaller houses only had one entrance with a metal door, and rooms were often separated with cloth barriers. Rooms could have small windows allowing limited light into the house. Higher quality windows had glass panes, but most remained open and some had wooden shutters. Houses were commonly enclosed in a walled compound, providing storage and space for working and cooking. Kitchens could be either open air, an alcove consisting of three walls and a roof, or a separate annex. When a separate kitchen was present, there was often only a door and a single window providing ventilation. Chimneys were not regularly employed to redirect cooking smoke. Table 2.1 Provides a summary of household characteristics data and Figure 2.2 shows a collage of typical kitchen set ups and home exterior conditions.

Table 2.1: Household Characteristics Summary Table (n = 628 households)

	Value/Number	Percentage
Average Number of Rooms (SD)	2.4 (0.7)	
Average Number of Stoves Used Regularly (SD)	1.2 (0.4)	
Kitchen Locations		
In Separate Building	515	82.0%
Outside the House	98	15.6%
Room Adjacent to Bedroom	10	1.6%
Separate from Bedroom, Inside	3	0.5%
Don’t Know	2	0.4%
Primary Stove Type		
Traditional Cookstove	611	97.3%
Charcoal Stove	13	2.1%
Other	4	0.8%

Figure 2.2: Collage of Typical Kitchen and Home Exterior Appearances. (A) Typical kitchen setup for a home with the kitchen in a separate building. (B) Example of traditional stove. (C) Example of home exteriors.

2.5 Personal Exposure Monitoring

2.5.1 The UPAS V2 Plus

Personal $PM_{2.5}$ exposure sampling was conducted during visits 1 (baseline), 3, 4, 5, and 7 and consisted of wearing a UPAS V2 Plus (Ultrasonic Personal Aerosol Sampler; Access Sensor Technologies, Fort Collins CO) in the breathing zone for a continuous 48-hour period, during which participants went about their daily routines.[48] The UPAS is a wearable air quality monitor that uses a quiet piezoelectric pump to draw air at 1 L·min^{-1} through a 2.5 μm size-selective cyclone inlet and onto a 37 mm PTFE sampling filter (PT37 MTL LLC, Minneapolis, MN).[57] A separate stream pulls air into a light-scattering sensor (SPS30, Sensirion AG Stäfa, Switzerland) at the front of the unit to estimate $PM_{2.5}$ concentration at 30-second intervals.[58] The UPAS V2 Plus also records GPS, accelerometry, air temperature, relative humidity, and atmospheric pressure data at the same 30-second intervals.

2.5.2 The UPAS Harness

Participants were asked to wear the UPAS on their chest during waking hours, via a custom harness produced by a local tailor. The harness was designed to be as durable and nondisruptive to participants' daily lives as possible. A single length-adjustable shoulder strap allowed for a wide range of motion and orientation flexibility (depending on the participant's dominant arm). The lightweight locally sourced kitenge fabric provided breathability while minimizing any community stigma associated with participating in a foreign sponsored research project, and the locally sourced fishing net pouch (used to support the majority of the UPAS weight) facilitated ample air flow to and from the UPAS inlets and outlets while maintaining durability for the duration of 3-year study. Figure 2.3 shows an image of participants collecting a sample from the UPAS wearing the harness.

Figure 2.3: UPAS Harness. Three participants (man, woman, and child) wearing the UPAS V2 Plus in the locally produced kitenge fabric and fishnet harnesses.

2.5.3 The UPAS Charging Cradle

To obtain a continuous 48-hour sample, a small battery-powered charging station was provided to each participant to recharge their UPAS overnight. Participants were instructed to keep the UPAS and charging station as close to their breathing zone as feasible while they slept. The charging cradle consisted of a 20 Ah battery (INIU Portable Charger, 18W PD QC 20000mAh USB C Power Bank) connected to a magnetic microUSB connector housed within a 19 cm x 10 cm x 5 cm polystyrene enclosure. The outside of the cradle utilized a 3D-printed retainment structure to keep the UPAS upright, air vents exposed, and magnetic microUSB connection intact during the charging process. No device modification or setup was necessary for participants; they were instructed to simply take the UPAS out of their wearable harness and put it into the charging cradle before going to bed. Participants could also remove the UPAS and keep it nearby when bathing or using the restroom. An example of the UPAS charging cradle is provided in Figure 2.4

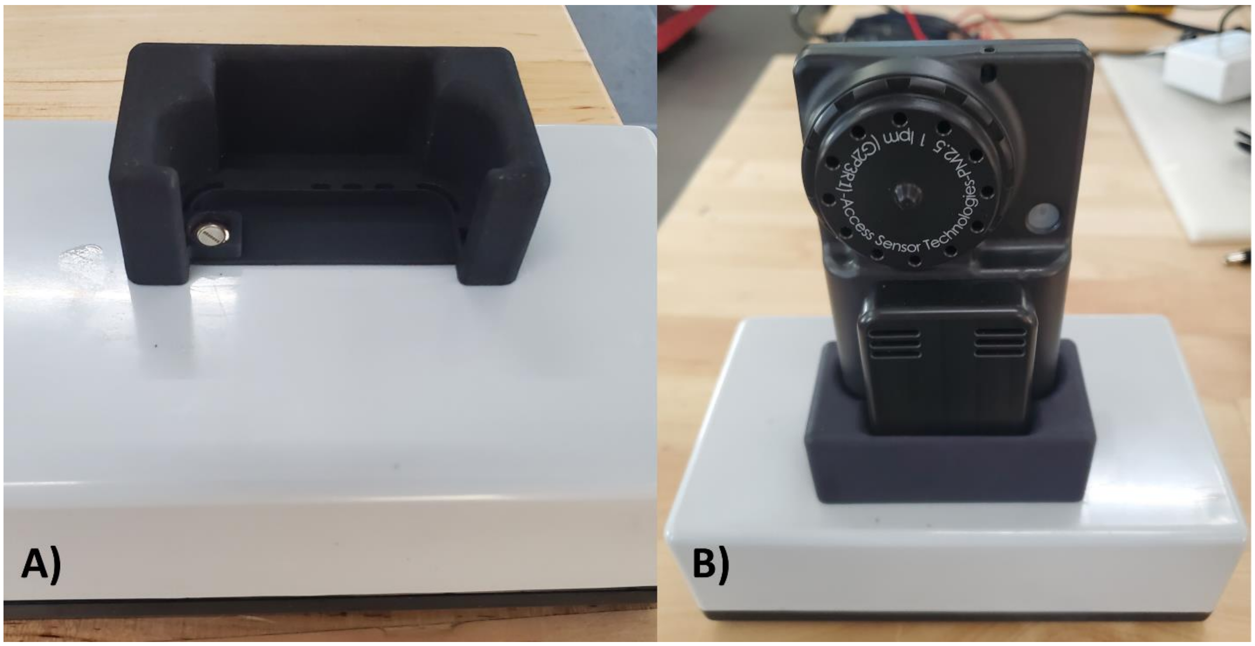

Figure 2.4: UPAS Charging Cradle. (A) Charging cradle without UPAS, showing magnetic connection port. (B) Charging cradle with UPAS.

2.5.4 UPAS Wearing Compliance

Device wearing compliance was assessed by UPAS accelerometry data, evaluated between the hours of 6:00 and 21:00 (waking hours) When the UPAS was not on the charging cradle. To establish the compliance metric, the 80% of samples with a working accelerometer were partitioned into 15-minute windows and the standard deviation (SD) of x-axis acceleration (mG) was calculated for the 30-second observations from each. Then, the distribution of the 15-minute window SDs for times when the UPAS was and was not connected to the charging cradle were examined, Figure 2.5.

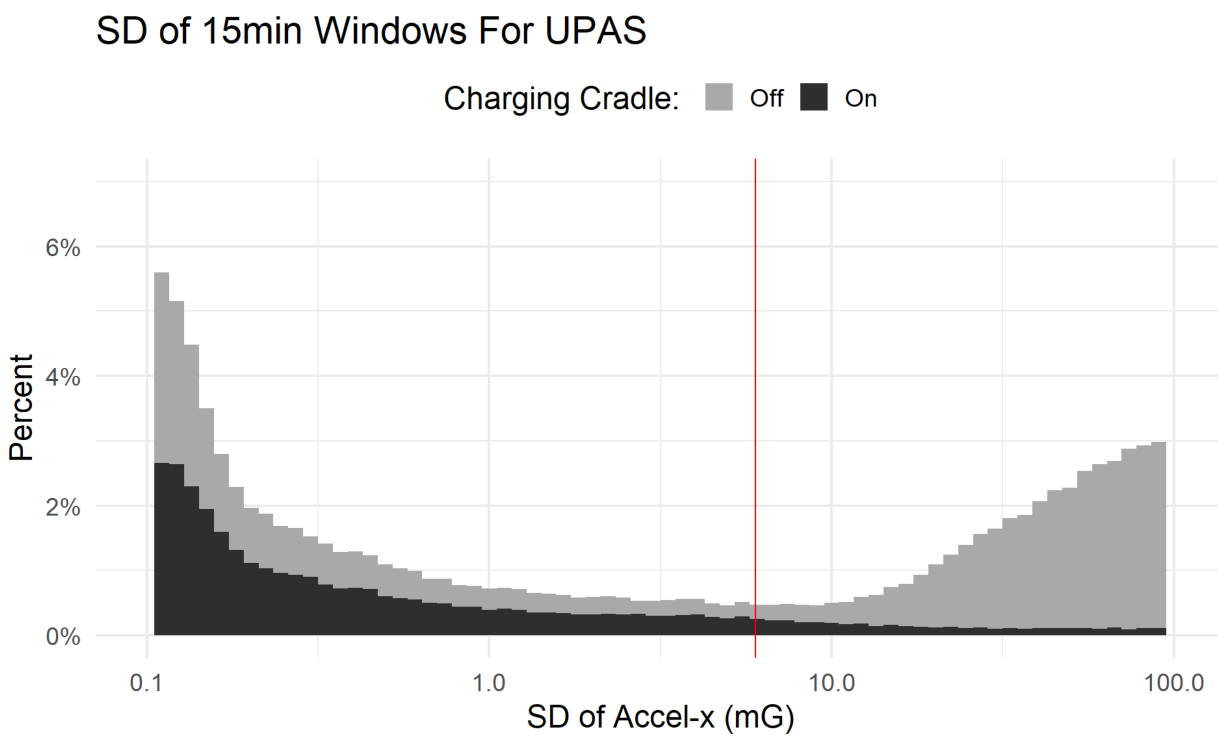

Figure 2.5: Standard Deviation of UPAS Acceleration. The distribution of standard deviations for acceleration in the x-axis (mG) among 15-minute time windows while the UPAS was on and off the charging cradle. The red line represents the 6 mG cutoff value determined as a threshold for adequate movement for a 15-minute time window.

It was determined that a 6 mG (red line) or greater SD for a 15-minute window meant the UPAS detected sufficient movement during the time window to suggest the participant was wearing the UPAS in that window. After establishing this movement cutoff value of 6 mG SD for the 15-minute windows, the fraction of time windows having SDs beyond the threshold for each sample were calculated. Results from this user compliance analysis (stratified by demographic and age) are provided in section *3.2.6* for the baseline samples and in section *4.2.6* for the intervention phase samples. Compliance was incentivized among participants by promising compensation worth approximately 7000 RWF to households with study members (adults and children) who wear the UPAS for at least 75% of the time during waking hours for the 4 study visits that included monitoring (they also must complete all 7 visits in total).

2.5.5 *Gravimetric Filter Handling and Analysis*

The time integrated gravimetric filter data were used to correct the UPAS's 30-second $PM_{2.5}$ concentration data on a per-sample basis using methods outlined in Tryner et al. 2020.[59] This correction was necessary because low-cost light scattering $PM_{2.5}$ sensors are sensitive to changes in aerosol size, refractive index, and ambient relative humidity, all of which can vary during sampling.[60] Post-sampling filters were stored in the SHEAR study office freezer (-20°C) between the bi-monthly air freight shipments back to Colorado State University where they were then stored in a -80 °C freezer before equilibration in climate-controlled environment (temperature: 20–23 °C; relative humidity: 30–40%) prior to gravimetric analysis. After equilibration, filters were weighed in triplicate using a high precision microbalance (XS3DU, Mettler-Toledo, Columbus, OH, USA) via an automated robotic process.[61] The same weighing process was applied to each filter prior to deployment in Rwanda, allowing for the calculation of filter sample loadings; the filter's post sampling weight – pre sampling weight (µg).

Before each UPAS deployment, a 'blank' filter was loaded into one of the UPAS units scheduled for use that day. This filter was left inside the turned-off unit for 1 to 5 minutes before being removed, labeled as a 'blank', and stored for shipment with the rest of the post-sampling filters in the SHEAR study office freezer. These blank filters were weighed via the same process as the sample filters, both pre- and post-deployment in Rwanda, and their loadings were calculated as 'blank filter loadings'. Filter loadings from personal samples were subtracted by the monthly average 'blank filter loading' for each sample's corresponding month (i.e., the monthly arithmetic mean of all blank filter loadings was subtracted from the filter loading of each personal exposure sample), providing background-corrected sample filter loadings; accounting for potential measurement artifacts encountered during shipping and handling. A time series plot of blank filter loadings for the duration of the study is shown in Appendix A1.

A gravimetric limit of detection (LOD) value was calculated for each month using the blank filter loadings, defined by Equation 1.

$$LOD = \mu_b + 3\sigma_b \qquad (1)$$

Where μ_b is the mean blank filter loading for the month and σ_b is the blank filter loading standard deviation for the month. The 3 comes from the probability density function for the normal distribution, implying values above the LOD have a 99:1 chance of being correctly identified as above zero (i.e. three standard deviations away from the normal distribution center at μb). The few filter loadings found to be below the LOD for their associated month were replaced by $\frac{LOD}{\sqrt{2}}$ as prescribed by Hewett and Ganser 2007.[62] However, all the samples with filter loadings below the LOD (for both the baseline and intervention phases) ended up excluded from our analysis anyways due to invalid sampling criteria (described in the subsequent chapters). A timeseries plot of our estimated gravimetric LOD values by month is shown in Appendix A2.

2.5.6 Gravimetric Correction for Real-time $PM_{2.5}$ Estimates

Background-corrected, LOD-adjusted filter loadings were divided by the total volume of air passed through each filter during sampling to find the gravimetrically derived average $PM_{2.5}$ sample concentration. Then, the average real-time light scattering sensor reported sample concentration (averaged only for times when the filter pump was on) was divided by this gravimetrically derived average concentration, producing a real-time to gravimetric correction ratio for each sample. This calculation is represented by Equation 2.

$$Correction\ Ratio = \frac{C_{Real-time}}{C_{Filter}} \qquad (2)$$

Where $C_{Real\text{-}time}$ is the sample average real-time reported $PM_{2.5}$ concentration (30-second observations) for times the filter was in use, and C_{Filter} is the gravimetrically derived concentration based on the filter loading and the recorded volumetric flowrate. The inverse of this correction ratio was multiplied to each 30-second $PM_{2.5}$ concentration estimate for each corresponding sample. This process provided 30-second $PM_{2.5}$ concentration estimates uniquely corrected for each 48-hour sample by its own gravimetric correction ratio.

To maintain sample quality, our field staff removed and cleaned the interior surfaces of all UPAS cyclones on a weekly basis. Our QA/QC procedures at CSU also noted any tears, holes or other anomalies in the filters during weighing, including documenting evidence of "spotting", "overloading", or unusual particle deposition across the filter surface. None of the filters used in our analysis were flagged for large particle breakthrough.

2.6 Linear Mixed Effect Models

All Data analyses were conducted using R (version 4.2.2). Linear mixed models were developed to examine the statistical significance, at a type 1 error rate of 5%, for the differences in personal exposures among men, women, and children while accounting for household using random intercepts. $PM_{2.5}$ exposure concentrations were natural log-transformed to meet the model assumptions (reducing right-skewedness and heteroscedasticity), taking the form of Equation 3:

$$Y_{ij} = \beta_0 + \boldsymbol{\beta}^T \boldsymbol{X_{ij}} + \alpha_i + \epsilon_{ij} \qquad (3)$$

Where Y_{ij} is the log-transformed average $PM_{2.5}$ exposure concentration from the ith household and the jth participant, $\boldsymbol{X_{ij}}$ is the set of fixed predictor variables, $\boldsymbol{\beta}$ is the vector of coefficients for the predictor variables, α_i is a random intercept term for household i and ϵ_{ij} represents the residual model error (assumed to be normally distributed with mean zero and constant variance). For the ITT analysis, an interaction term was specified between the demographic and study group variables to test specific pairwise differences.

2.7 Ambient Air Quality Monitoring

2.7.1 The AMODs

Ambient $PM_{2.5}$ levels were routinely monitored using 4 Aerosol Mass and Optical Depth monitors (AMODs, developed at Colorado State University) set upon 4m (13.1 ft) poles at two central and two edge locations in Karambi, shown as the blue dots in Figure 2.1.[63–66] These ambient air quality monitors functioned similarly to the UPAS personal exposure monitors.

The AMODs had both a real-time PM light scattering sensor (Plantower PMS8003), and a separate $PM_{2.5}$ filter train. This setup provides the AMODs with similar gravimetrically corrected real-time $PM_{2.5}$ concentration estimations to the ones calculated for the UPAS personal exposure monitors. The main differences are that the AMODs had more weatherproof enclosures, larger batteries, and a different $PM_{2.5}$ light scattering sensor. The AMODs also record $PM_{2.5}$ concentrations at 10-minute intervals instead of 30-second ones like the UPAS because ambient $PM_{2.5}$ concentrations change a lot slower than personal exposures, and a 10-minute resolution was decided on as a reasonable compromise allowing for longer battery runtimes.

These ambient air quality monitoring units were set up at least 4m above the ground (and away from household kitchens) to avoid tampering during sampling campaigns. As a result, these units monitored background (ambient) $PM_{2.5}$ levels within the village. See Figure 2.6 for an image of one of the AMODs and its sampling pole set up.

Figure 2.6: AMOD and Sampling Location. On the left is an image of one of the modified AMODs (with the AOD turret covered) used for ambient $PM_{2.5}$ monitoring. The dark-green circle at the front of the unit is the size-selective ($d_p < 2.5$ µm) cyclone inlet that sits in front of the PTFE filter for collecting gravimetric samples. The black inlet on the left face of the unit is the real-time $PM_{2.5}$ light scattering sensor port. The right side of the figure shows one of the original wooden sampling poles and its replacement metal pole used to hold the units ~4 m above the ground while sampling. The AMODs were set up on wooden poles for the first 5 months of the study before getting replaced by metal ones to ensured greater longevity for the remainder of the 3-year study.

2.7.2 Stripping of the AMOD abilities

The AMODs were originally designed to monitor aerosol optical depth (AOD) along with real-time $PM_{2.5}$ concentration. They used a camera attached to a turret on top of the unit that swiveled to find the sun every 20 minutes.[63] The camera measured the intensity of light when aimed directly at the sun throughout the day to calculate the AOD. However, to allow for longer battery runtimes for the SHEAR study, this feature was disabled and the AOD turret was covered up. The AMODs used in the SHEAR study only monitored the real-time $PM_{2.5}$ concentrations while collecting an integrated filter sample, along with recording other real-time environmental conditions like atmospheric temperature, pressure, etc.

2.7.3 Gravimetric Filter Handling and Analysis

Filters were not collected with every sample as they were with the personal exposure UPAS samples due to the bandwidth of the field staff and the assumption that ambient air quality has less compositional variation than personal exposures. The 4 AMODs were typically deployed on Friday afternoons and recorded real-time $PM_{2.5}$ concentration estimates every 10-minutes until their batteries died. These sampling periods (i.e. the battery life) lasted about 3 days when a gravimetric filter sample was collected in parallel, and around 5 days when only real-time data was monitored.

'Blank' filter collection, background subtraction, and real-time correction ratios were all conducted in a similar manner to the UPAS personal exposure samples (detailed in sections *2.5.5* and *2.5.6*), but the AMODs did not have a unique correction ratio for each deployment because filters were not collected for every sampling period. Instead, the median real-time to gravimetric $PM_{2.5}$ correction ratio was used to correct all filter and non-filter AMOD samples. Filter samples were typically collected every 4th AMOD deployment, averaging about one ambient air filter sample per month. The median correction ratio was determined to be the best option for the correction of all samples due to the smaller sample size of ambient air filter deployments and the large standard deviation among these samples. Appendix A3 depicts a histogram of the ambient filter sample calculated real-time to gravimetric $PM_{2.5}$ correction ratios along with the median line value used for in the analysis for all ambient real-time $PM_{2.5}$ corrections (median correction ratio value used: 1.94). A temporal analysis for daily average ambient $PM_{2.5}$ concentrations by AMOD location over the course of the SHEAR study is provided in Appendix A4.

2.8 SHEAR Field Team

Monitor deployment, collection, in-field filter handling, and participant interactions were conducted by trained local staff. Integrating staff from the community improved the project's rapport among participants and helped establish trust within the larger community, as most participants only spoke Kinyarwanda.

CHAPTER 3: FAMILIAL DIFFERENCES IN BASELINE PERSONAL $PM_{2.5}$ EXPOSURE EXPLAINED WITH SPATIOTEMPORAL APPORTIONMENT

3.1 Introduction

Exposure to $PM_{2.5}$ was responsible for an estimated 7.8 million premature deaths and 231 million disability-adjusted life years lost globally in 2021.[1,2] Health outcomes attributed to $PM_{2.5}$ exposure include incidence and exacerbation of chronic obstructive pulmonary disease, asthma, ischemic heart disease, acute lower respiratory tract infections, stroke, and lung cancer, among others.[3–7] The $PM_{2.5}$ disease burden, however, remains uncertain for many demographic groups and across various geographic regions due to a lack of collected personal $PM_{2.5}$ exposure data. For example, a recent review of 140 personal exposure studies that met established quality-control criteria (having at least 10 unique participants, a minimum of 20 hours of continuous monitoring, and the use of the same type of monitoring equipment throughout the duration of the study) found that none of these studies compared personal $PM_{2.5}$ exposure among men, women, and children in either low-income or low-middle-income countries (LICs and LMICs).[12] To date, most personal $PM_{2.5}$ exposure studies in sub-Saharan Africa have focused on women and/or young children (0 to 5 years), as these groups are assumed most likely to have the closest proximity to cooking emissions.[13,26,31–35] Exposure data are lacking for men and children (5 to 17 years) in these settings; these data are necessary to define exposure burden more accurately as a function of population demographics.

Personal exposure (i.e., data collected from within one's breathing zone) is considered the "gold standard" for estimating individual risks because it accounts for variations in exposure that occur as a function of time, location, activity, and behavior. Personal exposure data are especially important for risk assessment differentiation between various demographic groups within the same geographical region.[12,45,46] When personal exposure data are lacking, mortality and morbidity burden estimates rely on a combination of satellite imagery, chemical transport modeling, regional source-receptor estimates, and fixed-site outdoor concentration measurements (which can be several km away from many at risk populations).[12,44,46,67–70] These methods are commonly used to estimate exposure-response relationships for ambient $PM_{2.5}$, but they are less reliable at quantifying indoor air pollution exposure, which is characterized by more spatial and temporal variation.[26,28,52] Understanding individual $PM_{2.5}$ exposure patterns in sub-Saharan Africa is crucial since this region accounts for an estimated 31% of global deaths related to household air pollution, despite having only 15% of the global population in 2021.[1,47] Unfortunately, personal $PM_{2.5}$ exposure studies are often limited due to a lack of wearable, robust, accurate and scalable (i.e. quickly deployable with standardized quality assurance measures) $PM_{2.5}$ monitoring technology.[45] However, recent improvements in personal $PM_{2.5}$ monitoring technology have increased our ability to track exposures in space and time with less disruption to individual's daily routines.

The primary objectives of the work in this chapter were to quantify the $PM_{2.5}$ exposures and demographic variations among adults (both men and women) and adolescent/pre-adolescent children (aged between 8 and 17 at the time of enrollment) in a rural sub-Saharan African community that relied on solid biomass fuel as their sole form of household cooking energy. Space-and-time-resolved personal exposure data, a machine-learning cluster analysis, and geocoded land-use feature data were combined to apportion personal $PM_{2.5}$ exposures into unique time-activity patterns. These patterns helped reveal source-receptor relationships for

$PM_{2.5}$ exposure that explain demographic variations in daily exposures among men, women, and children in this rural setting.

3.2 Methods

3.2.1 Study Setting and Participant Eligibility

The SHEAR project (Sustainable Household Energy Adoption in Rwanda) is a 3-year randomized control clean household energy intervention trial (2022-2025; US ID: NCT05668624) located in the communities of Karambi and Isangano within the Eastern Province of Rwanda (see Figure 2.1 for a map of the study region). The villages were chosen because they will not be receiving distributed electricity during the study period (there is a plan to connect them to the national grid eventually) and solid fuels for cooking are used nearly universally amongst the households in the study area. These villages typify rural sub-Saharan African subsistence farming communities with limited resources and virtually no access to modern forms of household energy (e.g. grid electricity or pumped natural gas). Data presented in this chapter were collected during the SHEAR baseline period, prior to the intervention that introduced LPG for cooking and solar-based electric lamps for lighting. A total of 630 households were initially enrolled in SHEAR with the following inclusion criteria: (1) located in the study area of Isangano and Karambi; (2) had an adult male and female, or a single adult, head of household over 18 years, and at least one child 8 to 17 years of age; (3) non-smoking; (4) primarily used an open fire or wood/charcoal stove; (5) did not do any commercial cooking; (6) were not currently pregnant (women); and (7) did not plan to move within the next 3 years. Participants provided informed consent approved by the Rwanda National Ethics Committee (# 00001497) and by the Institutional Review Board at Colorado State University (IRB # 3946).

Additional details on the SHEAR study design, enrollment criteria, household characteristics, and participant surveys are provided in sections *2.2* through *2.4*.

3.2.2 Personal $PM_{2.5}$ Exposure Monitoring

Personal $PM_{2.5}$ exposure sampling consisted of wearing a UPAS V2 Plus (Ultrasonic Personal Aerosol Sampler; Access Sensor Technologies, Fort Collins CO) in the breathing zone for a continuous 48-hour period, during which participants went about their daily routines. The UPAS is a wearable air quality monitor that uses a quiet piezoelectric pump to draw air at 1 $L \cdot min^{-1}$ through a 2.5 μm size-selective cyclone inlet and onto a 37 mm PTFE sampling filter(PT37 MTL LLC, Minneapolis, MN).[57] A separate stream pulls air into a light-scattering sensor (SPS30, Sensirion AG Stäfa, Switzerland) at the front of the unit to estimate $PM_{2.5}$ concentration at 30-second intervals.[58] The UPAS V2 Plus also records GPS, accelerometry, air temperature, relative humidity, and atmospheric pressure data at the same 30-second intervals. Air sampling filters were pre- and post-weighed in triplicate (XS3DU, Mettler-Toledo, Columbus, OH, USA) inside a climate controlled environment via an automated robotic process at Colorado State University and shipped to and from the field via air freight every other month.[61] Filters were stored in an on-site freezer (-20 °C) after sample collection between the bi-monthly air freight shipments. Post-sampling filters were stored in a -80 °C freezer once received by CSU before equilibration in the climate-controlled weighing chamber prior to gravimetric analysis. Filter field blanks were collected at the beginning of each sampling day and used to account for potential measurement artifacts encountered during shipping and handling.

Participants were asked to wear the UPAS on their chest during waking hours, via a custom harness (Figure 2.3) produced by a local tailor. To obtain a continuous 48-hour sample, a small battery-powered charging station was provided to each participant to recharge their UPAS overnight (Figure 2.4). Participants were instructed to keep the UPAS and charging station as close to their breathing zone as feasible while they slept (see sections *2.5.2* and *2.5.3* for additional details). Participants could also remove the UPAS and keep it nearby when bathing or using the restroom. Device wearing compliance was assessed by UPAS accelerometry data, evaluated between the hours of 6:00 and 21:00 (see section *2.5.4* for more details). Data presented in this chapter are from the SHEAR baseline survey of study participants; each sample represents a single 48-hr measurement (n=1,280 samples total with no repeated measures). All real-time $PM_{2.5}$ estimates used in this analysis were corrected using the gravimetric correction ratios described in section *2.5.6*.

3.2.3 GPS Cleaning

Each 30-second $PM_{2.5}$ observation was apportioned into one of 8 distinct microenvironments based upon its GPS coordinates: home, near home, agricultural field, school, in transit (within village), in transit (outside of village), other, and no-GPS. To do this, first a GPS cleaning algorithm was applied to all the raw GPS observations removing nonsensical outliers. This algorithm set the latitude and longitude values of observations to "NA" if the calculated speed of a participant based on sequential observations exceeded 18 km/h (very few people drove vehicles in the village and bike traffic was often slow due to the many hills, foot traffic, and unpaved roads). All the successive coordinates of an initial "bad point" were also set to "NA" until the coordinates indicated a participant was either back in one of the study villages, or within 2 km of the last previous "good" GPS observation.

3.2.4 Clustering Algorithm

A machine-learning clustering algorithm (dbscan, from the fpc package) was then used to categorize participants' GPS coordinates into distinct clusters.[71] This function employs an unsupervised learning non-linear algorithm to categorize data into groups with similar characteristics or clusters. The three inputs used for the function were a data frame containing all the latitude and longitude points from a participant's sample, the eps (epsilon neighborhood radius, i.e. the maximum radius used to define cluster neighborhoods)[72], and MinPts or the minimum number of points within the neighborhood radius required for establishing/addition to a cluster. For our analysis the eps was set to 0.00018, which is the GPS degree equivalent of ~20 m (calculated using the Haversine formula), and our MinPts to 60 which is equivalent to 30 minutes for our data, which had a 30-second time resolution.

The algorithm established a cluster for a participant when one GPS point had 60 or more GPS points within a 20 m radius. The 60 GPS points used to establish the cluster were only labeled as being a part the cluster if they also had 60 points within a 20 m radius of them (including points already labeled as part of the cluster). The process continued until the edge points of the cluster were established, where points further away had less than 60 other points within a 20 m radius of them. These points with less than 60 other points inside their 20 m radius were assigned to cluster "0", or "no cluster".

This process established "hot spots" or clusters of GPS locations where a participant spent at least 30 minutes of their sampling time. It should be noted that these clusters were not limited just to the 20 m radius of the initial GPS point used to establish the cluster, as the radius shifted to determine additional points within clusters iteratively for every GPS point in a participant's sample. An example of one participant's cluster map is displayed in Figure 3.1.

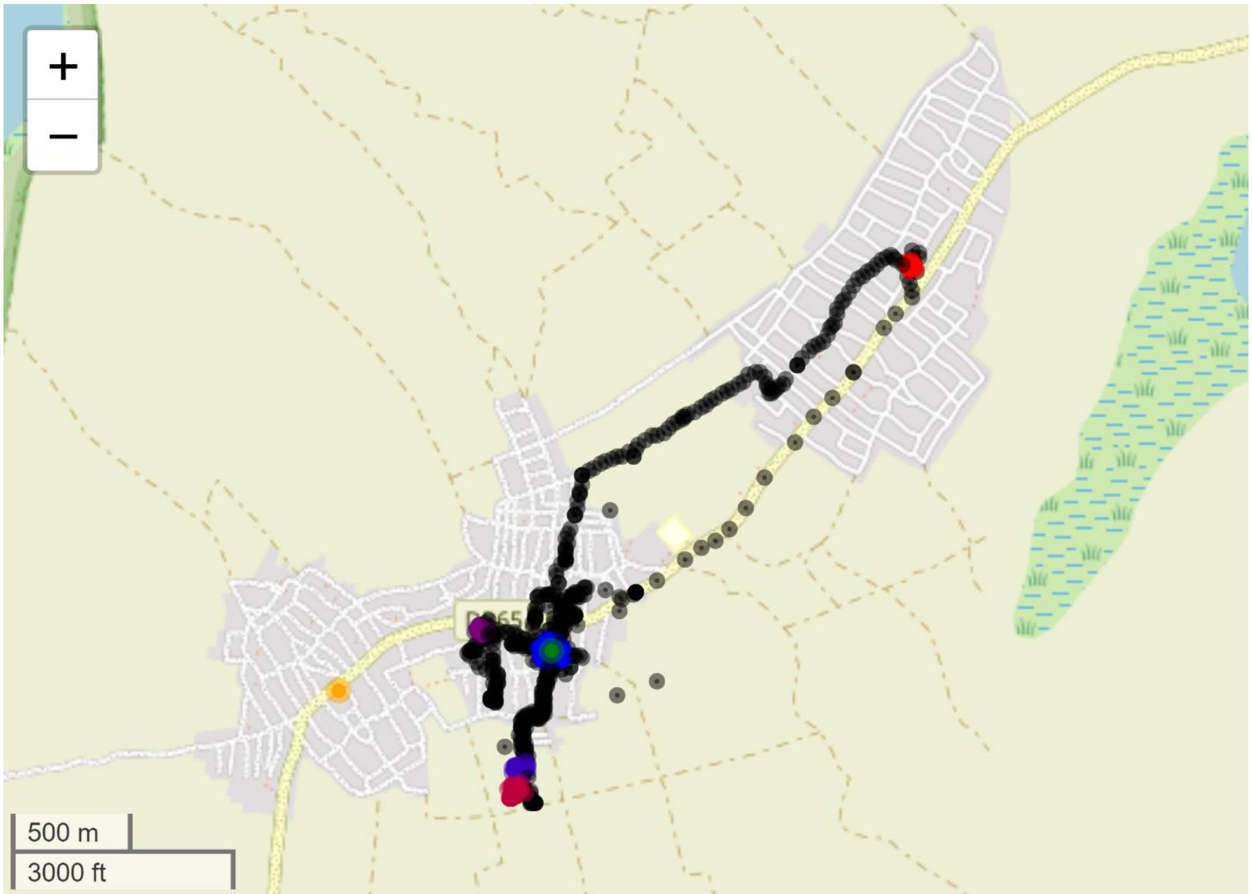

Figure 3.1: Example of a Participant's Clustering Map. The green dot represents the preestablished coordinates of this participant's home, and the orange dot represents the location of the SHEAR study office. All the other dots are GPS coordinates recorded for this participant's sampling period. Black dots indicate locations not part of any cluster (i.e. the participant spent less than 30 minutes within a 20 m radius of these points), and colored dots show the different clusters that were established.

3.2.5 Microenvironmental Assignment

The field staff provided GPS coordinates along with a brief description for various gathering spots within the study communities. From these initial points polygons were drawn around the boundaries of the gathering spots using Google Earth, then converted to .shp files. For the "field" microenvironment, 7 separate polygons were originally created to distinguish the different fields people worked in, but due to similarities in exposures among the fields we decided to agglomerate them all into one general “field” microenvironment (this same procedure was applied to churches, schools, and restaurants). These .shp files were input into R creating a geocoded boundary matrix that when combined with the clustering analysis outputs described above, helped to assign each unique 30-second GPS observation to one of the following microenvironments: home, near home, field, school, church, restaurant, fishing, community center, in transit (within village), in transit (outside of village), other, and no-GPS.

To assign observations to the ‘home’ microenvironment, the participant’s cluster whose centroid had the minimum distance to the median GPS coordinates of one of the household members (typically the woman) was determined between the hours of 23:00 and 4:00 (it was assumed participants were home during this time). This was then stratified this further by assigning all points within this “home” cluster that were > 30 m away from the household centroid as “near home”, and the points closer than 30 m as “home”. GPS points that were part of a cluster but had more than half of their points outside any of the geocoded microenvironmental boundaries were assigned to the “other” microenvironment. Clusters with over half of their points within one of the geocoded microenvironment polygons were all assigned to that microenvironment, and points that were not assigned to any cluster, regardless of whether they were within one of the geocoded microenvironmental boundaries or not, were labeled either as “in transit (within village)” or “in transit (outside of village)” depending on whether the point was inside or outside of one of the two geocoded village boundaries. An exception was made for children within one of the two “school” polygons, all these points regardless of belonging to a cluster or not were assigned to the “school” microenvironment. Finally, all observations that did not have GPS recorded, or had their GPS coordinates removed during the GPS cleaning stage were assigned to the “no GPS” microenvironment, 8.6% of the 30-s observations.

3.2.6 Valid Sample Criteria

Three metrics were used to determine whether a participant's personal exposure sample was retained for analysis. The first was that logged real-time $PM_{2.5}$ data must have exceeded 36 hours. This threshold was determined by comparing the Spearman and Pearson correlations between samples' mean 48-hour $PM_{2.5}$ concentration and their respective mean 48 - n hour concentrations (where 'n' is the number of hours taken away from the end of the sample). The goal of this analysis was to find the shortest amount of sampling time that was still representative of full 48-hour exposures. Figure 3.2 depicts the results from this analysis.

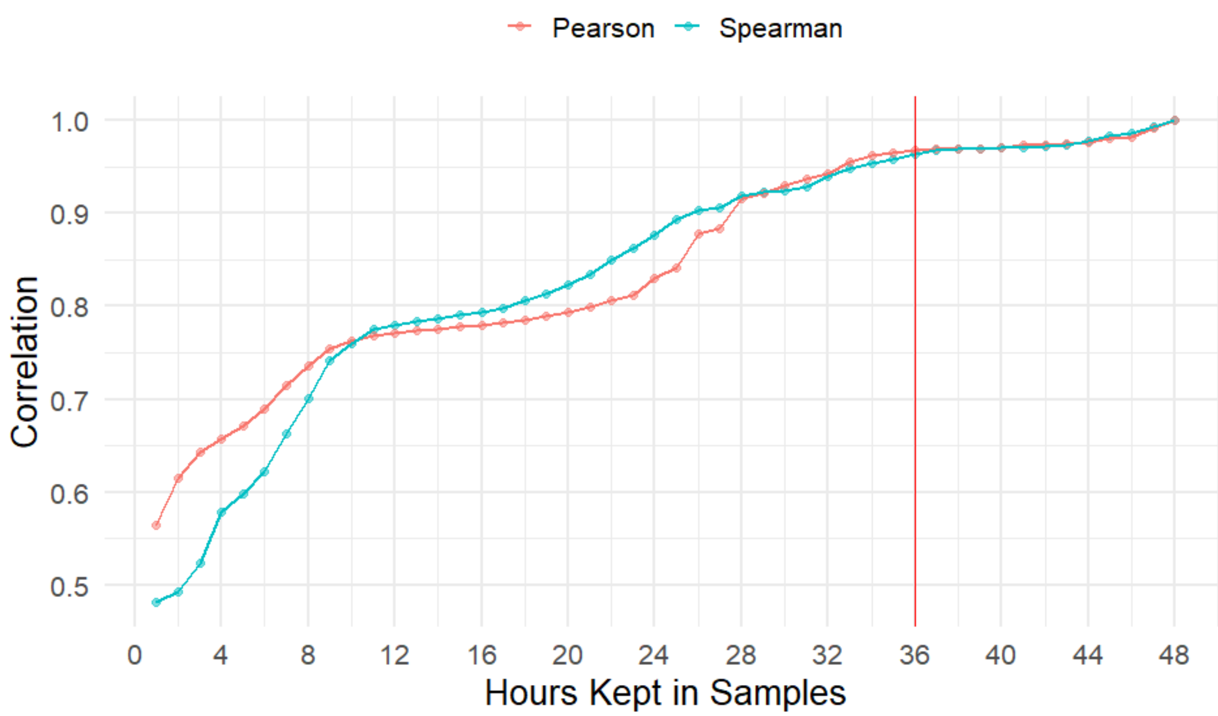

Figure 3.2: Correlation (r, ρ) Between 48-hour Sample Mean $PM_{2.5}$ Concentrations and Their Respective 48 - n Hour Sample Mean Concentrations.

With the 899 samples that had at least 48-hours of logged $PM_{2.5}$ concentration data, we initially found each one's mean 48-hour concentration. Then, each of these samples' mean 48 - n $PM_{2.5}$ concentration (where n represents lagged hours prior) was found, iteratively removing one hour at a time and calculating a new mean $PM_{2.5}$ concentration for each sample, eventually calculating the mean for only the first hour of each sample's runtime. Next, the Pearson (r) and Spearman (rho) correlations were determined between the means of the full 48-hour sample concentrations and their respective mean 48 - n hour concentrations. These correlations were plotted against the number of hours kept in the samples in Figure 3.2 to determine that 36 hours was a reasonable threshold time for a valid sample. Samples with at least 36 hours of data were representative of their full 48-hour average $PM_{2.5}$ concentrations to 92% confidence. A total of 139 personal exposure samples were removed from the analysis for having less than 36 hours of real-time $PM_{2.5}$ data.

Samples were also removed from the analysis if the acceleration threshold was not achieved for over 75% of a sample's 15-minute windows during waking hours (the acceleration threshold for a 15-minute window was previously described in section *2.5.4*). The baseline data illustrated a high rate of compliance with little variation among demographics and ages (Figure 3.3). Based on this criterion, 46 total samples (~4%) were removed from the analysis due to insufficient wearing compliance. An hourly breakdown of compliance among the three demographic groups is provided in Appendix B1. The 20% of samples that did not have any acceleration data recorded for analysis were retained. We assumed there was no systematic reason for a difference in UPAS wearing compliance among samples with/without working accelerometers, therefore it was inferred that ~4% of the 296 samples without working accelerometers likely had insufficient wearing compliance, or about 12 samples. This means about 0.9% of samples used in our analysis may report data that does not accurately reflect the participant's true breathing zone exposures.

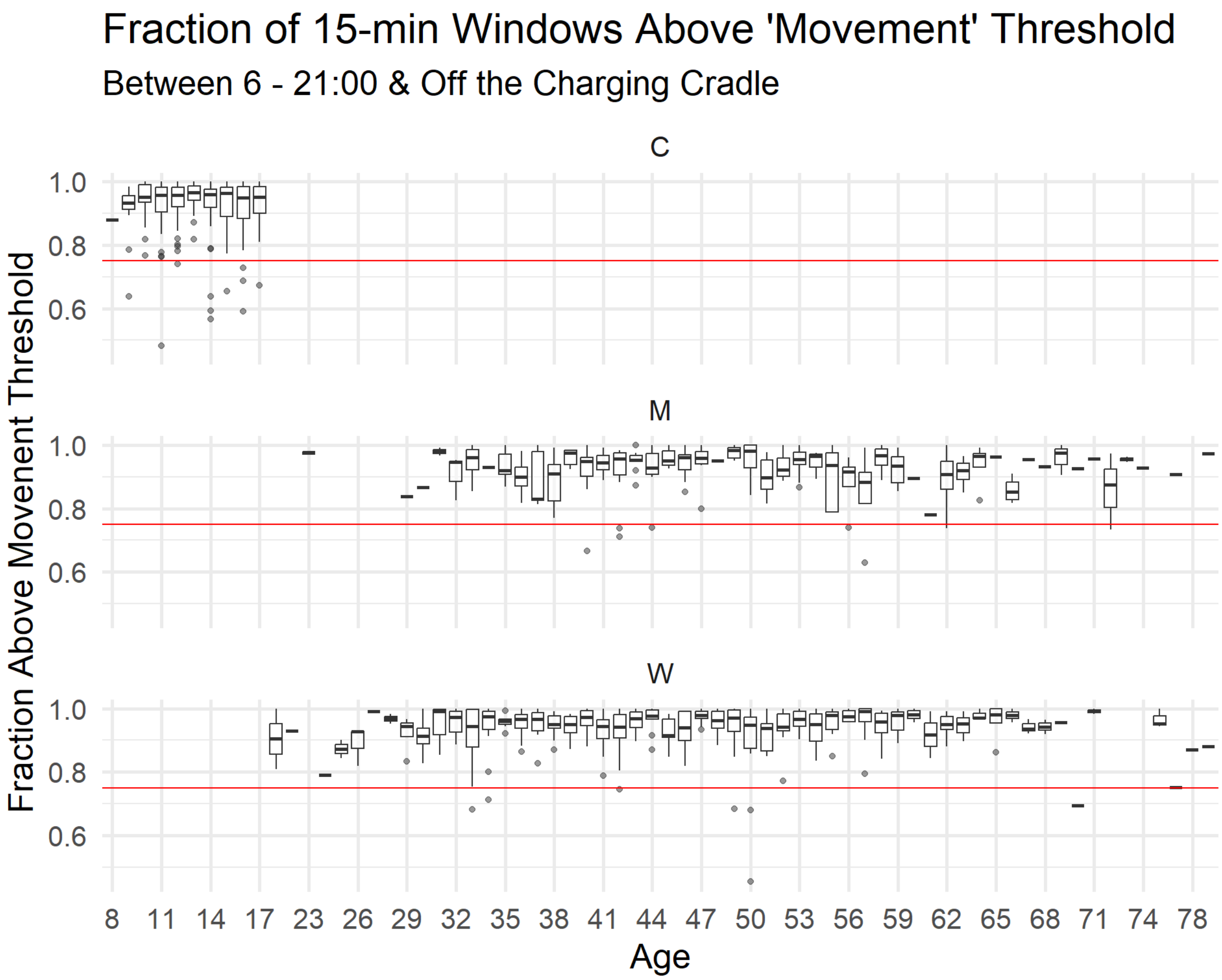

Figure 3.3: UPAS Wearing Compliance. The distributions of the fraction of samples' 15-minute windows where the UPAS accelerometer measured standard deviations above background levels (6 mG) during waking hours (6:00 -21:00) off the charging cradle vs age and demographic. The red line shows the 75% compliance cutoff threshold used for sample retention.

The final criteria used to remove samples from the analysis was if they had gravimetric to real-time $PM_{2.5}$ concentration ratios beyond +/- 2 geometric standard deviations from the sample population's geometric mean (as described in section *2.5.6*). This criterion removed an additional 53 samples from the baseline analysis (Appendix B2).

3.3 Results and Discussion

3.3.1 Sample Culling

This analysis included a total of 1,280 valid samples. In total 199 samples were removed from an initial 1,479, providing a final sample size of 1,280 valid samples. Table 3.1 illustrates how many samples were removed based on the different validation criteria for each demographic. From the initial 606 households with sampled data, 579 were retained. In total 304 samples from men, 495 from women, and 481 from children used in this baseline personal exposure analysis. 139 (9%) samples were flagged for inadequate runtime, 46 (3%) were flagged for poor wearing compliance, and 53 (3.5%) were flagged for having filter-to-sensor $PM_{2.5}$ correction ratios beyond 2 geometric standard deviations from the geometric sample mean (see section *3.2.6* for more details). Some samples were flagged for multiple validation criteria but were only removed once. Men, women, and children had similar percentages of valid samples, 89.4, 89.0, and 82.5%, respectively.

Table 3.1: Valid Sample Removal Criteria. Samples were removed from the analysis if flagged for not meeting one or more of the validation criteria. Some samples were flagged for multiple validation criteria but were only removed once.

Demographic	**Initial Samples Collected**	**Runtime < 36 hours**	**Poor User Wearing Compliance**	**Invalid Filter-to-Real-time Correction Ratio**	**Total Removed**	**Total Used**
Children	583	76	21	25	102	481
Women	556	41	14	20	61	495
Men	340	22	11	8	36	304
All	1,479	139	46	53	199	1,280
Households	606				27	579

3.3.2 Overall Personal $PM_{2.5}$ Exposures

Overall, children had the highest 48-hour time-averaged $PM_{2.5}$ exposures with a median concentration of 193 $\mu g \cdot m^{-3}$. Women had the second highest exposures with a median concentration of 174 $\mu g \cdot m^{-3}$, and men had the lowest exposures with a median of 94 $\mu g \cdot m^{-3}$ (Figure 3.4, Table 3.2). These exposure levels greatly exceeded the WHO annual average interim 1 target (IT-1) of 35 $\mu g \cdot m^{-3}$.[73] This guideline was chosen as an optimistic milestone for this study population since the median daily average ambient $PM_{2.5}$ concentration observed during this baseline period was 23.0 $\mu g \cdot m^{-3}$. The mean ambient $PM_{2.5}$ concentration for these study villages was 27.0 $\mu g \cdot m^{-3}$, which falls below the WHO IT-1 target of 35 $\mu g \cdot m^{-3}$; however personal exposures greatly exceeded that target. This finding demonstrates that even regions with low ambient $PM_{2.5}$ levels can still have population exposures far exceeding health-based guidelines. A Wilcoxon signed rank test suggested the difference between children's and women's exposures within the household was distinct from 0 $\mu g \cdot m^{-3}$ (CI: -46.6, -19.0 $\mu g \cdot m^{-3}$). The same test suggested children's exposures were even more distinct from the men's within their household (CI: -103.8, -71.5 $\mu g \cdot m^{-3}$). Descriptive statistics for the 48-hour personal $PM_{2.5}$ exposure data are provided in Table 3.2.

Table 3.2. Descriptive statistics for 48-hour average $PM_{2.5}$ concentrations ($\mu g \cdot m^{-3}$) as a function of familial demographics. IQR = Inter-quartile range.

		48-hour Sample Average $PM_{2.5}$ Concentration ($\mu g \cdot m^{-3}$)							
	Sample Size (n)	**Mean**	**Standard Deviation**	**Geometric Mean**	**Geometric SD[a]**	**Median**	**Min**	**Max**	**IQR**
Children	481	248	177	199	1.96	193	31	1,235	214
Women	495	227	233	174	2.01	174	28	3,551	173
Men	304	127	101	98	2.06	94	16	739	104
All	1,280	212	194	160	2.11	158	16	3,551	170

(a) Geometric standard deviation is dimensionless.

Linear mixed modeling (n = 1280 participants in 579 unique households) accounting for household as a random effect suggests children were exposed to 14% (CI: 6, 22%) higher $PM_{2.5}$ concentrations than women in their household and 100% (CI: 85, 117%) higher concentrations than the men (See Appendix B3 for details). All participant exposures were higher than the median ambient air concentration, 23.0 $\mu g{\cdot}m^{-3}$, indicating personal exposures were dominated by proximity to localized PM sources. The demographic exposure differences, along with ambient $PM_{2.5}$ concentrations, are illustrated in Figure 3.4.

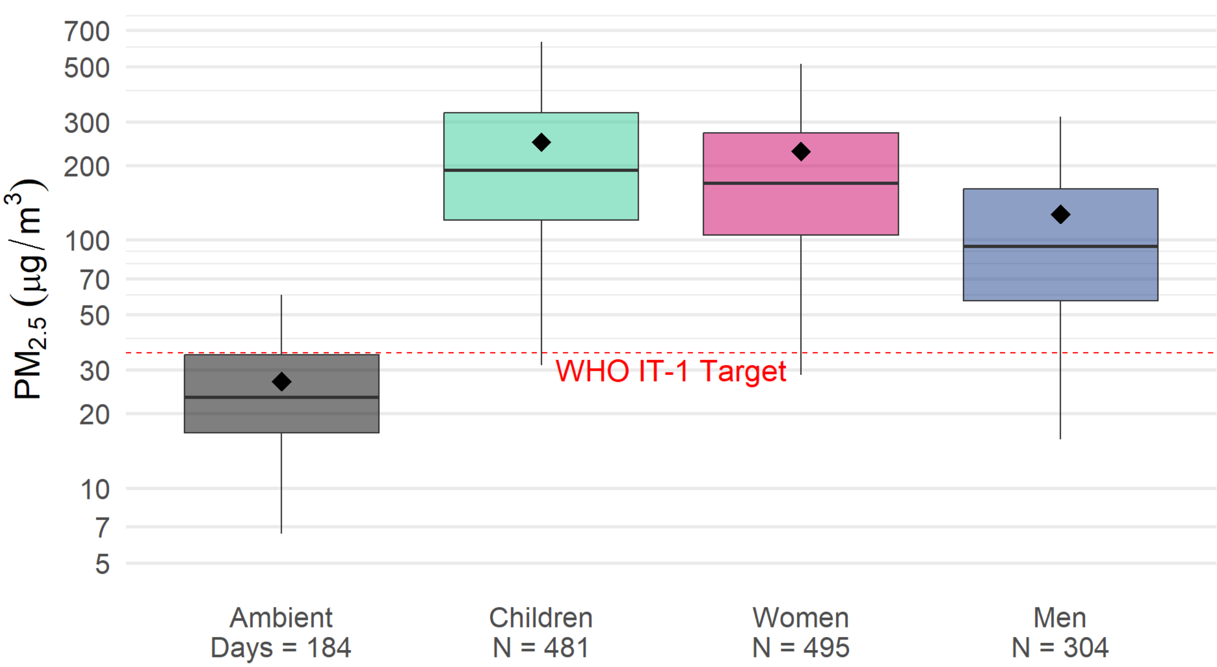

Figure 3.4: Boxplots represent the average (~48-hr for personal samples, and 24-hr for ambient) $PM_{2.5}$ concentration distribution among ambient air, and personal exposure samples of men, women, and children. The Y-axis is logscale. The ambient box depicts the distribution of all the daily average $PM_{2.5}$ concentrations recorded across all sampling locations within the same 15-month window when personal exposure sampling occurred. Center lines delineate the median; boxes represent the interquartile range, and whiskers represent the extent of observations within +/- 1.5·IQR. The red line is the WHO interim 1 target of 35 of $\mu g{\cdot}m^{-3}$. The black diamonds represent the means.

The finding that children had significantly higher $PM_{2.5}$ exposure levels than their mothers was unexpected, given prior reports of household air pollution exposures in

Africa.[12,31,33] Children are a particularly vulnerable demographic to the effects of air pollution due to their developing respiratory and immune systems; yet, their primary guardians (often assumed to be their mother) are frequently used as a proxy for their exposure due to assumed similarities in daily activity patterns.[37,42] Based on participant survey responses, women did the majority of the household cooking tasks; 65% of women report being the "Primary Cook" and 39% report being "Both the primary cook and head of my household". Cooking was the only major source of $PM_{2.5}$ within the community (vehicular traffic and trash burning were infrequent), so it was notable that children had the highest levels of $PM_{2.5}$ exposure among the demographics. A prior study of personal $PM_{2.5}$ exposures in rural Africa reported that Ugandan women had 51% and 574% (60 and 151 $\mu g \cdot m^{-3}$) higher 24-hour average exposures than their female and male children respectively (aged 6 - 17 years old); Ethiopian women were shown to have 53% and 578% (71 and 175 $\mu g \cdot m^{-3}$) higher average exposures than female and male children respectively.[31]

The children's $PM_{2.5}$ exposures reported here were also higher than children from LMIC and LICs as reviewed by Lim et al. (2022). Children from our study had a median $PM_{2.5}$ exposure of 193 $\mu g \cdot m^{-3}$ compared to the 65 $\mu g \cdot m^{-3}$ reported for the groups of children from other LMICs and LICs (n = 15 studies).[12] Further, Lim et al. reported that all of the adult groups (n=26) from LMICs and LICs had median $PM_{2.5}$ exposures of 79.5 $\mu g \cdot m^{-3}$. These adults groups were not linked to the children groups (different samples from different studies), but across all the studies reviewed, the children had lower median $PM_{2.5}$ exposures.[12] There are several potential reasons for the relatively higher exposures found in the SHEAR study, including the differences between rural/urban environments and artifacts of the PM measurement techniques. Our results have implications for mortality and morbidity estimates from household air pollution for low- and middle-income countries around the world.[1,7,43,74–76] The elevated exposure ratio experienced by children relative to women contradicts common assumptions made by the global burden of disease study and highlights the need for additional research examining demographic variation in personal $PM_{2.5}$ exposure.[43]

For the SHEAR baseline data, personal $PM_{2.5}$ exposures between male and female children were not significantly different. Linear mixed modeling suggested that boys had only 3% higher $PM_{2.5}$ exposures (CI: -10 – 16%) than girls (see Appendix B4 for details) and that sex was only a significant predictor of exposure differences for adults (See Figure 3.4 and Table 3.2). Linear mixed modeling also suggested that along with gender, neither age nor height was a significant predictor in $PM_{2.5}$ exposures among children (see Appendix B5 for details).

To examine why this analysis found that children had the highest exposures, the personal $PM_{2.5}$ exposure concentrations were stratified by hour of the day (Figure 3.5). Diurnal exposure patterns revealed that participants tended to receive their highest exposures between the hours of 18:00 and 20:00. During the daily peak at 19:00, children's exposures diverged substantially from men's and women's, with the children exposed to 47% (CI: 33 – 61%) higher concentrations than women and 100% (CI: 79 – 122%) higher than men when accounting for household as a random effect (See Appendix B6 for model details). This diurnal peak (which coincides with observed dinner times) suggests that the majority of personal $PM_{2.5}$ exposures for this population occur during evening meal preparation. These data suggest that children likely participate in cooking or fire maintenance tasks and may also be near the fire as a source of lighting to complete homework during this time window.[23] These notions were supported by observational reports from project field staff.

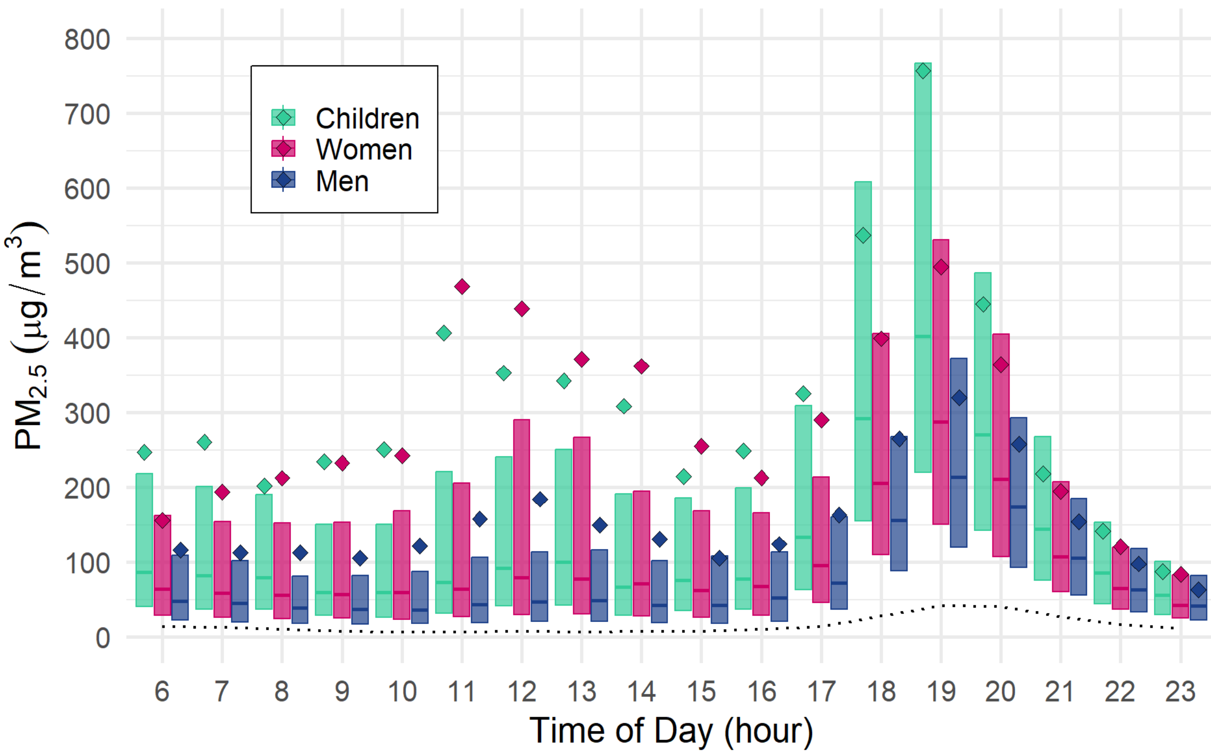

Figure 3.5: Boxplots display the diurnal variation in $PM_{2.5}$ concentrations for personal exposures among men, women, and children. The black dotted line shows the median ambient air $PM_{2.5}$ concentration. Hours 0 – 5 have been removed from plot due to similarity to other early morning hours. Diamonds represent arithmetic means of $PM_{2.5}$ exposure for each demographic-hour.

3.3.3 Spatiotemporal Analysis

Spatiotemporal exposure apportionment assigned 91.4% of all recorded observations to a classified microenvironment, with the remaining 8.6% labeled as 'no GPS' observations. Men, women, and children had an equal distribution of time apportioned to microenvironments, 90.0, 92.0, and 91.7%, respectively. Hourly microenvironmental apportionment results are depicted in Figure 3.6, stratified by demographic group. This figure indicates the average percentage of time that participants spent in each microenvironment, for each hour of the day.

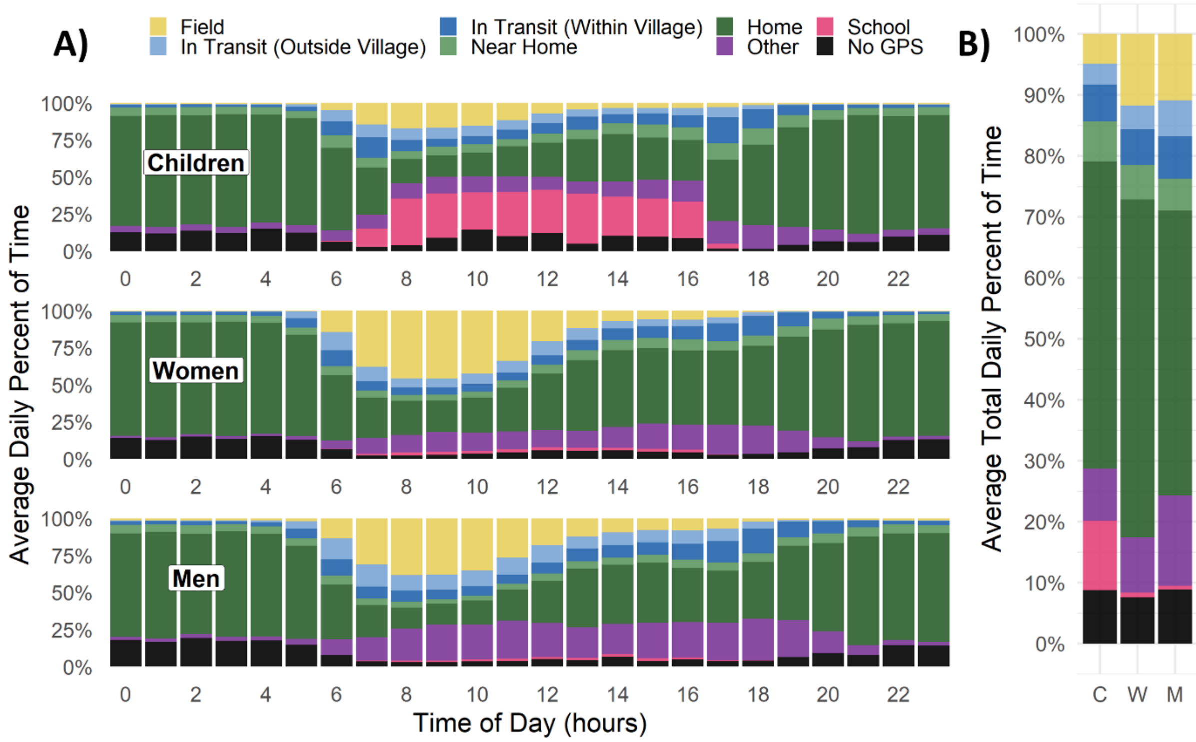

Figure 3.6: (A) Spatiotemporal distribution plot showing average percent of time spent in various microenvironments at each hour of the day among the different demographic groups. (B) The microenvironmental make up of full 48-hour sample averages among demographics. These data are only representative of weekday activity patterns, as samples were not collected on the weekend.

During the peak $PM_{2.5}$ exposure hour (19:00), children were at home 67% of the time, women 63%, and men 50%. Men spent a lot of time in "other" environments throughout the day with some staying in these locations until 20:00, after which most returned home. Children did not spend as much time working in the fields compared to men and women. Instead, children were more likely to be in school during the middle of the day, typically returning home around 17:00. Adults, men in particular, traveled outside the village during morning hours, with the average microenvironmental apportionment for 'In Transit (Outside Village)' peaking around 8:00. Similarly, the average 'Field' microenvironment apportionment peaked in the morning for both men and women, around 8:00. These activity patterns suggest adults often left the home in the morning to run errands and/or do agricultural work before returning home, or for some men, to 'other' environments around mid-day.

Shown in Figure 3.7 are average diurnal distributions of $PM_{2.5}$ exposure by microenvironment, depicting the timing, location, and magnitude of $PM_{2.5}$ exposures for the three demographic groups. In this figure, overall bar heights represent hourly average exposure across participant groups, with the proportion of exposure by microenvironment indicated by color.

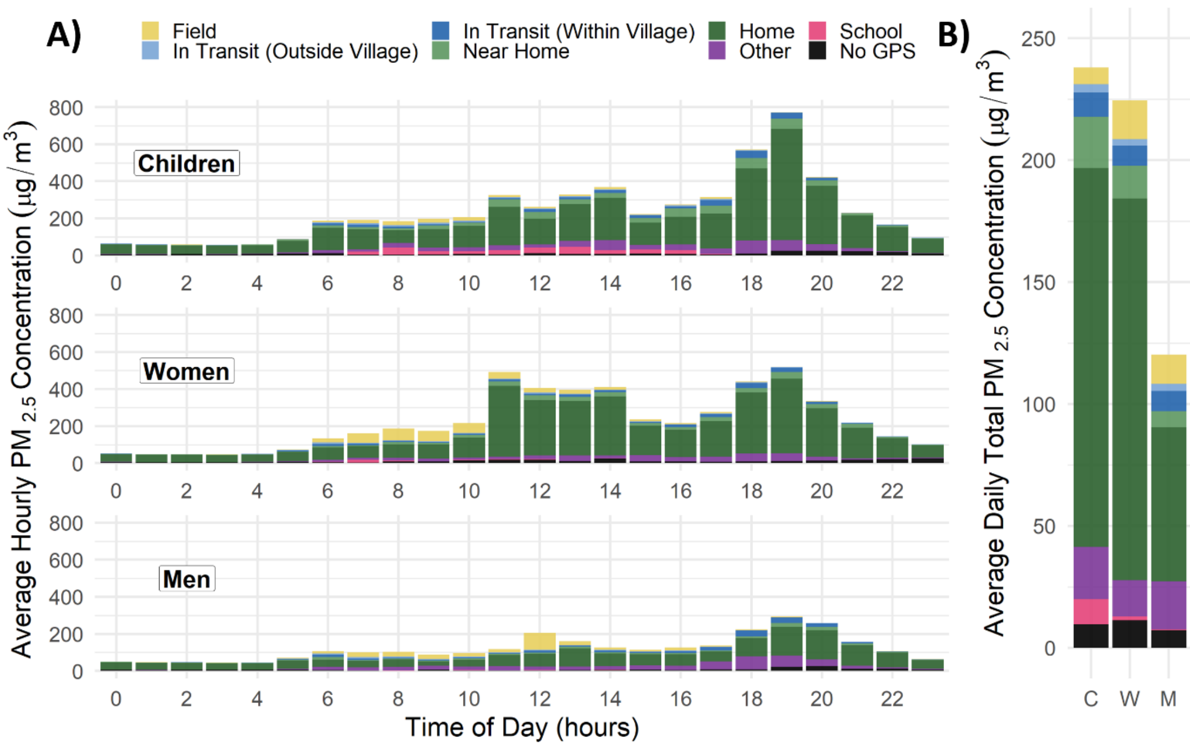

Figure 3.7: (A) Spatiotemporal distribution plot showing, on average, when and where different demographics received proportions of their daily $PM_{2.5}$ exposures. (B) The full 48-hour sample average $PM_{2.5}$ exposure variation between demographics among microenvironments. These data are only representative of weekday activity patterns, as participants were not sampled during the weekend.

Participants received the majority of their daily $PM_{2.5}$ exposure at home, suggesting that localized cookstove emissions within the home were the largest contributing source for this population's $PM_{2.5}$ exposures (see Appendix B7 for a zoomed in version highlighting non-home environments). Adult women spent an average of 58% of their time at home, compared with men at 50%, and children at 53%. Women were also the only demographic likely to receive a large portion of their $PM_{2.5}$ exposure around 11:00, suggesting some women performed a mid-day cooking event independent of men and children, who were most likely at school or in “other” environments at this time. However, when children were home in the evenings, they experienced the highest overall increase in $PM_{2.5}$ exposure among all the demographics, with exposures 47% (CI: 33 – 61%) higher than the woman and 100% (CI: 79 – 122%) higher than the man in their home at 19:00. Anecdotal evidence from our field staff suggests that children are often tasked with starting and maintaining cooking fires when they are home and available, while the women do most of the food preparation and cooking. Children are also known to use fire for lighting in the evenings while completing their homework.[23] These behaviors are a possible explanation for why children often have the highest in-home exposures, since the ignition and refueling steps are usually the highest polluting stages of working with fire.[77,78]

To corroborate observations from our field staff suggesting that children perform most fire maintenance tasks, the variation in women’s $PM_{2.5}$ exposures at different times of the day, depending on whether their child was present, were examined in Figure 2.3. Although only one child was monitored per household (and other children who did not participate in the study were unaccounted for in our exposure assessment), the results in Figure 3.8 suggest that women’s exposures to $PM_{2.5}$ may have been reduced when the monitored child was present at home during the 19:00 hour.

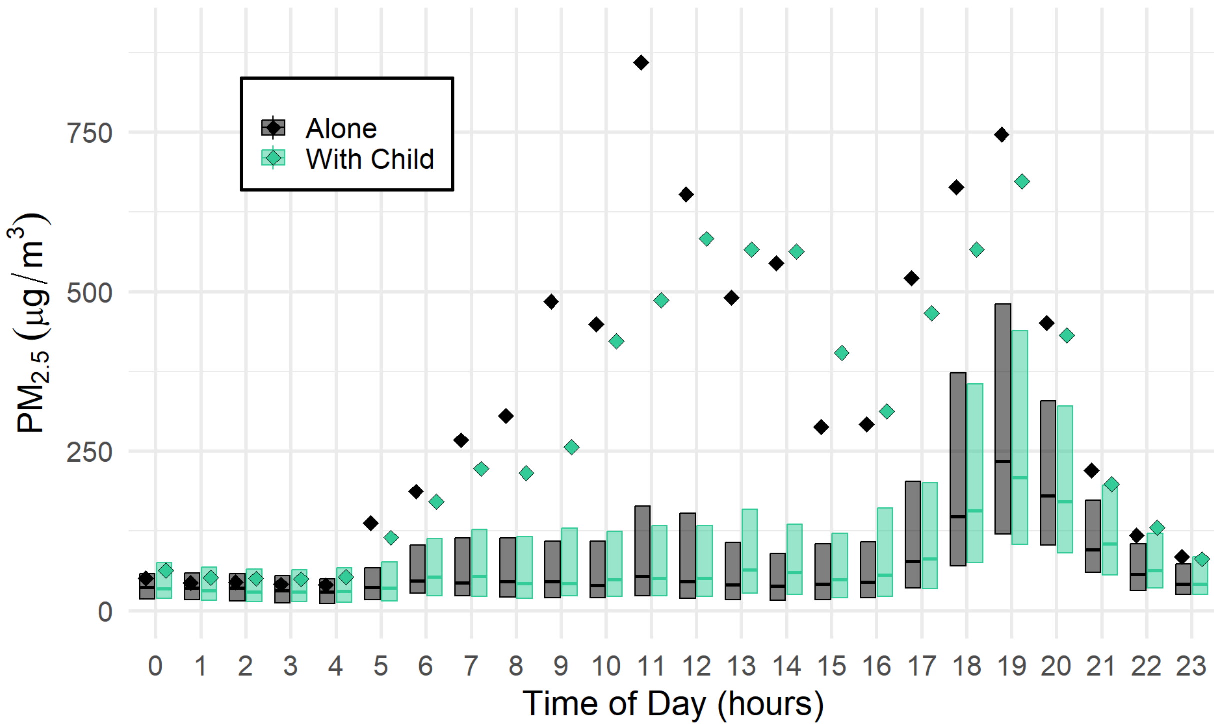

Figure 3.8: Boxplots and median connection lines showing how women's in-home personal exposures change throughout the day depending on whether a child was with them or not. Diamonds represent the means.

For most of the day, women's in-home exposures were unaffected by whether or not they had the child being sampled home with them. However, at 19:00, women who were home with the monitored child had exposures 4% (CI: 2 – 7%) lower than women who were 'alone' (see Appendix B8 for details). This provides additional evidence to suggest that many children do help with fire maintenance tasks, because having a child home with the woman in the evening, on average significantly lowered her $PM_{2.5}$ exposures. While this reported 4% difference is small, the mean number of children households in the study had between the ages of 5 and 17 was 2.3, of which only one was monitored. Therefore, it is likely that the woman's decrease in exposure would be even more significant if all the children were accounted for rather than just the one monitored child.

Within the home environment, men were exposed to 48.9% less $PM_{2.5}$ than women and 54.7% less than children (see Table 3.3), on average. This suggests a behavioral difference between men, women, and children within the home environment. Observational evidence from the field team alludes to men performing almost no meal preparation work compared to women and children, with quantitative evidence from the spatiotemporal analysis supporting this notion (Appendix B9). This analysis suggests clean cooking access may greatly reduce the PM exposure burden for women and children within this and similar rural communities throughout the world.

Table 3.3. Descriptive statistics for microenvironmental $PM_{2.5}$ exposure ($\mu g \cdot m^{-3}$)

	Demographic	**Time (days)**	**Mean**	**Median**	**Max**	**Min**	**IQR**
Home	Children	505	309	254	1,678	12	246
	Women	572	274	207	4,440	17	208
	Men	299	140	108	515	13	126
Near Home	Children	70	299	182	6,351	14	246
	Women	59	264	162	2,465	13	244
	Men	32	145	76	3,455	6	112
Fields	Children	37	134	65	733	2	143
	Women	86	123	55	1,452	1	98
	Men	52	97	31	3,031	2	61
Other	Children	81	222	120	3,076	3	201
	Women	86	149	91	1,789	2	141
	Men	86	138	93	2,402	3	123
School	Children	83	90	71	459	5	80
	Women	6	96	44	915	9	38
	Men	2	83	66	217	13	81
In Transit (Within Village)	Children	57	165	117	1,366	11	138
	Women	59	158	106	1,577	9	129
	Men	41	116	81	846	12	97
In Transit (Outside Village)	Children	29	106	63	2,269	1	76
	Women	31	95	44	3,353	2	74
	Men	29	59	38	851	3	56
No GPS	Children	77	187	75	10,902	5	110
	Women	79	224	75	23,454	0	144
	Men	57	86	54	685	2	84

3.3.4 Seasonal Effects

Seasonal cycles also played a role in determining individual's $PM_{2.5}$ exposures, with the dry seasons (June to August and December to April) on average leading to 30% (CI: 19 – 43%) higher personal exposure concentrations than the wet seasons (see Appendix B10 for details). Weather data collected by a nearby Rwandan meteorological weather station (NDEGO AWS6 Station, about 2 km from the SHEAR study site) suggested the study region received 7.9 times more rainfall during the wet season vs. the dry. This increased precipitation likely scrubbed much of the ambient $PM_{2.5}$ from the atmosphere, increased the humidity in the region, and in turn decreased the background $PM_{2.5}$ pollution levels. Therefore, the observed seasonal difference in personal exposure is likely due to several factors, such as dust suppression (from elevated humidity) and washout of $PM_{2.5}$ from rainfall during the wet season. Similar seasonal variations in ambient $PM_{2.5}$ levels have been reported previously for sub-Saharan Africa.[79–81]

Appendix B11 shows our reported differences in sample average $PM_{2.5}$ exposures among the demographics and between the seasons. It should also be noted that children had significantly lower exposures during schooling months than during their school-break months (July and August), with exposures 52% (CI: 44 – 60%) lower during their schooling months (see Appendix B12 for details). We want to clarify that seasonal effects did not impact the household-level analyses, since each family member from a household was sampled once during the same 48-hr period.

CHAPTER 4: THE EFFECT OF A WHOLE-HOUSEHOLD ENERGY INTERVENTION ON PERSONAL $PM_{2.5}$ EXPOSURE AMONG MEN, WOMEN AND CHILDREN IN RURAL RWANDA

4.1 Introduction

$PM_{2.5}$ exposure (particulate matter with an aerodynamic diameter less than 2.5 µm) is a leading cause of death and disease globally, with an estimated 7.8 million premature deaths and 231 million disability-adjusted life years (DALYs) lost globally in 2021.[1,2] Health outcomes attributed to $PM_{2.5}$ exposure include incidence and exacerbation of chronic obstructive pulmonary disease, asthma, ischemic heart disease, acute lower respiratory tract infections, stroke, and lung cancer, among others.[3–7] Black carbon (BC) a fractional component of $PM_{2.5}$ often associated with PM produced from combustion, has also been implicated in the contribution to many adverse health effects including stroke, cardiopulmonary morbidity, and premature mortality.[8–11]

In many part of the world, the majority of people's $PM_{2.5}$ exposures come from solid fuel (biomass) burning for daily cooking and heating needs.[14,15,73] Additionally, many of these same communities rely on kerosene burning lamps for lighting. This style of lighting has been shown to produce high concentrations of $PM_{2.5}$ on its own, however when combined with the emissions from biomass burning cookstoves, the health effects associated with household air pollution are exacerbated.[22–25] Liquefied petroleum gas (LPG) stoves have been identified as a clean alternative to traditional biomass burning cookstoves, producing much lower $PM_{2.5}$ and BC emissions than their traditional, and improved-biomass-burning, counterparts in both in laboratory and field environments.[21,82–85] Previous studies have shown LPG interventions can result in significant reductions in personal $PM_{2.5}$ and BC exposures, however these studies were limited in only focusing on female adults in their populations, and only addressed emissions associated with traditional cooking (not whole-household energy).[27–30,86] The reason for this focus is because women are the primary cooks for the vast majority of homes in these regions and are therefore assumed to be at greatest risk for health complications attributed to household air pollution exposure.

However, results from the baseline phase of the SHEAR study (Chapter 3) indicate that the children in this population had 14% (CI: 6, 22%) higher $PM_{2.5}$ exposures than their mothers and 100% (CI: 85, 117%) higher than their fathers. This is concerning because children are a particularly vulnerable demographic to the adverse health effects of air pollution due to their heightened breathing rate, developing respiratory system, and immature immune system.[37–41] Children's personal exposures are often assumed to be identical to their primary guardian (usually their mother) due to perceived similarity in daily activities and exposure patterns.[42] However, spatiotemporal analysis of the baseline data, along with anecdotal evidence from the field staff suggest that children within this community likely participate in cooking or fire maintenance tasks and may also be near the cookstove fire in the evening as a source of lighting to complete homework.

Kerosene lamps are often overlooked due to their relatively smaller emissions factors compared to biomass burning cookstoves, but self-reported use of kerosene lamps in the SHEAR pilot study was associated with an 80% increase in personal $PM_{2.5}$ exposures ($p<0.001$). Integrated exposure curves have been developed for describing the non-linear relationships between personal $PM_{2.5}$ exposures and various associated health risks (COPD, ischemic heart disease, etc.).[6] These curves indicate that the reductions in personal $PM_{2.5}$ exposures associated with LPG interventions may be enough to mitigate some health risks; however, it is unclear whether they are enough to mitigate the risk for more sensitive conditions, like stroke incidence. Therefore addressing PM emissions from all forms of household energy has been proposed as a way to lower personal exposures to a level that mitigates all associated health risks.[23]

There have been several notable interventions studies reporting personal $PM_{2.5}$ exposure reductions due to an LPG intervention, such as HAPIN (an LPG intervention study taking place across 4 countries with one arm in rural Rwanda) which reported $PM_{2.5}$ exposure reductions among 3,195 pregnant women and 418 woman aged 40 – 79, and GRAPHS (a clean cooking intervention study taking place in rural Ghana with an LPG arm) which reported exposure reductions for 361 pregnant women.[27,84,86] However, to the best of our knowledge there have been no studies to date investigating personal $PM_{2.5}$ exposure reductions resulting from a whole-household energy intervention among men, women, and children within a biomass burning community. The novel aspect of the SHEAR study is its approach to personal PM exposure reductions from a whole-household energy perspective, and its monitoring of men and children along with women within the households.

In this chapter an intent-to-treat (ITT) analysis is used to evaluate the impact of a fully subsidized whole-household energy intervention on the personal $PM_{2.5}$ and BC exposures among men, women, and children within a rural sub-Saharan African community that relied on traditional forms of household energy (biomass fuel for cooking and kerosene fuel for lighting) prior to the study intervention. Using linear mixed effect models, the variation in exposure reductions between men, women and children are examined at both the household and community levels.

4.2 Methods

4.2.1 Study Overview

The SHEAR project (Sustainable Household Energy Adoption in Rwanda) is a 3-year randomized control clean household energy intervention trial (2022-2025; US ID: NCT05668624) located in the communities of Karambi and Isangano within the Eastern Province of Rwanda (see Figure 2.1 for a map of the study region). The villages were chosen because they will not be receiving distributed electricity during the study period (there is a plan to connect them to the national grid eventually) and traditional energy sources for cooking and lighting were used nearly universally amongst the households in the region, prior to the energy intervention. These villages typify rural sub-Saharan African subsistence farming communities with limited resources and virtually no access to modern forms of household energy (e.g., distributed forms of electricity or natural gas). The SHEAR study recruited one man, one woman, and one child from 624 households within the villages tracking their $PM_{2.5}$ exposures and health measures over the course of a whole-household energy intervention that replaced solid fuel combustion with liquefied petroleum gas (LPG) and kerosene lamps with solar-based electric lighting.

Households are visited up to seven times over the course of the study for: responding to surveys, collecting data on their health metrics, and participating in personal $PM_{2.5}$ exposure sampling sessions. After the first visit (when baseline health metrics and $PM_{2.5}$ exposure estimates were collected), households were randomized into the 3 arms of the study. The full subsidy arm consisting of 248 homes who received LPG and solar electricity free of charge, the random subsidy arm consisting of 141 homes that had to pay for LPG and solar electricity at various discounted rates, and the control arm consisting of 235 homes who did not receive any clean energy for the duration of the study. For randomization, participants drew pieces of paper out of an envelope indicating which study arm they would be a part of for the duration of the 3-year study. Blinding was not possible for the households, field staff, or the researchers due to the nature of the study (i.e. participants would know if they were in the full subsidy arm because they would receive LPG/solar electricity for free). No household received any clean energy technology at the first visit, used to establish participants' baseline health measures and PM exposure levels under normal conditions.

Results reported here are presented as an ITT analysis representing the personal $PM_{2.5}$ and BC exposure changes from the baseline and follow-up (intervention) visits for the full subsidy (treatment) and control arms of the SHEAR study. Since the study is still ongoing as of the writing of this report, only data collected up to visit 5 will be reported. The baseline phase of the study lasted ~16 months from November 2022 through March 2024 while the intervention phase (up to visit 5) lasted ~17 months, from December 2023 through May 2025. Initially, a total of 651 households were consented into SHEAR with the following inclusion criteria: (1) located in the study area of Isangano and Karambi; (2) had an adult male and female, or a single adult, head of household over 18 years, and at least one child 8 to 17 years of age; (3) non-smoking; (4) primarily used an open fire or wood/charcoal stove; (5) did not do any commercial cooking; (6) were not currently pregnant (women); and (7) did not plan to move within the next 3 years. Participants provided informed consent approved by the Rwanda National Ethics Committee (# 00001497) and by the Institutional Review Board at Colorado State University (IRB # 3946). Additional details on the SHEAR study setting, experimental design, enrollment criteria eligibility criteria, and household characteristics are discussed in sections *2.1* through *2.4*.

4.2.2 Study Visits

Home visits for $PM_{2.5}$ monitor deployments, health measures, in-field filter handling, and participant surveys were conducted by trained local staff. Participants were visited on a weekday up to seven times over the study period. Weekends and holidays were excluded due to field staff availability and to avoid potential unusual cooking practices. Personal $PM_{2.5}$ exposure monitoring was conducted for everyone on visits 1 (baseline) and 7. For visits 3, 4, and 5 participants conducted personal exposure monitoring on two out of the three visits. No personal PM exposure monitoring took place on visits 2 or 6.

4.2.3 LPG Distribution and Solar Electricity

Participants in the full subsidy (treatment) arm received LPG equipment following their randomization assignment after the first visit. The SHEAR field team installed the LPG stoves, fuel tanks, and wooden tables (to support the stove) at each home. The primary cook of the household received training on how to operate the LPG stove safely. Posters were also given to participants with visual and written instructions to provide additional safety, and cooking techniques. Through the course of the study, the SHEAR field team provided LPG tank refills for households whenever they scheduled service by contacting a SHEAR team member at the local study office, or over the phone. To reduce the risk of households completely running out of fuel, two 12 kg LPG cylinders were provided to each household during LPG installation and participants were instructed to request a refill whenever the first tank had been emptied. During the refill visits, tank weights were recorded to document LPG usage.

Participants in the treatment group, who were not already receiving Solar Home Systems from the Rwandan government, were connected to micro solar grids. Mesh Power established and maintained the microgrids used in the SHEAR study. Solar panels were installed at a host household, and power was distributed over cables to neighboring households. Households connected to the grid received energy for lighting and phone charging. These treatment group households received unlimited lighting and charging for the duration of the study while control group homes did not receive any additional solar electricity.

4.2.4 Personal $PM_{2.5}$ Exposure Monitoring

Personal $PM_{2.5}$ exposure sampling consisted of wearing a UPAS V2 Plus (Ultrasonic Personal Aerosol Sampler; Access Sensor Technologies, Fort Collins CO) in the breathing zone for a continuous 48-hour period, during which participants went about their daily routines.[48] The UPAS is a wearable air quality monitor that uses a silent piezoelectric pump to draw air at 1 $L \cdot min^{-1}$ through a 2.5 µm size-selective cyclone inlet and onto a 37 mm PTFE sampling filter (PT37 MTL LLC, Minneapolis, MN).[57] A parallel air stream passes through a light-scattering sensor (SPS30, Sensirion AG Stäfa, Switzerland) to estimate $PM_{2.5}$ concentration at 30-second intervals.[58] The UPAS V2 Plus also records GPS, accelerometry, air temperature, relative humidity, and atmospheric pressure data at the same 30-second intervals. Air sampling filters were pre- and post-weighed in triplicate inside a climate controlled environment (temperature: 20–23 °C; relative humidity: 30–40%) via an automated robotic process at Colorado State University, and shipped to and from the field via air freight on a bi-monthly basis.[61] Filters were stored in an on-site freezer (-20 °C) after sample collection between the bi-monthly air freight shipments. Post-sampling filters were stored in a -80 °C freezer once received by CSU before equilibration in the climate-controlled weighing chamber prior to gravimetric analysis. Filter field blanks were collected at the beginning of each sampling day and used to account for potential measurement artifacts encountered during shipping and handling.

Participants were asked to wear the UPAS on their chest during waking hours, via a custom harness (Figure 2.3) produced by a local tailor. To obtain a continuous 48-hour sample, a small battery-powered charging station was provided to each participant to recharge their UPAS overnight (Figure 2.4). Participants were instructed to keep the UPAS and charging station as close to their breathing zone as feasible while they slept (see sections *2.5.2* and *2.5.3* for additional details). Participants could also remove the UPAS and keep it nearby when bathing or using the restroom. Device wearing compliance was assessed by UPAS accelerometry data, evaluated between the hours of 6:00 and 21:00 (see section *2.5.4* for more details). The data presented in this chapter are from households assigned to either the control or full subsidy (treatment) arms during the baseline (visit 1) and intervention (visits 3, 4, and 5) phases of the SHEAR study. Baseline measures each represent a single 48-hr measurement (n=1,006 samples with no repeated measures). Intervention measures can have repeated samples from a participant, since each individual was scheduled for 2 separate PM exposure samples between visit 3 and visit 5 (n = 1,198 total intervention PM samples collected with an average of 1.38 repeated measures per participant). All $PM_{2.5}$ estimates used in this analysis were corrected using the gravimetric correction ratios described in section *2.5.6*.

4.2.5 Black Carbon Measurements

Black Carbon filter loadings were estimated by measuring the attenuation of 880 nm light passing through the filter using an optical transmissometer.[61] Attenuation measurements were performed for every filter—both field blanks and sample filters—before and after sampling. These measurements were conducted as part of the same robotic process used for gravimetric weighing. The attenuation system consisted of a tungsten halogen light source (HL-2000-LL, OceanOptics, Cincinnati, OH, USA) and a wide-band spectrometer (FLAME-S-VIS-NIR, OceanOptics, Cincinnati, OH, USA), connected via fiber-optic cables. Light from the source was directed through the filter, and the transmitted spectrum was recorded by the spectrometer across the visible to near-infrared range. 48-hour sample average BC concentration were calculated in a four-step process:

1. ***Blank Correction***. Net attenuation at 880 nm was calculated for each filter as the difference between pre- and post- sampling values. To account for handling and background artifacts, the monthly average net attenuation from field blank filters (SD: 1.62) was subtracted from each sample. If a monthly average blank attenuation value was not available, the study average was used (8 out of 27 months, Appendix C1).
2. ***LOD Adjustment***. A limit of detection (LOD) value was calculated monthly using the field blank filter attenuations, via an analogous process as that described for the gravimetric mass in section *2.5.6*. Attenuations below the LOD were replaced by $\frac{LOD}{\sqrt{2}}$ as prescribed by Hewett and Ganser 2007.[62] A timeseries plot of calculated attenuation LOD values by month is provided in Appendix C2.
3. ***Conversion to BC Mass***. Background-corrected, LOD-adjusted attenuation values were converted to surface mass concentrations ($\mu g \cdot cm^{-2}$) using a mass absorption cross-section (MAC) of 9 $m^2 \cdot g^{-1}$ and then to total BC per filter (μg) using the effective sampling area of the filter (7.55 cm^2), following Presler-Jur et al. 2017.[87,88]
4. ***Conversion to Air Concentration.*** Surface loadings were then converted to 48-hour sample average BC concentrations in air ($\mu g \cdot m^{-3}$) using the volume of air passed through the filter during the sampling process.

4.2.6 Valid Sample Criteria

Three metrics were used to determine whether a participant's personal exposure sample was retained for analysis. The first was that logged real-time $PM_{2.5}$ data must have exceeded 30 hours. This threshold was determined using the Spearman and Pearson correlations between baseline samples' mean 48-hour $PM_{2.5}$ concentration and their respective mean 48 - n hour concentrations (where 'n' is the number of hours taken away from the end of the sample) and adjusting for intervention visit's sample retention. Details of this analysis are available in section *3.2.6*. Samples were also removed from the analysis if the acceleration threshold was not achieved for over 70% of a sample's 15-minute windows during waking hours (previously described in section *2.5.4*). Baseline samples illustrated a higher rate of UPAS wearing compliance than the intervention samples (Figure 4.1). The 26% of samples that did not have any acceleration data recorded for analysis were retained based on the reasoning outlined in section *3.2.6*. The final criteria used to remove samples from our analysis was if they had gravimetric to real-time $PM_{2.5}$ concentration ratios beyond +/- 2 geometric standard deviations from the sample population's geometric mean (as described in section *2.5.6*). Appendix C3 provides a temporal distribution of the gravimetric to real-time $PM_{2.5}$ concentration ratios for all personal $PM_{2.5}$ exposure samples collected over the course of the study, with the associated cutoff thresholds.

Details on the statistical models used to determine effect magnitude and significance can be found in section *2.6*.

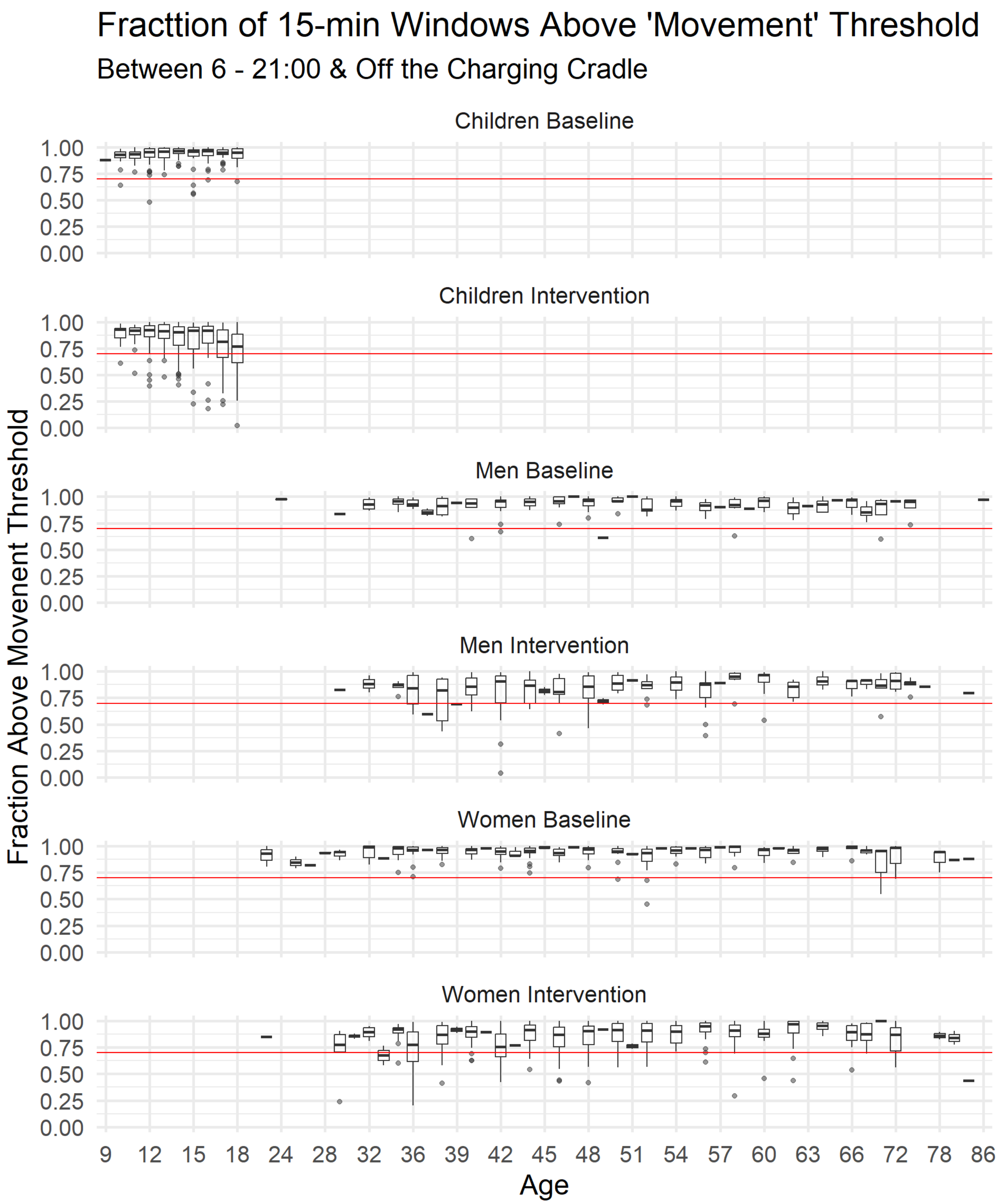

Figure 4.1: UPAS Wearing Compliance. The distributions of the fraction of samples' 15-minute windows where the UPAS accelerometer measured standard deviations above background levels (6 mG) during waking hours (6:00 -21:00) off the charging cradle vs age and demographic and sample set. The red line shows the 70% compliance cutoff threshold used for sample retention.

4.3 Results and Discussion

4.3.1 Sample Retention

Figure 4.2 depicts the participant follow-up flow diagram, illustrating the number of participants still enrolled in the study at visit checkpoints, and how many personal $PM_{2.5}$ exposure samples were collected during these visits. We should note many participants were not available during some visits, but also did not officially withdraw from the study, meaning they were "followed" for those visits but did not have PM data collected. Some participants also had to skip visits 5 and 6, jumping straight into visit 7 due to funding limits encountered by the study.

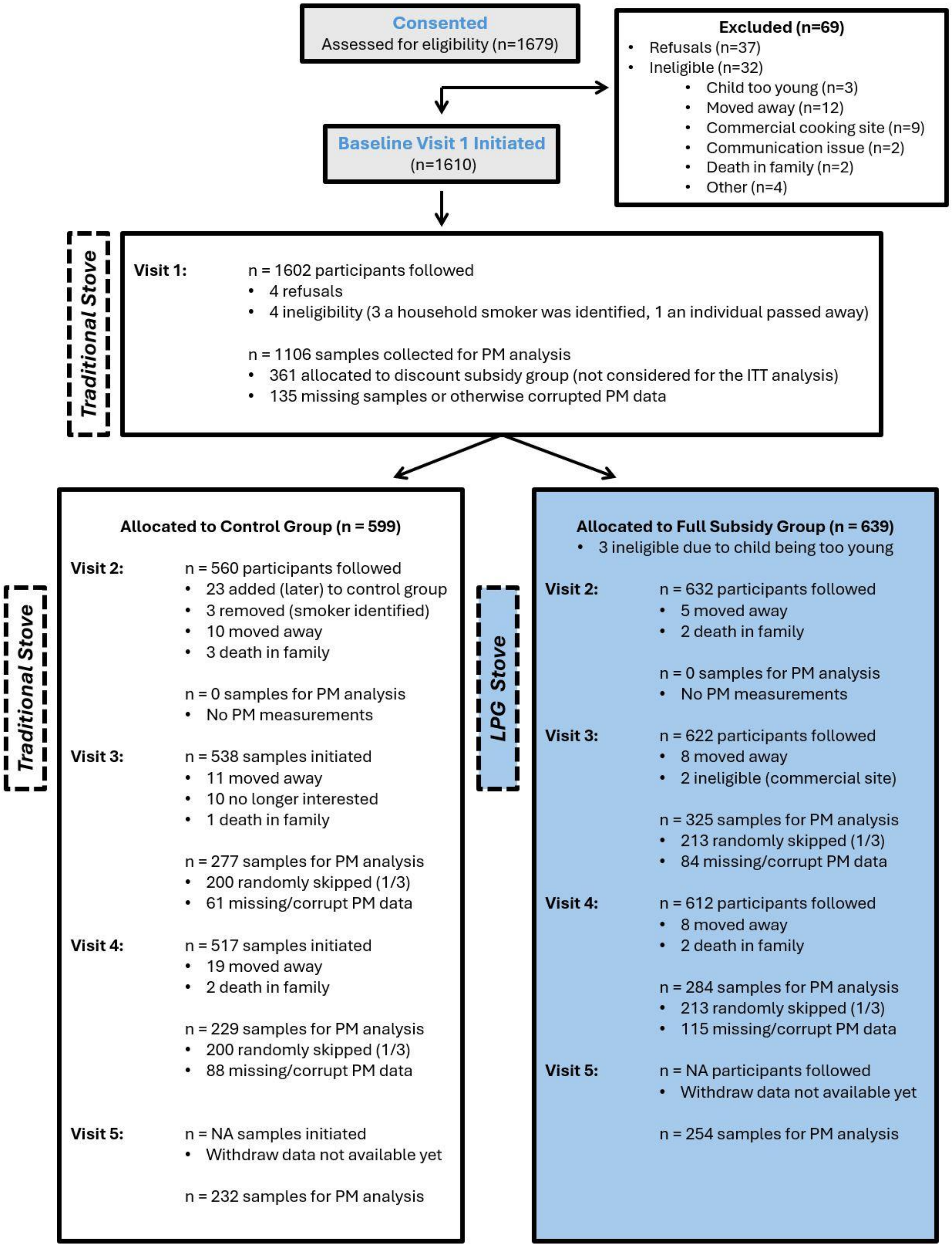

Figure 4.2: Participant follow-up flow diagram. Visit 7 samples have been excluded from our analysis due to ongoing data collection, visit 6 did not have personal exposure samples collected and visit 5 does not have all the withdraw data gathered yet.

A total of 2,707 PM personal exposure samples were collected from visits 1 to 5. In total 503 samples were removed due to invalid sampling criteria (described in section *4.2.6*) providing a final sample size of 2,204 valid samples. Table 4.1 illustrates how many samples were removed based on the different validation criteria for each demographic and each sample set. From the initial 651 households consented in SHEAR, 468 were retained for the ITT analysis (all random subsidy arm homes were removed). In total 520 samples from men, 857 from women, and 827 from children. 309 (11%) samples were flagged for removal due to inadequate runtime, 202 (7.5%) were flagged for poor wearing compliance, and 57 (2.1 %) were flagged for having filter-to-sensor $PM_{2.5}$ correction ratios beyond 2 geometric standard deviations from the geometric sample. Samples were removed from the analysis if flagged for not meeting one or more of the validation criteria. Men, women, and children had similar percentages of valid samples, 83.9, 84.1, and 77.4%, respectively. The BC data presented is a subset of the samples with valid PM data (those that had BC attenuation measurements and a calculated BC concentration lower than its sample's $PM_{2.5}$ concentration, n = 1,661). A sensitivity analysis was conducted to see how results varied based on sample inclusion criteria (section *4.3.4*).

Table 4.1: Valid Sample Removal Criteria. Samples were removed from the analysis if flagged for not meeting one or more of the validation criteria. Some samples were flagged for multiple validation criteria but were only removed once. A household was counted if at least one member had a valid $PM_{2.5}$ exposure sample.

	Initial Samples Collected	Runtime < 30 hours	Poor User Wearing Compliance	Invalid Filter-to-Real-time Correction Ratio	Total Removed	Total Used	Total % Used
Baseline Samples							
Children	433	47	9	3	54	379	87.5%
Women	416	20	7	6	27	389	93.5%
Men	257	10	5	4	19	238	92.6%
All	1,106	77	21	13	100	1,006	91.0%
Households	454				9	445	98.0%
Control Samples							
Children	298	54	30	13	84	214	71.8%
Women	283	29	38	7	64	219	77.4%
Men	157	18	14	4	27	130	82.8%
All	738	101	82	24	175	563	76.3%
Households	198				9	189	95.5%
Treatment Samples							
Children	337	68	39	8	103	234	69.4%
Women	320	35	37	6	71	249	77.8%
Men	206	28	23	6	54	152	73.8%
All	863	131	99	20	228	635	73.6%
Households	225				10	215	95.6%

4.3.2 $PM_{2.5}$: Intervention Effect

Overall, women had the largest differences in personal exposures to $PM_{2.5}$ between control and treatment groups, with median 48-hour time-averaged $PM_{2.5}$ exposure differences of 94.5 $\mu g \cdot m^{-3}$. Children had the second largest reductions with reported median exposure differences of 64.1 $\mu g \cdot m^{-3}$. Men had the smallest reductions in personal exposures, with differences between treatment and control groups of 17.5 $\mu g \cdot m^{-3}$ for $PM_{2.5}$. Table 4.2 provides descriptive statistics for the 48-hour average personal $PM_{2.5}$ exposures among the demographics and study groups. Across all demographics there was no significant difference in the baseline

$PM_{2.5}$ exposures between the control and treatment groups (Welch two sample t-test: $p = 0.9$, Appendix C4).

Table 4.2: Descriptive statistics for 48-hour average $PM_{2.5}$ concentrations ($\mu g \cdot m^{-3}$) as a function of familial demographic and between study groups. IQR = Inter-quartile range. The baseline portion of the table shows the control and treatment groups' data combined (no significant difference).

		48-hour Sample Average $PM_{2.5}$ Concentration ($\mu g \cdot m^{-3}$)							
	Sample Size (n)	**Mean**	**Standard Deviation**	**Geometric Mean**	**Geometric SD[a]**	**Median**	**Min**	**Max**	**IQR**
				Baseline Samples					
Children	379	245	179	194	1.99	190	17	1,235	197
Women	389	217	176	170	2.00	167	19	1,386	164
Men	238	121	93	94	2.04	92	19	525	98
				Control Samples					
Children	214	295	258	226	2.08	231	31	2,039	248
Women	219	310	249	227	2.36	245	1	1,441	264
Men	130	162	134	124	2.14	124	4	966	119
				Treatment Samples					
Children	234	223	248	163	2.2	164	24	3,188	189
Women	249	208	169	159	2.11	165	19	1,365	173
Men	152	161	181	113	2.41	112	1	1575	110

(a) Geometric standard deviation is dimensionless.

While the treatment group had the lowest 48-hour sample average personal $PM_{2.5}$ exposures, concentrations still greatly exceeded the WHO annual average interim 1 target (IT-1) of 35 $\mu g \cdot m^{-3}$ for all demographics.[73] The treatment and baseline groups had ~50% of their total samples conducted in the wet season, while about ~63% of the control group's samples were taken during the wet season. Seasonal cycles played a role in determining individuals' $PM_{2.5}$ exposures, with the dry seasons (June to August and December to April) on average leading to 32% (CI: 23 – 41%) higher personal exposure concentrations than the wet seasons. When isolating samples from the treatment group, this effect became even more pronounced, with the dry season leading to an estimated 51% (CI: 33 – 71%) increase in personal $PM_{2.5}$ exposures. There was a lot of dust in the community (Figure 2.2) likely contributing to the elevated exposures seen in the dry season.

However, even the group with lowest recorded exposures, men in the treatment arm during the wet season (n = 75) still had their 48-hour average $PM_{2.5}$ exposures well above the WHO IT-1 target, with a median concentration of 83 μg·m^{-3}. A comparison of the 48-hour sample average $PM_{2.5}$ exposures among demographics and study groups for samples taken during the intervention phase of the study is provided in Figure 4.3. A temporal distribution of $PM_{2.5}$ concentrations between intervention groups among the demographics is provided in Appendix C5.

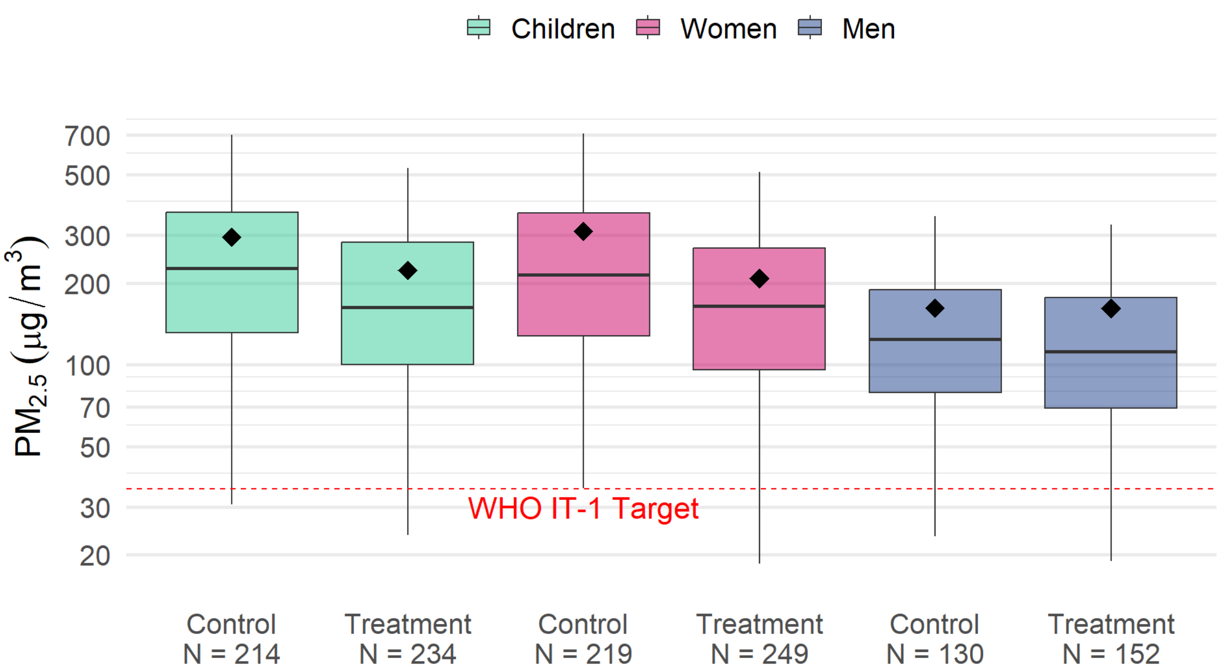

Figure 4.3: Boxplots represent the average (~48-hr for personal samples) $PM_{2.5}$ concentration distribution among ambient air, and personal exposure samples of men, women, and children from the control and treatment groups during the intervention phase of the study. The Y-axis is logscale. Center lines delineate the median; boxes represent the interquartile range, and whiskers represent the extent of observations within +/- 1.5·IQR. The red line is the WHO interim 1 target of 35 of μg·m^{-3}. The black diamonds represent the means.

Exposures among all demographic groups during the intervention were higher than the median ambient air concentration, 25.6 μg·m^{-3}, indicating personal exposures were dominated by proximity to localized PM sources, even in the treatment group. This suggests stove stacking (using a separate biomass burning stove) or neighbor visitations for meals could have played a large role in the personal exposure measurements for participants in the treatment group.[29,49] Another study conducted just a few years before SHEAR examined personal $PM_{2.5}$ exposures among pregnant women within a similar, yet slightly more urbanized, village in Eastern Rwanda (the HAPIN study) over the course of an LPG intervention. HAPIN reported the Rwandan women in their treatment group to have median 24-hour average personal $PM_{2.5}$ exposures of 33.6 $\mu g \cdot m^{-3}$ (IQR: 23.8 – 50 $\mu g \cdot m^{-3}$) and for the women in their control group, 79.6 $\mu g \cdot m^{-3}$ (IQR: 48.5 – 129.6 $\mu g \cdot m^{-3}$).[86] These exposures were substantially lower than our reported median 48-hour exposure concentrations of 165 $\mu g \cdot m^{-3}$ (IQR: 96 – 269 $\mu g \cdot m^{-3}$) and 245 $\mu g \cdot m^{-3}$ (IQR: 129 – 393 $\mu g \cdot m^{-3}$) for the women in our treatment and control groups respectively. Pope et al. conducted a review of other LPG intervention studies and reported a pooled mean exposure concentration of 58 $\mu g \cdot m^{-3}$ for participants in treatment groups among the 6 studies included in their analysis.[84]

While these studies reported values much lower than what was found for the women in the SHEAR treatment group, the PURE study (which observed non-intervention personal $PM_{2.5}$ exposures from men and women in 120 rural communities, spanning 8 countries) reported the personal $PM_{2.5}$ exposure geometric mean for African women using LPG and biomass fuels to be 146 and 153 $\mu g \cdot m^{-3}$ respectively.[49] These values are much closer to our monitored geometric means among the women in our control and treatment groups of 159 and 227 $\mu g \cdot m^{-3}$ respectively. However, it is important to note the PURE study was an observational study, so all participants from the LPG group were paying for their own fuel and likely used biomass (stove stacking) intermittently when needed. The wide range in reported exposures for both LPG and biomass users in sub-Saharan Africa illustrates how important it is to account for variations in individual exposure patterns between demographics at the community scale. A spaciotemporal analysis (as reported for the baseline data in section *3.3.3*) could illuminate differences in exposure patterns among participants in these studies providing a clearer picture for the most important variables impacting exposures. For example, a spaciotemporal analysis on our treatment group would show if participants still received the majority of their exposures in the home environment, which would suggest stove stacking, or if exposures were dominated by "other" environments during the intervention phase.

Linear mixed modeling (as described in section *2.6*) using the average personal $PM_{2.5}$ exposure among intervention visits per participant (since many participants had more than 1 intervention visit with PM exposure monitoring) accounting for interaction between demographic and intervention group variables and using household as a random intercept (n = 868 participants in 404 unique households) suggests the intervention had a significant reduction in overall $PM_{2.5}$ exposures for women and children. Model results estimated reductions for personal $PM_{2.5}$ exposures in women and children of 28.2% (CI: 15.8, 38.8%) and 22.4% (CI: 8.6, 34.2%) respectively. HAPIN reported an estimated reduction of 61% (59, 63%) between control and treatment groups among all the women in their study.[86] For men in the SHEAR study, the estimated reduction was not significant, at 11.5% (CI: -7.9, 27.5%). The model ICCs showed high within-household variability (compared to between-household variability, ICC = 0.21) suggesting on average large differences in personal exposures between members of the same household. The reported ICC for repeated measurements among individuals was 0.23, suggesting a similarly high variability between samples taken from the same person.

These results contradict the hypothesis that children would experience the largest reduction in personal $PM_{2.5}$ exposure from the whole-household energy intervention, which was based on findings from the spaciotemporal analysis conducted in section *3.3.3*. However, they validate data collected from participant surveys, where 65% of women report being the "Primary Cook" and 39% report being "Both the primary cook and head of my household" within the community.

Welch two sample t-tests estimated absolute reductions in $PM_{2.5}$ exposures associated with the whole-household energy intervention to be 64.5 $\mu g \cdot m^{-3}$ (CI: 35.6, 89 $\mu g \cdot m^{-3}$) for the women and 55.2 $\mu g \cdot m^{-3}$ (CI: 28, 78.6 $\mu g \cdot m^{-3}$) for the children in the SHEAR study. This absolute effect size is similar to what was seen in the HAPIN study where women were reported to have personal $PM_{2.5}$ exposure reductions of 68 $\mu g \cdot m^{-3}$ (CI: 63, 74 $\mu g \cdot m^{-3}$) due to their LPG intervention.[86] A Wilcoxon signed rank test suggested the difference between children's and women's exposures within the SHEAR study households was not significant (CI: -31.6, 40.9 $\mu g \cdot m^{-3}$) for control homes or for treatment homes (CI: -29.3, 16.0 $\mu g \cdot m^{-3}$). This furthers the distinction from data collected during the baseline phase of the study, where the same test suggested the difference between children's and women's exposures within the household was 32.8 $\mu g \cdot m^{-3}$ (CI: 48.5, 15.6 $\mu g \cdot m^{-3}$).

4.3.3 Black Carbon: Intervention Effect

Spearman correlations between $PM_{2.5}$ and BC concentrations for participants in the control and treatment groups were $\rho = 0.67$ and 0.73 respectively ($R^2 = 0.37$ and 0.38 respectively, Appendix C6). HAPIN reported lower correlations for their treatment group, with Spearman rho values for $PM_{2.5}$ and BC between (0.68 - 0.87) and (0.46 - 0.73) for control and treatment groups.[86]

For the SHEAR study, similar to $PM_{2.5}$, women and children had the largest and second largest reductions in personal exposures to BC between control and treatment groups. The median 48-hour average BC exposure difference between control and treatment groups was 4.1 and 3.1 $\mu g \cdot m^{-3}$ for women and children, respectively. Likewise, Men had the smallest reductions in personal exposures to BC, with a treatment to control group difference in exposures of 0.8 μg·m-3. Table 4.3 provides descriptive statistics for sample average personal BC exposures, and Appendix C7 provides a comparison of the 48-hour average BC exposures among demographics for the intervention groups. Across all demographics there was no significant difference in the baseline BC exposures (Welch two sample t-test, $p = 0.3$) between the control and treatment groups (Appendix C8). A temporal distribution of BC concentrations between intervention groups among the demographics is provided in Appendix C9. We should also note that BC concentrations are highly sensitive to the MAC value, and we used a MAC of 9 $m^2 \cdot g^{-1}$ which is relatively higher than what was used in previous studies and was based on the assumed composition of the PM collected.

Table 4.3: Descriptive statistics for 48-hour average BC concentrations ($\mu g \cdot m^{-3}$) as a function of familial demographic and between treatment groups. IQR = Inter-quartile range.

		48-hour Sample Average BC Concentration ($\mu g \cdot m^{-3}$)							
	Sample Size (n)	**Mean**	**Standard Deviation**	**Geometric Mean**	**Geometric SD[a]**	**Median**	**Min**	**Max**	**IQR**
Baseline Samples									
Children	310	10.3	6	8.6	1.87	9.7	1	38	7
Women	327	11.3	7	9.3	1.91	9.9	1	49	8
Men	205	7.1	6	5.4	2.09	5.4	1	34	7
Control Samples									
Children	136	13.9	6	12.5	1.64	13.4	2	33	7
Women	137	14.7	7	13.4	1.57	13.6	3	48	8
Men	88	9.8	5	8.7	1.72	8.9	1	25	5
Treatment Samples									
Children	166	10.7	7	9.2	1.78	10.3	1	71	7
Women	182	9.9	4	8.9	1.62	9.5	2	32	6
Men	110	9	6	7.8	1.75	8.1	1	53	5

(a) Geometric standard deviation is dimensionless.

HAPIN reported the Rwandan women in their treatment group to have median 24-hour average personal BC exposures of 4.2 $\mu g \cdot m^{-3}$ (IQR: 2.9 – 5.9 $\mu g \cdot m^{-3}$) and 10 μg·m-3 (IQR: 7 – 13.9 $\mu g \cdot m^{-3}$) for the women in their control group.[86] Similar to overall $PM_{2.5}$, these exposures were lower than our reported median 48-hour BC exposure concentrations of 9.5 $\mu g \cdot m^{-3}$ (IQR: 7 – 13 $\mu g \cdot m^{-3}$) and 13.6 μg·m-3 (IQR: 10 – 18 $\mu g \cdot m^{-3}$) for women in our treatment and control groups respectively.

An analogous linear mixed effects model to the one described for $PM_{2.5}$ exposures (section *4.3.2,* with model details provided in section *2.6*) was conducted for black carbon exposure data (n = 693 participants in 341 unique households). This model suggests the intervention reduced BC exposures for women and children by 33.3% (CI: 24.8, 40.7%) and 26.2% (CI: 16.7, 34.6%) respectively. However, unlike for overall $PM_{2.5}$, the model also reported a slight but significant decrease in exposures to BC for men in the treatment group of 15.2% (CI: 1.7, 26.8%). Figure 4.4 displays the contrast ratios between the treatment and control groups among demographics for both $PM_{2.5}$ and BC.

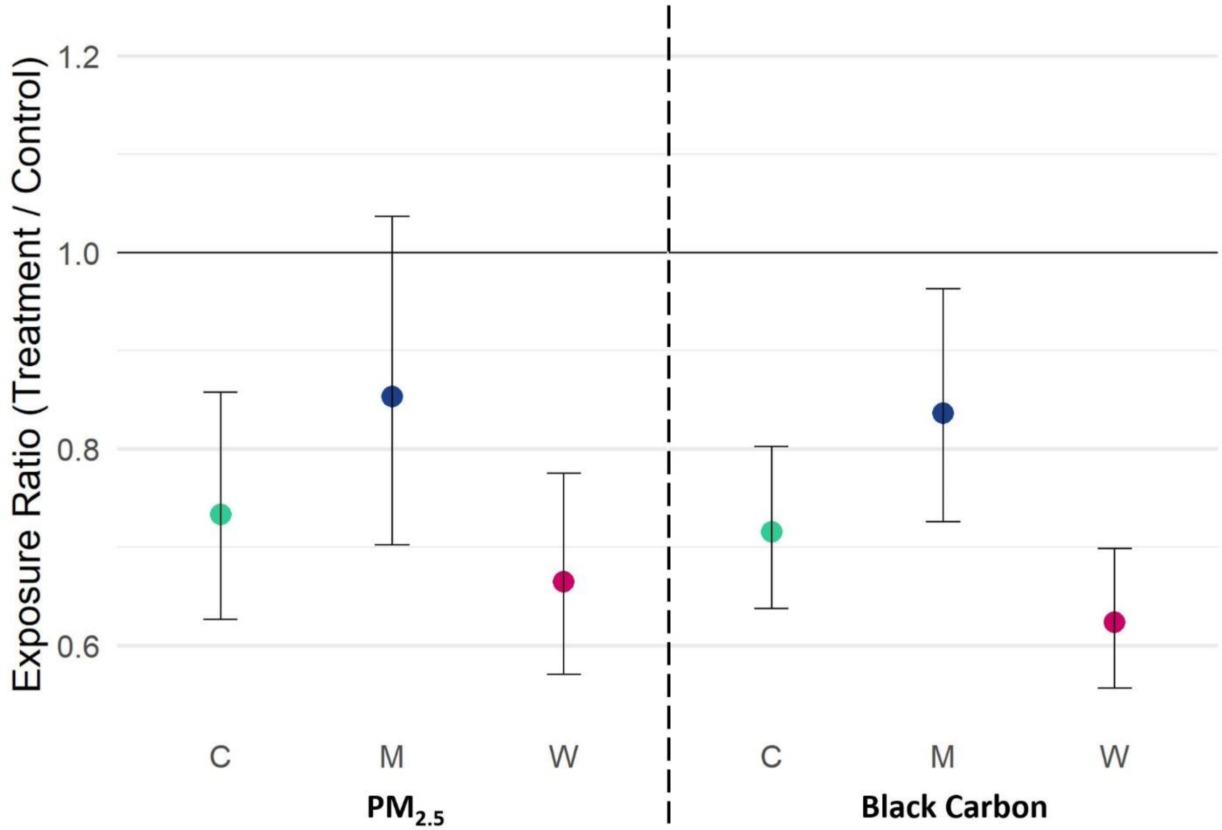

Figure 4.4: Contrast ratios produced by linear mixed effect models, accounting for interaction between demographic and intervention groups and household as a random effect. This illustrates the whole-household energy intervention effect for overall $PM_{2.5}$ and BC exposures among the demographic groups. Error bars illustrate the 95% confidence for the exposure ratios.

4.3.4 Inclusion Criteria Sensitivity Analysis

Results from a sensitivity analysis that retained all the samples for linear mixed effect modeling (i.e. none of the samples that failed to meet the 'valid sample criteria' were removed, as described in section *4.3.1*, n = 503 additional samples) were minimally different from the primary study model (Figure 4.5).

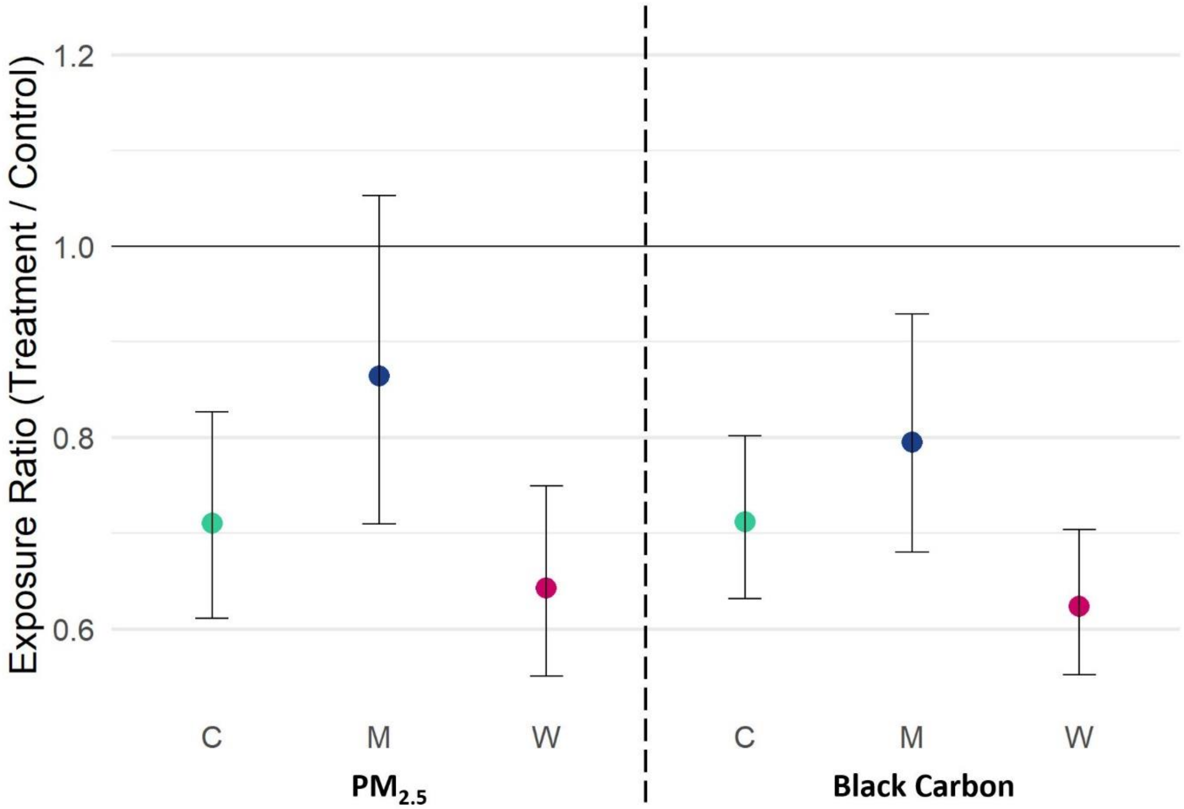

Figure 4.5: Contrast ratios produced by linear mixed effect models when all the collected samples are included. Accounting for interaction between demographic and intervention groups and household as a random effect. Error bars illustrate the 95% confidence for the exposure ratios.

Women still had the greatest personal exposure reductions for both personal $PM_{2.5}$ and BC of 35.8% (CI: 25.1, 45%) and 37.7% (CI : 29.6, 44.8%) respectively. Children still had the second greatest reductions due to the whole-household energy intervention of 29% (CI : 17.3, 38.9%) and 28.8% (CI : 19.8, 36.8%) for $PM_{2.5}$ and BC, respectively. Men had the largest change in exposure reductions for this sensitivity analysis, but not in a way that meaningfully impacts the results. Men still had the smallest exposure contrast ratios, with estimated exposure reductions of 13.6% (CI : -5.3, 29.1%) and 20.5% (CI : 7.1, 32%) for $PM_{2.5}$ and BC, respectively.

CHAPTER 5: CONCLUSIONS AND FUTURE WORK

Recent improvements in monitoring technology allowed us to track personal $PM_{2.5}$ exposures as a function of time and location with an ease and at a scale never before seen. In this work, data collected from the SHEAR study was used to examine baseline demographic variation in $PM_{2.5}$ exposure within a rural Rwandan community and provided an intent-to-treat analysis highlighting the efficacy of a whole-household energy intervention within that community. This project is the first of its kind to provide personal $PM_{2.5}$ exposure variations between men, women, and children in a rural sub-Saharan African community, from both an observational (baseline) and whole-household energy intervention perspective.

Findings from the baseline analysis suggest that $PM_{2.5}$ exposures were the highest among children, second highest among women, and lowest for men. This is a concerning trend because children are a particularly susceptible demographic to the adverse effects of air pollution. Anecdotal evidence suggests cookstove fire maintenance and proximity to cookstove fires for lighting (to complete homework) as likely reasons for these heightened exposures. We propose behavioral modifications targeting children's cooking tasks and homework settings could help reduce the exposure disparity between children and their parents in these rural sub-Saharan African settings. However, all participant's exposures exceeded WHO recommended levels (IT-1 target of 35 $\mu g \cdot m^3$), implying behavioral modifications alone will not be enough to produce meaningful health impacts.

This is where the whole-household energy intervention provided additional insight. Results from the intervention phase ITT analysis suggested the household energy intervention did produce meaningful reductions in personal $PM_{2.5}$ and BC exposure burdens for women and children. However, even homes in the treatment group (who were provided free access to LPG and solar electricity) did not experience exposure reductions great enough to put them below, or near the WHO IT-1 target. Men's $PM_{2.5}$ exposures were not significantly impacted by the intervention, but their BC exposures showed a moderately significant decrease. Additionally, during the intervention no significant difference was found in the $PM_{2.5}$ or BC exposures experience between women and children within the same household, contrary to results from the baseline exposure analysis.

For future work, we suggest a spaciotemporal analysis on the exposure data from the intervention phase of the SHEAR study. This could illuminate the behavioral changes that occurred between the baseline and intervention phases of the study potentially causing the differences in exposures patterns for women and children. A spaciotemporal analysis could also provide insight into whether or not stove stacking contributed to the diluted personal exposure reductions experienced by the treatment group for the SHEAR study. Overall, this work further highlights how complex and varied personal exposures to household air pollution are at the regional, community, household, and individual level. There is so much left to learn about the demographic patterns influencing personal exposure burdens.

I hope this work will contribute to improving the lives of the people in Karambi, Isangano, and the entire Ndego Cell. This work built upon the efforts of everyday scientists who for decades have searched for solutions to improve the quality of life for people in this community, their communities, and the thousands of similar communities all around the world. We cannot afford to stop building upon this research now; in many ways we have become a global community, and we are currently in the midst of an unprecedented storm. We cannot expect our ship to stay afloat unless the entire hull is properly maintained.

REFERENCES

(1) *GBD Compare*. Institute for Health Metrics and Evaluation. http://vizhub.healthdata.org/gbd-compare (accessed 2023-02-02).
(2) *Household air pollution*. https://www.who.int/news-room/fact-sheets/detail/household-air-pollution-and-health (accessed 2024-10-01).
(3) Brook, R. D.; Rajagopalan, S.; Pope, C. A.; Brook, J. R.; Bhatnagar, A.; Diez-Roux, A. V.; Holguin, F.; Hong, Y.; Luepker, R. V.; Mittleman, M. A.; Peters, A.; Siscovick, D.; Smith, S. C.; Whitsel, L.; Kaufman, J. D. Particulate Matter Air Pollution and Cardiovascular Disease. *Circulation* **2010**, *121* (21), 2331–2378. https://doi.org/10.1161/CIR.0b013e3181dbece1.
(4) mU.S. EPA. Integrated Science Assessment for Particulate Matter (December 2019). **2019**.
(5) Fedak, K. M.; Good, N.; Walker, E. S.; Balmes, J.; Brook, R. D.; Clark, M. L.; Cole-Hunter, T.; Devlin, R.; L'Orange, C.; Luckasen, G.; Mehaffy, J.; Shelton, R.; Wilson, A.; Volckens, J.; Peel, J. L. Acute Changes in Lung Function Following Controlled Exposure to Cookstove Air Pollution in the Subclinical Tests of Volunteers Exposed to Smoke (STOVES) Study. *Inhal. Toxicol.* **2020**, *32* (3), 115–123. https://doi.org/10.1080/08958378.2020.1751750.
(6) Burnett, R. T.; Pope, C. A.; Ezzati, M.; Olives, C.; Lim, S. S.; Mehta, S.; Shin, H. H.; Singh, G.; Hubbell, B.; Brauer, M.; Anderson, H. R.; Smith, K. R.; Balmes, J. R.; Bruce, N. G.; Kan, H.; Laden, F.; Pr, üss-U. A.; Turner, M. C.; Gapstur, S. M.; Diver, W. R.; Cohen, A. An Integrated Risk Function for Estimating the Global Burden of Disease Attributable to Ambient Fine Particulate Matter Exposure. *Environ. Health Perspect.* **2014**, *122* (4), 397–403. https://doi.org/10.1289/ehp.1307049.
(7) Lee, K. K.; Bing, R.; Kiang, J.; Bashir, S.; Spath, N.; Stelzle, D.; Mortimer, K.; Bularga, A.; Doudesis, D.; Joshi, S. S.; Strachan, F.; Gumy, S.; Adair-Rohani, H.; Attia, E. F.; Chung, M. H.; Miller, M. R.; Newby, D. E.; Mills, N. L.; McAllister, D. A.; Shah, A. S. V. Adverse Health Effects Associated with Household Air Pollution: A Systematic Review, Meta-Analysis, and Burden Estimation Study. *Lancet Glob. Health* **2020**, *8* (11), e1427–e1434. https://doi.org/10.1016/S2214-109X(20)30343-0.
(8) Janssen, N. A. H.; Hoek, G.; Simic-Lawson, M.; Fischer, P.; van Bree, L.; ten Brink, H.; Keuken, M.; Atkinson, R. W.; Anderson, H. R.; Brunekreef, B.; Cassee, F. R. Black Carbon as an Additional Indicator of the Adverse Health Effects of Airborne Particles Compared with PM10 and PM2.5. *Environ. Health Perspect.* **2011**, *119* (12), 1691–1699. https://doi.org/10.1289/ehp.1003369.
(9) Ljungman, P. L. S.; Andersson, N.; Stockfelt, L.; Andersson, E. M.; Nilsson Sommar, J.; Eneroth, K.; Gidhagen, L.; Johansson, C.; Lager, A.; Leander, K.; Molnar, P.; Pedersen, N. L.; Rizzuto, D.; Rosengren, A.; Segersson, D.; Wennberg, P.; Barregard, L.; Forsberg, B.; Sallsten, G.; Bellander, T.; Pershagen, G. Long-Term Exposure to Particulate Air Pollution, Black Carbon, and Their Source Components in Relation to Ischemic Heart Disease and Stroke. *Environ. Health Perspect.* **2019**, *127* (10), 107012. https://doi.org/10.1289/EHP4757.
(10) Baumgartner, J.; Zhang, Y.; Schauer, J. J.; Huang, W.; Wang, Y.; Ezzati, M. Highway Proximity and Black Carbon from Cookstoves as a Risk Factor for Higher Blood Pressure in Rural China. *Proc. Natl. Acad. Sci.* **2014**, *111* (36), 13229–13234. https://doi.org/10.1073/pnas.1317176111.
(11) Gu, Y.; Zhang, W.; Yang, Y.; Wang, C.; Streets, D. G.; Yim, S. H. L. Assessing Outdoor Air Quality and Public Health Impact Attributable to Residential Black Carbon Emissions in Rural China. *Resour. Conserv. Recycl.* **2020**, *159*, 104812. https://doi.org/10.1016/j.resconrec.2020.104812.
(12) Lim, S.; Bassey, E.; Bos, B.; Makacha, L.; Varaden, D.; Arku, R. E.; Baumgartner, J.; Brauer, M.; Ezzati, M.; Kelly, F. J.; Barratt, B. Comparing Human Exposure to Fine Particulate Matter in Low and High-Income Countries: A Systematic Review of Studies Measuring Personal PM2.5 Exposure. *Sci. Total Environ.* **2022**, *833*, 155207. https://doi.org/10.1016/j.scitotenv.2022.155207.

(13) Panchal, R.; Benyon, M.; Laban, T.; Kwatala, N.; Wernecke, B.; Wright, C. Y.; Vande Hey, J. Reviewing the Methodologies Used to Assess Household PM2.5 Air Pollution in Sub-Saharan Africa. *Build. Environ.* **2024**, *266*, 112099. https://doi.org/10.1016/j.buildenv.2024.112099.
(14) Bonjour, S.; Adair-Rohani, H.; Wolf, J.; Bruce, N. G.; Mehta, S.; Prüss-Ustün, A.; Lahiff, M.; Rehfuess, E. A.; Mishra, V.; Smith, K. R. Solid Fuel Use for Household Cooking: Country and Regional Estimates for 1980–2010. *Environ. Health Perspect.* **2013**, *121* (7), 784–790. https://doi.org/10.1289/ehp.1205987.
(15) Stoner, O.; Lewis, J.; Martínez, I. L.; Gumy, S.; Economou, T.; Adair-Rohani, H. Household Cooking Fuel Estimates at Global and Country Level for 1990 to 2030. *Nat. Commun.* **2021**, *12* (1), 5793. https://doi.org/10.1038/s41467-021-26036-x.
(16) IEA; IRENA; UNSD; World Bank; WHO. *2022. Tracking SDG 7: The Energy Progress Report*; 2022.
(17) Bond, T. C.; Bhardwaj, E.; Dong, R.; Jogani, R.; Jung, S.; Roden, C.; Streets, D. G.; Trautmann, N. M. Historical Emissions of Black and Organic Carbon Aerosol from Energy-Related Combustion, 1850–2000. *Glob. Biogeochem. Cycles* **2007**, *21* (2). https://doi.org/10.1029/2006GB002840.
(18) Bradbrook, A. J.; Gardam, J. G. Placing Access to Energy Services within a Human Rights Framework. *Hum. Rights Q.* **2006**, *28* (2), 389–415.
(19) Martin. *Energy*. United Nations Sustainable Development. https://www.un.org/sustainabledevelopment/energy/ (accessed 2025-06-11).
(20) Bilsback, K. R.; Eilenberg, S. R.; Good, N.; Heck, L.; Johnson, M.; Kodros, J. K.; Lipsky, E. M.; L'Orange, C.; Pierce, J. R.; Robinson, A. L.; Subramanian, R.; Tryner, J.; Wilson, A.; Volckens, J. The Firepower Sweep Test: A Novel Approach to Cookstove Laboratory Testing. *Indoor Air* **2018**, *28* (6), 936–949. https://doi.org/10.1111/ina.12497.
(21) Johnson, M. A.; Garland, C. R.; Jagoe, K.; Edwards, R.; Ndemere, J.; Weyant, C.; Patel, A.; Kithinji, J.; Wasirwa, E.; Nguyen, T.; Khoi, D. D.; Kay, E.; Scott, P.; Nguyen, R.; Yagnaraman, M.; Mitchell, J.; Derby, E.; Chiang, R. A.; Pennise, D. In-Home Emissions Performance of Cookstoves in Asia and Africa. *Atmosphere* **2019**, *10* (5), 290. https://doi.org/10.3390/atmos10050290.
(22) *World Energy Outlook 2024 Free Dataset - Data product*. IEA. https://www.iea.org/data-and-statistics/data-product/world-energy-outlook-2024-free-dataset (accessed 2025-06-22).
(23) Lam, N. L.; Muhwezi, G.; Isabirye, F.; Harrison, K.; Ruiz-Mercado, I.; Amukoye, E.; Mokaya, T.; Wambua, M.; Bates, M. N. Exposure Reductions Associated with Introduction of Solar Lamps to Kerosene Lamp-Using Households in Busia County, Kenya. *Indoor Air* **2018**, *28* (2), 218–227. https://doi.org/10.1111/ina.12433.
(24) *WHO Guidelines for indoor air quality: Household fuel combustion*. https://www.who.int/publications/i/item/9789241548885 (accessed 2025-06-22).
(25) Lam, N. L.; Chen, Y.; Weyant, C.; Venkataraman, C.; Sadavarte, P.; Johnson, M. A.; Smith, K. R.; Brem, B. T.; Arineitwe, J.; Ellis, J. E.; Bond, T. C. Household Light Makes Global Heat: High Black Carbon Emissions From Kerosene Wick Lamps. *Environ. Sci. Technol.* **2012**, *46* (24), 13531–13538. https://doi.org/10.1021/es302697h.
(26) Johnson, M.; Pillarisetti, A.; Piedrahita, R.; Balakrishnan, K.; Peel, J. L.; Steenland, K.; Underhill, L. J.; Rosa, G.; Kirby, M. A.; D, íaz-A. A.; McCracken, J.; Clark, M. L.; Waller, L.; Chang, H. H.; Wang, J.; Dusabimana, E.; Ndagijimana, F.; Sambandam, S.; Mukhopadhyay, K.; Kearns, K. A.; Campbell, D.; Kremer, J.; Rosenthal, J. P.; Checkley, W.; Clasen, T.; Naeher, L.; null, null. Exposure Contrasts of Pregnant Women during the Household Air Pollution Intervention Network Randomized Controlled Trial. *Environ. Health Perspect.* **2022**, *130* (9), 097005. https://doi.org/10.1289/EHP10295.
(27) Ye, W.; Campbell, D.; Johnson, M.; Balakrishnan, K.; Peel, J. L.; Steenland, K.; Underhill, L. J.; Rosa, G.; Kirby, M. A.; Díaz-Artiga, A.; McCracken, J.; Thompson, L. M.; Clark, M. L.; Waller, L. A.; Chang, H. H.; Wang, J.; Dusabimana, E.; Ndagijimana, F.; Sambandam, S.; Mukhopadhyay, K.; Chiang, M.; Hartinger, S. M.; Nicolaou, L.; Williams, K.; Piedrahita, R.; Kearns, K. A.; Kremer, J.; Ghosh, A.; Rosenthal, J. P.; Checkley, W.; Clasen, T.; Naeher, L.; Pillarisetti, A. Exposure Contrasts

of Women Aged 40–79 Years during the Household Air Pollution Intervention Network Randomized Controlled Trial. *Environ. Sci. Technol.* **2025**, *59* (1), 69–81. https://doi.org/10.1021/acs.est.4c06337.
(28) Chillrud, S. N.; Ae-Ngibise, K. A.; Gould, C. F.; Owusu-Agyei, S.; Mujtaba, M.; Manu, G.; Burkart, K.; Kinney, P. L.; Quinn, A.; Jack, D. W.; Asante, K. P. The Effect of Clean Cooking Interventions on Mother and Child Personal Exposure to Air Pollution: Results from the Ghana Randomized Air Pollution and Health Study (GRAPHS). *J. Expo. Sci. Environ. Epidemiol.* **2021**, *31* (4), 683–698. https://doi.org/10.1038/s41370-021-00309-5.
(29) Katz, J.; Tielsch, J. M.; Khatry, S. K.; Shrestha, L.; Breysse, P.; Zeger, S. L.; Kozuki, N.; Checkley, W.; LeClerq, S. C.; Mullany, L. C. Impact of Improved Biomass and Liquid Petroleum Gas Stoves on Birth Outcomes in Rural Nepal: Results of 2 Randomized Trials. *Glob. Health Sci. Pract.* **2020**, *8* (3), 372–382. https://doi.org/10.9745/GHSP-D-20-00011.
(30) Checkley, W.; Williams, K. N.; Kephart, J. L.; Fandiño-Del-Rio, M.; Steenland, N. K.; Gonzales, G. F.; Naeher, L. P.; Harvey, S. A.; Moulton, L. H.; Davila-Roman, V. G.; Goodman, D.; Tarazona-Meza, C.; Miele, C. H.; Simkovich, S.; Chiang, M.; Chartier, R. T.; Koehler, K. Effects of a Household Air Pollution Intervention with Liquefied Petroleum Gas on Cardiopulmonary Outcomes in Peru. A Randomized Controlled Trial. *Am. J. Respir. Crit. Care Med.* **2021**, *203* (11), 1386–1397. https://doi.org/10.1164/rccm.202006-2319OC.
(31) Okello, G.; Devereux, G.; Semple, S. Women and Girls in Resource Poor Countries Experience Much Greater Exposure to Household Air Pollutants than Men: Results from Uganda and Ethiopia. *Environ. Int.* **2018**, *119*, 429–437. https://doi.org/10.1016/j.envint.2018.07.002.
(32) Lim, S.; Said, B.; Zurba, L.; Mosler, G.; Addo-Yobo, E.; Adeyeye, O. O.; Arhin, B.; Evangelopoulos, D.; Fapohunda, V. T.; Fortune, F.; Griffiths, C. J.; Hlophe, S.; Kasekete, M.; Lowther, S.; Masekela, R.; Mkutumula, E.; Mmbaga, B. T.; Mujuru, H. A.; Nantanda, R.; Mzati Nkhalamba, L.; Ngocho, J. S.; Ojo, O. T.; Owusu, S. K.; Shaibu, S.; Ticklay, I.; Grigg, J.; Barratt, B. Characterising Sources of PM2·5 Exposure for School Children with Asthma: A Personal Exposure Study across Six Cities in Sub-Saharan Africa. *Lancet Child Adolesc. Health* **2024**, *8* (1), 17–27. https://doi.org/10.1016/S2352-4642(23)00261-4.
(33) Vanker, A.; Barnett, W.; Chartier, R.; MacGinty, R.; Zar, H. J. Personal Monitoring of Fine Particulate Matter (PM2.5) Exposure in Mothers and Young Children in a South African Birth Cohort Study – A Pilot Study. *Atmos. Environ.* **2023**, *294*, 119513. https://doi.org/10.1016/j.atmosenv.2022.119513.
(34) Van Vliet, E. D. S.; Asante, K.; Jack, D. W.; Kinney, P. L.; Whyatt, R. M.; Chillrud, S. N.; Abokyi, L.; Zandoh, C.; Owusu-Agyei, S. Personal Exposures to Fine Particulate Matter and Black Carbon in Households Cooking with Biomass Fuels in Rural Ghana. *Environ. Res.* **2013**, *127*, 40–48. https://doi.org/10.1016/j.envres.2013.08.009.
(35) Yip, F.; Christensen, B.; Sircar, K.; Naeher, L.; Bruce, N.; Pennise, D.; Lozier, M.; Pilishvili, T.; Loo Farrar, J.; Stanistreet, D.; Nyagol, R.; Muoki, J.; de Beer, L.; Sage, M.; Kapil, V. Assessment of Traditional and Improved Stove Use on Household Air Pollution and Personal Exposures in Rural Western Kenya. *Environ. Int.* **2017**, *99*, 185–191. https://doi.org/10.1016/j.envint.2016.11.015.
(36) Smith, K. R.; Bruce, N.; Balakrishnan, K.; Adair-Rohani, H.; Balmes, J.; Chafe, Z.; Dherani, M.; Hosgood, H. D.; Mehta, S.; Pope, D.; Rehfuess, E.; HAP CRA Risk Expert Group. Millions Dead: How Do We Know and What Does It Mean? Methods Used in the Comparative Risk Assessment of Household Air Pollution. *Annu. Rev. Public Health* **2014**, *35*, 185–206. https://doi.org/10.1146/annurev-publhealth-032013-182356.
(37) Dionisio, K. L.; Howie, S. R. C.; Dominici, F.; Fornace, K. M.; Spengler, J. D.; Donkor, S.; Chimah, O.; Oluwalana, C.; Ideh, R. C.; Ebruke, B.; Adegbola, R. A.; Ezzati, M. The Exposure of Infants and Children to Carbon Monoxide from Biomass Fuels in The Gambia: A Measurement and Modeling Study. *J. Expo. Sci. Environ. Epidemiol.* **2012**, *22* (2), 173–181. https://doi.org/10.1038/jes.2011.47.
(38) Gehring, U.; Gruzieva, O.; Agius, R. M.; Beelen, R.; Custovic, A.; Cyrys, J.; Eeftens, M.; Flexeder, C.; Fuertes, E.; Heinrich, J.; Hoffmann, B.; de Jongste, J. C.; Kerkhof, M.; Klümper, C.; Korek, M.; Mölter, A.; Schultz, E. S.; Simpson, A.; Sugiri, D.; Svartengren, M.; von Berg, A.; Wijga, A. H.;

Pershagen, G.; Brunekreef, B. Air Pollution Exposure and Lung Function in Children: The ESCAPE Project. *Environ. Health Perspect.* **2013**, *121* (11–12), 1357–1364. https://doi.org/10.1289/ehp.1306770.
(39) Holgate, S. T. 'Every Breath We Take: The Lifelong Impact of Air Pollution' – a Call for Action. *Clin. Med.* **2017**, *17* (1), 8–12. https://doi.org/10.7861/clinmedicine.17-1-8.
(40) Brumberg, H. L.; Karr, C. J.; Bole, A.; Ahdoot, S.; Balk, S. J.; Bernstein, A. S.; Byron, L. G.; Landrigan, P. J.; Marcus, S. M.; Nerlinger, A. L.; Pacheco, S. E.; Woolf, A. D.; Zajac, L.; Baum, C. R.; Campbell, C. C.; Sample, J. A.; Spanier, A. J.; Trasande, L.; COUNCIL ON ENVIRONMENTAL HEALTH. Ambient Air Pollution: Health Hazards to Children. *Pediatrics* **2021**, *147* (6), e2021051484. https://doi.org/10.1542/peds.2021-051484.
(41) Gauderman, W. J.; Vora, H.; McConnell, R.; Berhane, K.; Gilliland, F.; Thomas, D.; Lurmann, F.; Avol, E.; Kunzli, N.; Jerrett, M.; Peters, J. Effect of Exposure to Traffic on Lung Development from 10 to 18 Years of Age: A Cohort Study. *The Lancet* **2007**, *369* (9561), 571–577. https://doi.org/10.1016/S0140-6736(07)60037-3.
(42) Baumgartner, J.; Schauer, J. J.; Ezzati, M.; Lu, L.; Cheng, C.; Patz, J.; Bautista, L. E. Patterns and Predictors of Personal Exposure to Indoor Air Pollution from Biomass Combustion among Women and Children in Rural China. *Indoor Air* **2011**, *21* (6), 479–488. https://doi.org/10.1111/j.1600-0668.2011.00730.x.
(43) Bennitt, F. B.; Wozniak, S.; Causey, K.; Spearman, S.; Okereke, C.; Garcia, V.; Hashmeh, N.; Ashbaugh, C.; Abdelkader, A.; Abdoun, M.; Abdurebi, M. J.; Abedi, A.; Zuñiga, R. A. A.; Aboagye, R. G.; Abubakar, B.; Abu-Zaid, A.; Adane, M. M.; Adegboye, O. A.; Adekanmbi, V.; Adepoju, A. Brauer, M.; Burkart, K. Global, Regional, and National Burden of Household Air Pollution, 1990–2021: A Systematic Analysis for the Global Burden of Disease Study 2021. *The Lancet* **2025**, *405* (10485), 1167–1181. https://doi.org/10.1016/S0140-6736(24)02840-X.
(44) Burnett, R.; Chen, H.; Szyszkowicz, M.; Fann, N.; Hubbell, B.; Pope, C. A.; Apte, J. S.; Brauer, M.; Cohen, A.; Weichenthal, S.; Coggins, J.; Di, Q.; Brunekreef, B.; Frostad, J.; Lim, S. S.; Kan, H.; Walker, K. D.; Thurston, G. D.; Hayes, R. B.; Lim, C. C.; Turner, M. C.; Jerrett, M.; Krewski, D.; Gapstur, S. M.; Diver, W. R.; Ostro, B.; Goldberg, D.; Crouse, D. L.; Martin, R. V.; Peters, P.; Pinault, L.; Tjepkema, M.; van Donkelaar, A.; Villeneuve, P. J.; Miller, A. B.; Yin, P.; Zhou, M.; Wang, L.; Janssen, N. A. H.; Marra, M.; Atkinson, R. W.; Tsang, H.; Quoc Thach, T.; Cannon, J. B.; Allen, R. T.; Hart, J. E.; Laden, F.; Cesaroni, G.; Forastiere, F.; Weinmayr, G.; Jaensch, A.; Nagel, G.; Concin, H.; Spadaro, J. V. Global Estimates of Mortality Associated with Long-Term Exposure to Outdoor Fine Particulate Matter. *Proc. Natl. Acad. Sci.* **2018**, *115* (38), 9592–9597. https://doi.org/10.1073/pnas.1803222115.
(45) Clark, M. L.; Peel, J. L.; Balakrishnan, K.; Breysse, P. N.; Chillrud, S. N.; Naeher, L. P.; Rodes, C. E.; Vette, A. F.; Balbus, J. M. Health and Household Air Pollution from Solid Fuel Use: The Need for Improved Exposure Assessment. *Environ. Health Perspect.* **2013**, *121* (10), 1120–1128. https://doi.org/10.1289/ehp.1206429.
(46) Brokamp, C.; Brandt, E. B.; Ryan, P. H. Assessing Exposure to Outdoor Air Pollution for Epidemiological Studies: Model-Based and Personal Sampling Strategies. *J. Allergy Clin. Immunol.* **2019**, *143* (6), 2002–2006. https://doi.org/10.1016/j.jaci.2019.04.019.
(47) Schumacher, A. E.; Kyu, H. H.; Aali, A.; Abbafati, C.; Abbas, J.; Abbasgholizadeh, R.; Abbasi, M. A.; Abbasian, M.; ElHafeez, S. A.; Abdelmasseh, M.; Abd-Elsalam, S.; Abdelwahab, A.; Abdollahi, M.; Abdoun, M.; Abdullahi, A.; Abdurehman, A. M.; Abebe, M.; Abedi, A.; Abedi, A.; Abegaz, T. Lim, S. S.; Murray, C. J. L. Global Age-Sex-Specific Mortality, Life Expectancy, and Population Estimates in 204 Countries and Territories and 811 Subnational Locations, 1950–2021, and the Impact of the COVID-19 Pandemic: A Comprehensive Demographic Analysis for the Global Burden of Disease Study 2021. *The Lancet* **2024**, *403* (10440), 1989–2056. https://doi.org/10.1016/S0140-6736(24)00476-8.

(48) Volckens, J.; Quinn, C.; Leith, D.; Mehaffy, J.; Henry, C. S.; Miller-Lionberg, D. Development and Evaluation of an Ultrasonic Personal Aerosol Sampler. *Indoor Air* **2017**, *27* (2), 409–416. https://doi.org/10.1111/ina.12318.
(49) Shupler, M.; Hystad, P.; Birch, A.; Miller-Lionberg, D.; Jeronimo, M.; Arku, R. E.; Chu, Y. L.; Mushtaha, M.; Heenan, L.; Rangarajan, S.; Seron, P.; Lanas, F.; Cazor, F.; Lopez-Jaramillo, P.; Camacho, P. A.; Perez, M.; Yeates, K.; West, N.; Ncube, T.; Ncube, B.; Chifamba, J.; Yusuf, R.; Khan, A.; Hu, B.; Liu, X.; Wei, L.; Tse, L. A.; Mohan, D.; Kumar, P.; Gupta, R.; Mohan, I.; Jayachitra, K. G.; Mony, P. K.; Rammohan, K.; Nair, S.; Lakshmi, P. V. M.; Sagar, V.; Khawaja, R.; Iqbal, R.; Kazmi, K.; Yusuf, S.; Brauer, M. Household and Personal Air Pollution Exposure Measurements from 120 Communities in Eight Countries: Results from the PURE-AIR Study. *Lancet Planet. Health* **2020**, *4* (10), e451–e462. https://doi.org/10.1016/S2542-5196(20)30197-2.
(50) Daouda, M.; Mujtaba, M. N.; Yang, Q.; Seyram, K.; Lee, A. G.; Tawiah, T.; Ae-Ngibise, K. A.; Chillrud, S. N.; Jack, D.; Asante, K. P. Prediction of Personal Exposure to PM2.5 in Mother-Child Pairs in Rural Ghana. *J. Expo. Sci. Environ. Epidemiol.* **2022**, *32* (4), 629. https://doi.org/10.1038/s41370-022-00420-1.
(51) Li, X.; Baumgartner, J.; Barrington-Leigh, C.; Harper, S.; Robinson, B.; Shen, G.; Sternbach, T.; Tao, S.; Zhang, X.; Zhang, Y.; Carter, E. Socioeconomic and Demographic Associations with Wintertime Air Pollution Exposures at Household, Community, and District Scales in Rural Beijing, China. *Environ. Sci. Technol.* **2022**, *56* (12), 8308–8318. https://doi.org/10.1021/acs.est.1c07402.
(52) Koehler, K.; Good, N.; Wilson, A.; Mölter, A.; Moore, B. F.; Carpenter, T.; Peel, J. L.; Volckens, J. The Fort Collins Commuter Study: Variability in Personal Exposure to Air Pollutants by Microenvironment. *Indoor Air* **2019**, *29* (2), 231–241. https://doi.org/10.1111/ina.12533.
(53) Li, X.; Tryner, J.; Young, B. N.; Hernandez Ramirez, L.; Phillips, M.; WeMott, S.; Erlandson, G.; Kuiper, G.; Dean, D.; Martinez, N.; Sanpedro, L.; Magzamen, S.; Volckens, J. Application and Validation of a Wearable Monitor for Assessing Time- and Location-Resolved Exposures to Particulate Matter in California's Central Valley. *Aerosol Sci. Technol. 0* (0), 1–17. https://doi.org/10.1080/02786826.2024.2415481.
(54) Burrowes, V. J.; Piedrahita, R.; Pillarisetti, A.; Underhill, L. J.; Fandiño-Del-Rio, M.; Johnson, M.; Kephart, J. L.; Hartinger, S. M.; Steenland, K.; Naeher, L.; Kearns, K.; Peel, J. L.; Clark, M. L.; Checkley, W.; Investigators, H. Comparison of Next-Generation Portable Pollution Monitors to Measure Exposure to PM2.5 from Household Air Pollution in Puno, Peru. *Indoor Air* **2020**, *30* (3), 445–458. https://doi.org/10.1111/ina.12638.
(55) Do, K.; Yu, H.; Velasquez, J.; Grell-Brisk, M.; Smith, H.; Ivey, C. E. A Data-Driven Approach for Characterizing Community Scale Air Pollution Exposure Disparities in Inland Southern California. *J. Aerosol Sci.* **2021**, *152*, 105704. https://doi.org/10.1016/j.jaerosci.2020.105704.
(56) Johnson, M. A.; Abuya, T.; Wickramanayake, A.; Miller, H.; Sambu, D.; Mwanga, D.; Odwe, G.; Ndwiga, C.; Piedrahita, R.; Rossanese, M.; Gatari, M. J.; Giordano, M. R.; Westervelt, D. M.; Wotton, L.; Rajasekharan, S. Patterns and Drivers of Maternal Personal Exposure to PM2.5 in Informal Settlements in Nairobi, Kenya. *Environ. Sci. Atmospheres* **2024**, *4* (5), 578–591. https://doi.org/10.1039/D3EA00074E.
(57) Leith, D.; L'Orange ,Christian; Mehaffy ,John; and Volckens, J. Design and Performance of UPAS Inlets for Respirable and Thoracic Mass Sampling. *J. Occup. Environ. Hyg.* **2020**, *17* (6), 274–282. https://doi.org/10.1080/15459624.2020.1741595.
(58) AG, S. *SPS30-PM2.5 Sensor for HVAC and air quality applications SPS30*. Sensirion AG. https://sensirion.com/products/catalog/SPS30 (accessed 2024-09-23).
(59) Tryner, J.; L'Orange, C.; Mehaffy, J.; Miller-Lionberg, D.; Hofstetter, J. C.; Wilson, A.; Volckens, J. Laboratory Evaluation of Low-Cost PurpleAir PM Monitors and in-Field Correction Using Co-Located Portable Filter Samplers. *Atmos. Environ.* **2020**, *220*, 117067. https://doi.org/10.1016/j.atmosenv.2019.117067.

(60) Molina Rueda, E.; Carter, E.; L'Orange, C.; Quinn, C.; Volckens, J. Size-Resolved Field Performance of Low-Cost Sensors for Particulate Matter Air Pollution. *Environ. Sci. Technol. Lett.* **2023**, *10* (3), 247–253. https://doi.org/10.1021/acs.estlett.3c00030.
(61) L'Orange, C.; Neymark, G.; Carter, E.; Volckens, J. A High-Throughput, Robotic System for Analysis of Aerosol Sampling Filters. *Aerosol Air Qual. Res.* **2021**, *21* (11), 210037. https://doi.org/10.4209/aaqr.210037.
(62) Hewett, P.; Ganser, G. H. A Comparison of Several Methods for Analyzing Censored Data. *Ann. Occup. Hyg.* **2007**, *51* (7), 611–632. https://doi.org/10.1093/annhyg/mem045.
(63) Wendt, E. A.; Quinn, C. W.; Miller-Lionberg, D. D.; Tryner, J.; L'Orange, C.; Ford, B.; Yalin, A. P.; Pierce, J. R.; Jathar, S.; Volckens, J. A Low-Cost Monitor for Simultaneous Measurement of Fine Particulate Matter and Aerosol Optical Depth – Part 1: Specifications and Testing. *Atmospheric Meas. Tech.* **2019**, *12* (10), 5431–5441. https://doi.org/10.5194/amt-12-5431-2019.
(64) Ford, B.; Pierce, J. R.; Wendt, E.; Long, M.; Jathar, S.; Mehaffy, J.; Tryner, J.; Quinn, C.; van Zyl, L.; L'Orange, C.; Miller-Lionberg, D.; Volckens, J. A Low-Cost Monitor for Measurement of Fine Particulate Matter and Aerosol Optical Depth – Part 2: Citizen-Science Pilot Campaign in Northern Colorado. *Atmospheric Meas. Tech.* **2019**, *12* (12), 6385–6399. https://doi.org/10.5194/amt-12-6385-2019.
(65) Wendt, E. A.; Quinn, C.; L'Orange, C.; Miller-Lionberg, D. D.; Ford, B.; Pierce, J. R.; Mehaffy, J.; Cheeseman, M.; Jathar, S. H.; Hagan, D. H.; Rosen, Z.; Long, M.; Volckens, J. A Low-Cost Monitor for Simultaneous Measurement of Fine Particulate Matter and Aerosol Optical Depth – Part 3: Automation and Design Improvements. *Atmospheric Meas. Tech.* **2021**, *14* (9), 6023–6038. https://doi.org/10.5194/amt-14-6023-2021.
(66) A. Wendt, E.; Ford, B.; Cheeseman, M.; Rosen, Z.; R. Pierce, J.; H. Jathar, S.; L'Orange, C.; Quinn, C.; Long, M.; Mehaffy, J.; D. Miller-Lionberg, D.; H. Hagan, D.; Volckens, J. A National Crowdsourced Network of Low-Cost Fine Particulate Matter and Aerosol Optical Depth Monitors: Results from the 2021 Wildfire Season in the United States. *Environ. Sci. Atmospheres* **2023**, *3* (10), 1563–1575. https://doi.org/10.1039/D3EA00086A.
(67) De Hoogh, K.; Chen, J.; Gulliver, J.; Hoffmann, B.; Hertel, O.; Ketzel, M.; Bauwelinck, M.; Van Donkelaar, A.; Hvidtfeldt, U. A.; Katsouyanni, K.; Klompmaker, J.; Martin, R. V.; Samoli, E.; Schwartz, P. E.; Stafoggia, M.; Bellander, T.; Strak, M.; Wolf, K.; Vienneau, D.; Brunekreef, B.; Hoek, G. Spatial PM2.5, NO2, O3 and BC Models for Western Europe – Evaluation of Spatiotemporal Stability. *Environ. Int.* **2018**, *120*, 81–92. https://doi.org/10.1016/j.envint.2018.07.036.
(68) Evangelopoulos, D.; Katsouyanni, K.; Keogh, R. H.; Samoli, E.; Schwartz, J.; Barratt, B.; Zhang, H.; Walton, H. PM2.5 and NO2 Exposure Errors Using Proxy Measures, Including Derived Personal Exposure from Outdoor Sources: A Systematic Review and Meta-Analysis. *Environ. Int.* **2020**, *137*, 105500. https://doi.org/10.1016/j.envint.2020.105500.
(69) Dedoussi, I. C.; Eastham, S. D.; Monier, E.; Barrett, S. R. H. Premature Mortality Related to United States Cross-State Air Pollution. *Nature* **2020**, *578* (7794), 261–265. https://doi.org/10.1038/s41586-020-1983-8.
(70) Huang, J.; Pan, X.; Guo, X.; Li, G. Health Impact of China's Air Pollution Prevention and Control Action Plan: An Analysis of National Air Quality Monitoring and Mortality Data. *Lancet Planet. Health* **2018**, *2* (7), e313–e323. https://doi.org/10.1016/S2542-5196(18)30141-4.
(71) Hennig, C. Fpc: Flexible Procedures for Clustering, 2024. https://cran.r-project.org/web/packages/fpc/index.html (accessed 2025-01-06).
(72) Ester, M.; Kriegel, H.-P.; Xu, X. A Density-Based Algorithm for Discovering Clusters in Large Spatial Databases with Noise. **1996**.
(73) State of Global Air 2024. Special Report. *Health Eff. Inst.* **2024**.
(74) Shupler, M.; Balakrishnan, K.; Ghosh, S.; Thangavel, G.; Stroud-Drinkwater, S.; Adair-Rohani, H.; Lewis, J.; Mehta, S.; Brauer, M. Global Household Air Pollution Database: Kitchen Concentrations

and Personal Exposures of Particulate Matter and Carbon Monoxide. *Data Brief* **2018**, *21*, 1292–1295. https://doi.org/10.1016/j.dib.2018.10.120.
(75) Shupler, M.; Godwin, W.; Frostad, J.; Gustafson, P.; Arku, R. E.; Brauer, M. Global Estimation of Exposure to Fine Particulate Matter (PM2.5) from Household Air Pollution. *Environ. Int.* **2018**, *120*, 354–363. https://doi.org/10.1016/j.envint.2018.08.026.
(76) Nagpure, A. S.; Lal, R. M. PM2.5 Exposures Increased for the Majority of Indians and a Third of the Global Population during COVID-19 Lockdowns: A Residential Biomass Burning and Environmental Justice Perspective. *Environ. Res. Lett.* **2022**, *17* (11), 114017. https://doi.org/10.1088/1748-9326/ac9703.
(77) Parsons, S.; Tanner, K.; Champion, W.; Grieshop, A. The Effects of Modified Operation on Emissions from a Pellet-Fed, Forced-Draft Gasifier Stove. *Energy Sustain. Dev.* **2022**, *70*, 259–271. https://doi.org/10.1016/j.esd.2022.08.004.
(78) Fedak, K. M.; Good, N.; Dahlke, J.; Hecobian, A.; Sullivan, A.; Zhou, Y.; Peel, J. L.; Volckens, J. Chemical Composition and Emissions Factors for Cookstove Startup (Ignition) Materials. *Environ. Sci. Technol.* **2018**, *52* (16), 9505–9513. https://doi.org/10.1021/acs.est.8b02218.
(79) McFarlane, C.; Isevulambire, P. K.; Lumbuenamo, R. S.; Ndinga, A. M. E.; Dhammapala, R.; Jin, X.; McNeill, V. F.; Malings, C.; Subramanian, R.; Westervelt, D. M. First Measurements of Ambient PM2.5 in Kinshasa, Democratic Republic of Congo and Brazzaville, Republic of Congo Using Field-Calibrated Low-Cost Sensors. *Aerosol Air Qual. Res.* **2021**, *21* (7), 200619. https://doi.org/10.4209/aaqr.200619.
(80) Subramanian, R.; Kagabo, A. S.; Baharane, V.; Guhirwa, S.; Sindayigaya, C.; Malings, C.; Williams, N. J.; Kalisa, E.; Li, H.; Adams, P.; Robinson, A. L.; DeWitt, H. L.; Gasore, J.; Jaramillo, P. Air Pollution in Kigali, Rwanda: Spatial and Temporal Variability, Source Contributions, and the Impact of Car-Free Sundays. *Clean Air J.* **2020**, *30* (2). https://doi.org/10.17159/caj/2020/30/2.8023.
(81) Awokola, B.; Okello, G.; Johnson, O.; Dobson, R.; Ouédraogo, A. R.; Dibba, B.; Ngahane, M.; Ndukwu, C.; Agunwa, C.; Marangu, D.; Lawin, H.; Ogugua, I.; Eze, J.; Nwosu, N.; Ofiaeli, O.; Ubuane, P.; Osman, R.; Awokola, E.; Erhart, A.; Mortimer, K.; Jewell, C.; Semple, S. Longitudinal Ambient PM2.5 Measurement at Fifteen Locations in Eight Sub-Saharan African Countries Using Low-Cost Sensors. *Atmosphere* **2022**, *13* (10), 1593. https://doi.org/10.3390/atmos13101593.
(82) Bilsback, K. R.; Dahlke, J.; Fedak, K. M.; Good, N.; Hecobian, A.; Herckes, P.; L'Orange, C.; Mehaffy, J.; Sullivan, A.; Tryner, J.; Van Zyl, L.; Walker, E. S.; Zhou, Y.; Pierce, J. R.; Wilson, A.; Peel, J. L.; Volckens, J. A Laboratory Assessment of 120 Air Pollutant Emissions from Biomass and Fossil Fuel Cookstoves. *Environ. Sci. Technol.* **2019**, *53* (12), 7114–7125. https://doi.org/10.1021/acs.est.8b07019.
(83) Shen, G.; Hays, M. D.; Smith, K. R.; Williams, C.; Faircloth, J. W.; Jetter, J. J. Evaluating the Performance of Household Liquefied Petroleum Gas Cookstoves. *Environ. Sci. Technol.* **2018**, *52* (2), 904–915. https://doi.org/10.1021/acs.est.7b05155.
(84) Pope, D.; Johnson, M.; Fleeman, N.; Jagoe, K.; Duarte, R.; Maden, M.; Ludolph, R.; Bruce, N.; Shupler, M.; Adair-Rohani, H.; Lewis, J. Are Cleaner Cooking Solutions Clean Enough? A Systematic Review and Meta-Analysis of Particulate and Carbon Monoxide Concentrations and Exposures. *Environ. Res. Lett.* **2021**, *16* (8), 083002. https://doi.org/10.1088/1748-9326/ac13ec.
(85) Puzzolo, E.; Pope, D.; Stanistreet, D.; Rehfuess, E. A.; Bruce, N. G. Clean Fuels for Resource-Poor Settings: A Systematic Review of Barriers and Enablers to Adoption and Sustained Use. *Environ. Res.* **2016**, *146*, 218–234. https://doi.org/10.1016/j.envres.2016.01.002.
(86) Johnson, M.; Pillarisetti, A.; Piedrahita, R.; Balakrishnan, K.; Peel, J. L.; Steenland, K.; Underhill, L. J.; Rosa, G.; Kirby, M. A.; D, íaz-A. A.; McCracken, J.; Clark, M. L.; Waller, L.; Chang, H. H.; Wang, J.; Dusabimana, E.; Ndagijimana, F.; Sambandam, S.; Mukhopadhyay, K.; Kearns, K. A.; Campbell, D.; Kremer, J.; Rosenthal, J. P.; Checkley, W.; Clasen, T.; Naeher, L.; null, null. Exposure Contrasts of Pregnant Women during the Household Air Pollution Intervention Network Randomized Controlled Trial. *Environ. Health Perspect.* **2022**, *130* (9), 097005. https://doi.org/10.1289/EHP10295.

(87) Presler-Jur, P.; Doraiswamy, P.; Hammond, O.; Rice, J. An Evaluation of Mass Absorption Cross-Section for Optical Carbon Analysis on Teflon Filter Media. *J. Air Waste Manag. Assoc.* **2017**, *67* (11), 1213–1228. https://doi.org/10.1080/10962247.2017.1310148.
(88) Young, B. N.; Good, N.; Peel, J. L.; Benka-Coker, M. L.; Keller, J. P.; Rajkumar, S.; Walker, E. S.; Volckens, J.; L'Orange, C.; Quinn, C.; Africano, S.; Osorto Pinel, A. B.; Clark, M. L. Reduced Black Carbon Concentrations Following a Three-Year Stepped-Wedge Randomized Trial of the Wood-Burning Justa Cookstove in Rural Honduras. *Environ. Sci. Technol. Lett.* **2022**, *9* (6), 538–542. https://doi.org/10.1021/acs.estlett.2c00098.

APPENDIX A

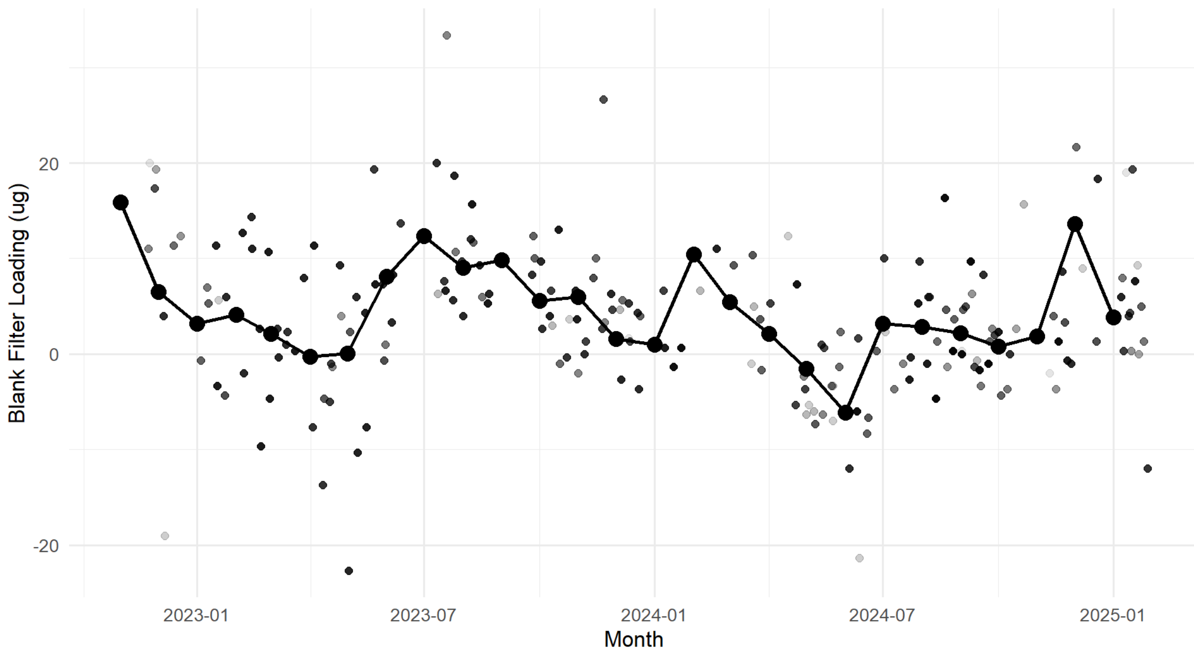

Appendix A1: UPAS Blank Filter Loadings. The small points represent each individual blank filter loading. The monthly averages are the large points connected by the line (used for filter sample background subtractions).

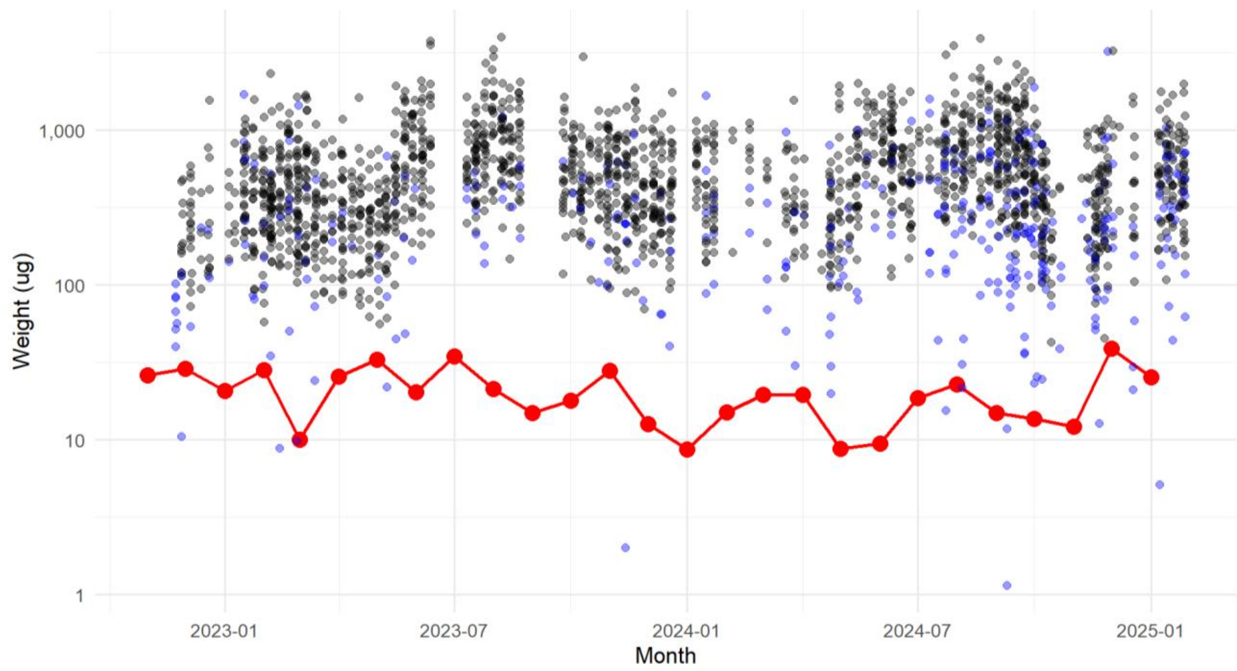

Appendix A2: The monthly calculated gravimetric limits of detection (Red) compared to sample filter loadings (black) over time. Blue points are samples that were excluded from analysis due to invalid compliance criteria.

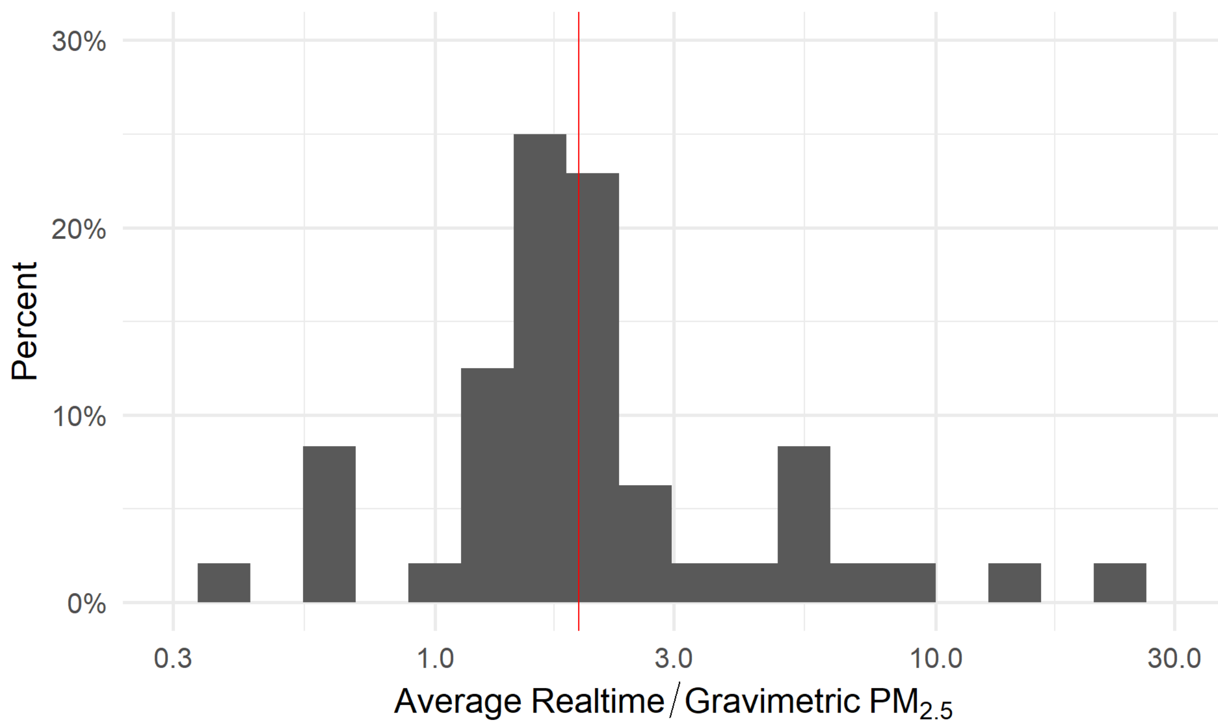

Appendix A3: AMOD Correction Ratios. A histogram of ratios for ambient samples' average Plantower, reported real-time $PM_{2.5}$ concentration (when the filter pump was on) divided by the gravimetric filter derived $PM_{2.5}$ concentration. The red line shows the median correction ratio used to correct all ambient sample's real-time $PM_{2.5}$ concentration data (1.94).

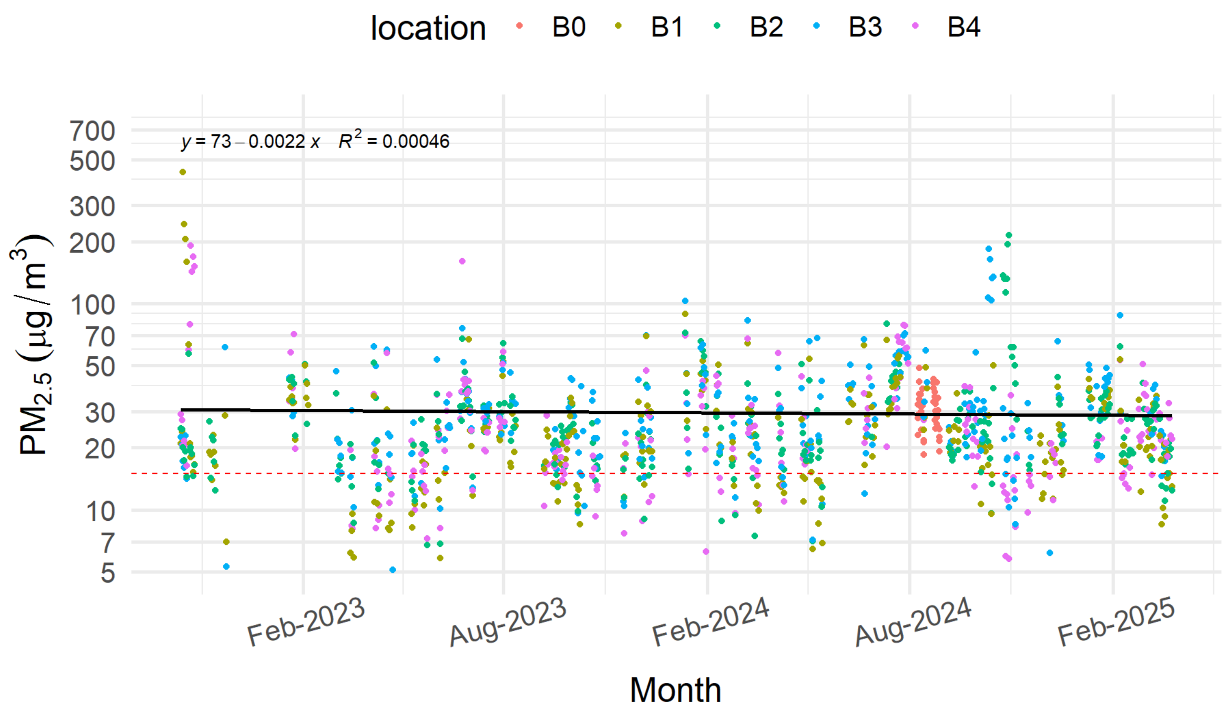

Appendix A4: Temporal distribution of daily average ambient $PM_{2.5}$ concentrations by AMOD deployment location**.** Each dot represents the filter corrected daily average ambient $PM_{2.5}$ concentration (by location). The black line shows the linear regression trend which is represented by the equation in the upper left corner of the plot (R^2 value is displayed next to the equation).

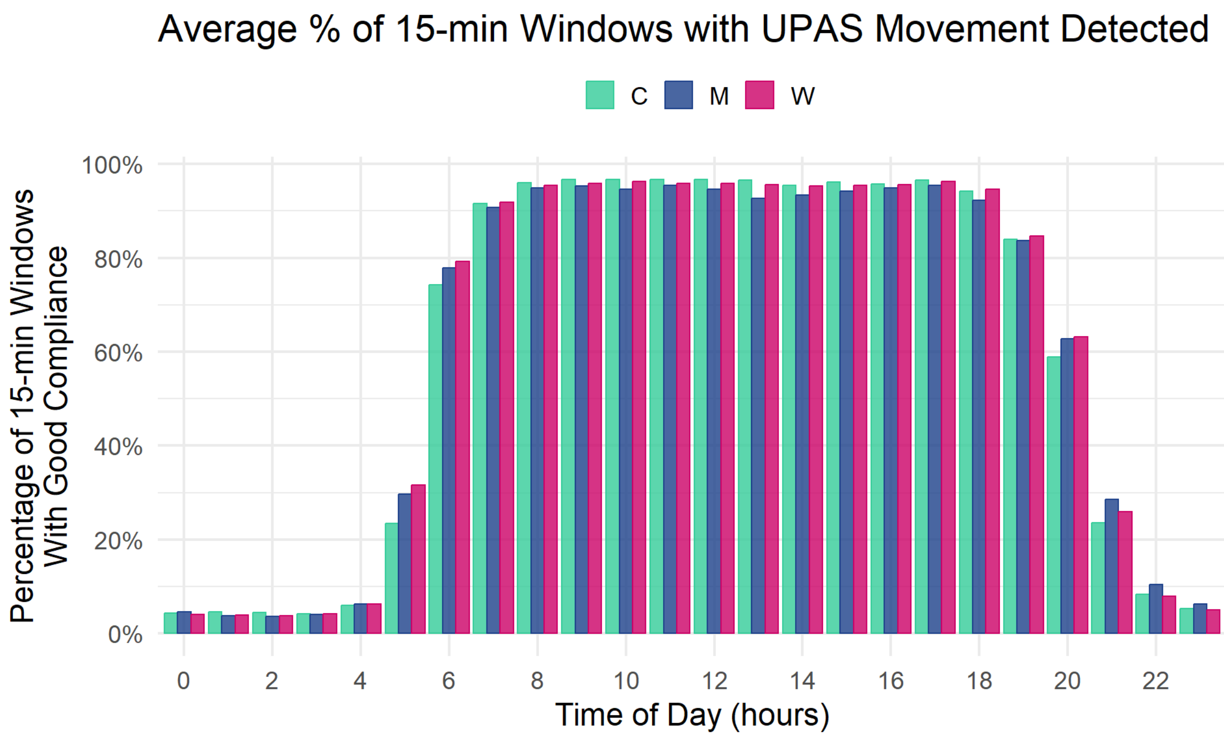

Appendix B1: UPAS Wearing Compliance by Hour of Day for the Baseline Samples. The average percentage of samples' 15-minute windows where the UPAS detected movement by demographic for each hour of the day.

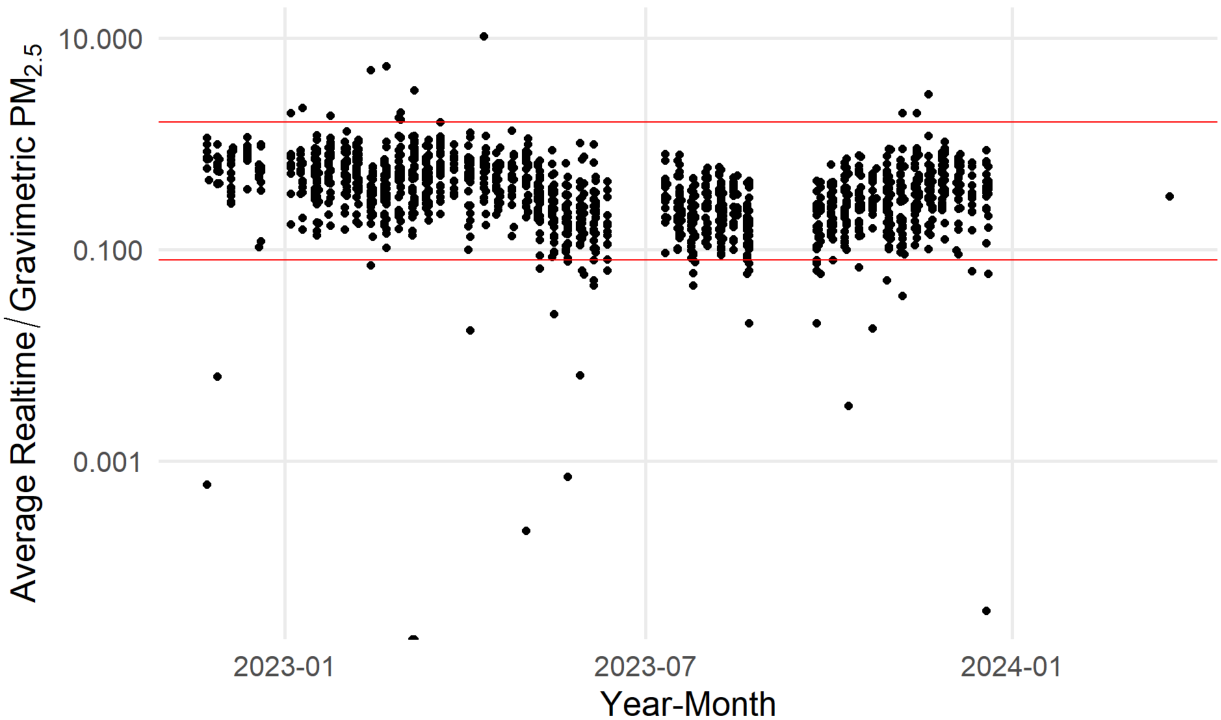

Appendix B2: UPAS Correction Ratios for Baseline Samples. Each dot represents a participant's time-averaged $PM_{2.5}$ concentration ratio between the Sensirion (real-time sensor) and the UPAS filter sample (for times when the filter pump was on). The red lines show the correction ratio thresholds, calculated as the geometric mean for the ratios +/- 2 geometric standard deviations (0.08, 1.62).

Appendix B3: Exponentiated coefficients from linear mixed effect modeling accounting for household as a random effect for examining associations between 48-hour sample average $PM_{2.5}$ concentrations ($\mu g \cdot m^{-3}$) among familial demographics (man vs. woman vs. child) as the fixed predictor variable.

Term	**Estimated Ratio**	**95% Confidence**
Intercept	201.7	(189.7, 214.4)
Women (n = 495)	0.88	(0.82, 0.94)
Man (n = 304)	0.50	(0.46, 0.54)

Appendix B4: Exponentiated coefficients from linear mixed effect modeling accounting for household as a random effect for examining associations between 48-hour sample average $PM_{2.5}$ concentrations ($\mu g \cdot m^{-3}$) among familial demographics (man vs. woman vs. boy vs. girl) as the fixed predictor variable.

Term	**Estimated Ratio**	**95% Confidence**
Intercept	199.4	(183.3, 216.9)
Boy (n = 201)	1.03	(0.91, 1.16)
Women (n = 495)	0.89	(0.81, 0.97)
Man (n = 304)	0.50	(0.45, 0.55)

Appendix B5: Exponentiated coefficients from linear mixed effect modeling examining associations between the 48-hour sample average $PM_{2.5}$ concentrations ($\mu g \cdot m^{-3}$) of children with their height, age, and gender as fixed predictor variables.

Term	Estimated Ratio	95% Confidence
Intercept	483.5	(203.8, 1,146.8)
Height	0.99	(0.98, 1.00)
Age	1.02	(0.97, 1.07)
Girl (n = 233)	1.00	(0.88, 1.13)

Appendix B6: Exponentiated coefficients from linear mixed effect modeling accounting for household as a random effect for examining associations between the average $PM_{2.5}$ concentrations ($\mu g \cdot m^{-3}$) at 19:00 among familial demographics (man vs. woman vs. child) as the fixed predictor variable.

Term	Estimated Ratio	95% Confidence
Intercept	476.6	(209.6, 259.5)
Women (n = 495)	0.68	(0.62, 0.75)
Man (n = 304)	0.50	(0.45, 0.56)

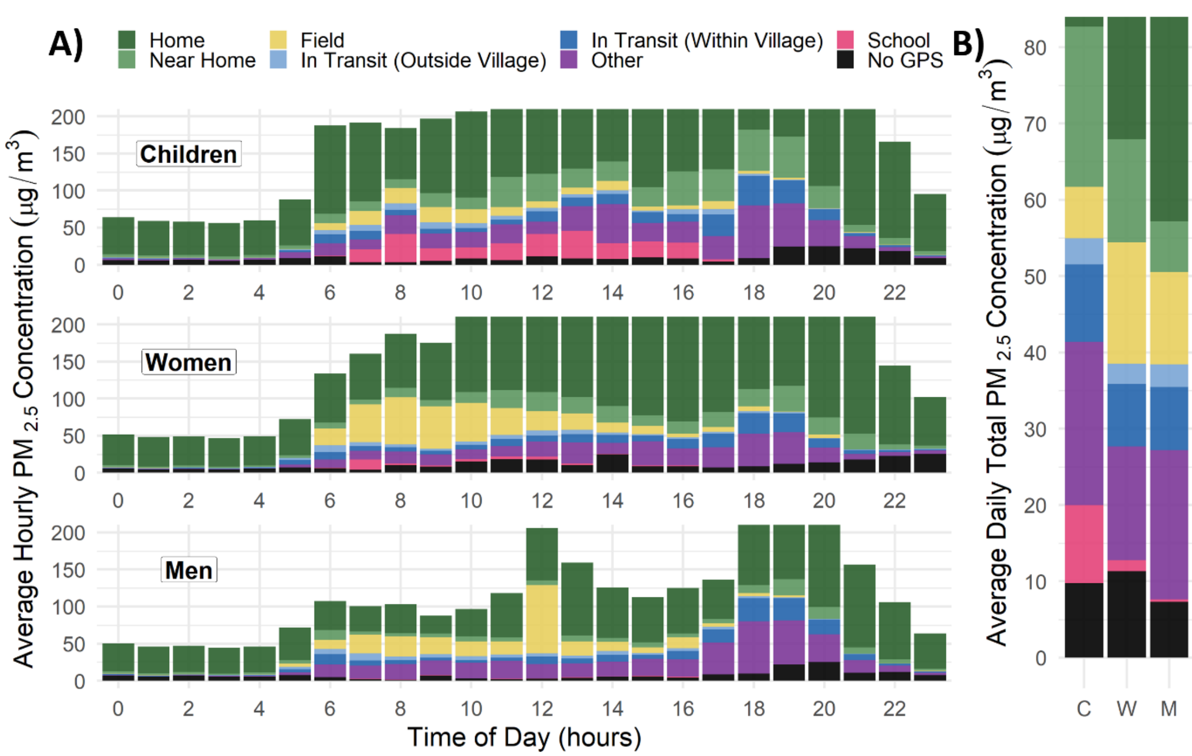

Appendix B7: (A) Zoomed in spatiotemporal distribution plot with the 'Home' environment largely cut off showing, on average, when and where different demographics received proportions of their daily $PM_{2.5}$ exposures. (B) The full 48- hour sample average $PM_{2.5}$ exposure variation between demographics among microenvironments with the 'Home' environment largely cut off. These data are only representative of weekday activity patterns, as participants were not sampled on the weekend.

Appendix B8: Exponentiated coefficients from linear mixed effect modeling accounting for household as a random effect for examining associations between the average $PM_{2.5}$ concentrations ($\mu g \cdot m^{-3}$) at 19:00 between women who were home with their child vs home without the child as the fixed predictor variable. Only one child per household had data collected.

Term	**Estimated Ratio**	**95% Confidence**
Intercept	239.8	(214.7, 267.8)
With Child (n = 434 hours)	0.96	(0.93, 0.98)

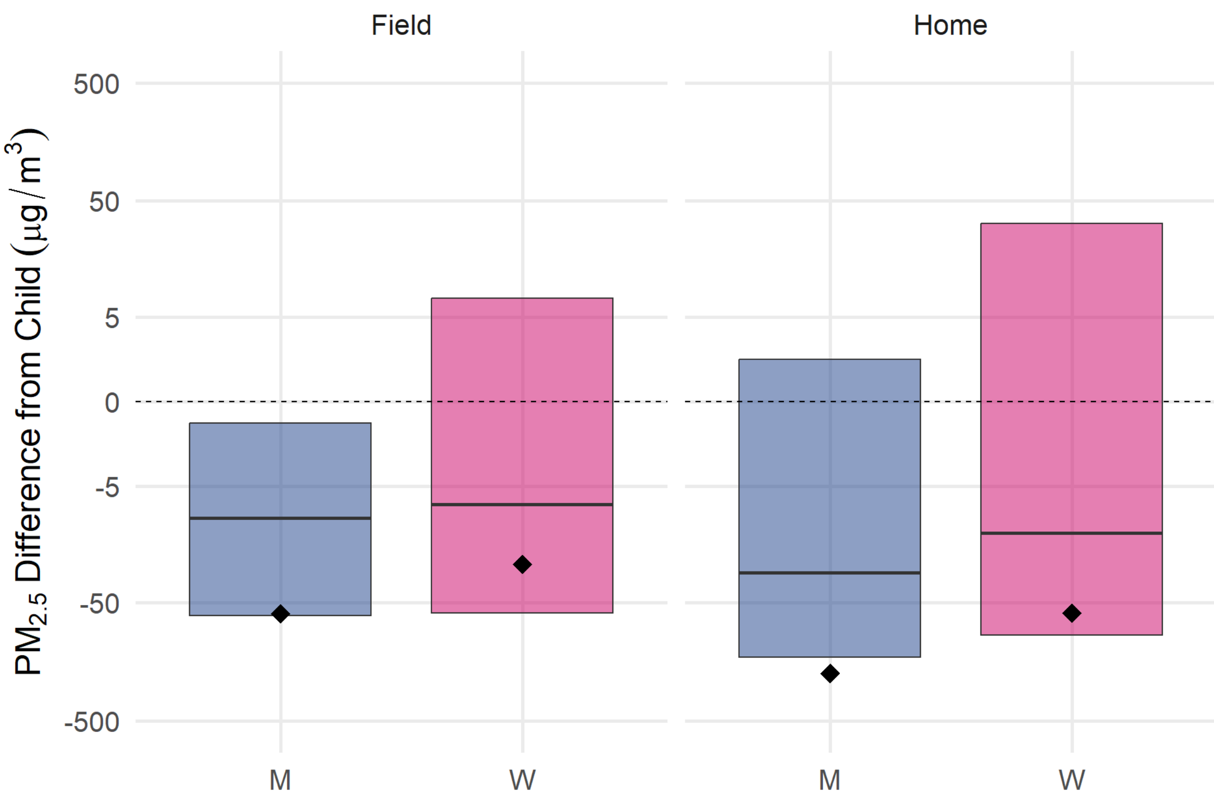

Appendix B9: The Distribution of differences in $PM_{2.5}$ exposures between adults and their adolescent children within the home and field microenvironments between the hours of 5:00 – 23:00. Boxplots represent the distribution in 30-second $PM_{2.5}$ concentration differences between adults and their children. Center lines delineate the median; boxes represent the interquartile range, and diamonds represent the average.

Appendix B10: Exponentiated coefficients from linear mixed effect modeling accounting for household as a random effect for examining associations between the average $PM_{2.5}$ concentrations ($\mu g \cdot m^{-3}$) during the wet vs. the dry season as the fixed predictor variable.

Term	**Estimated Ratio**	**95% Confidence**
Intercept	178.1	(165.35, 191.87)
Dry Season	1.30	(1.19, 1.43)

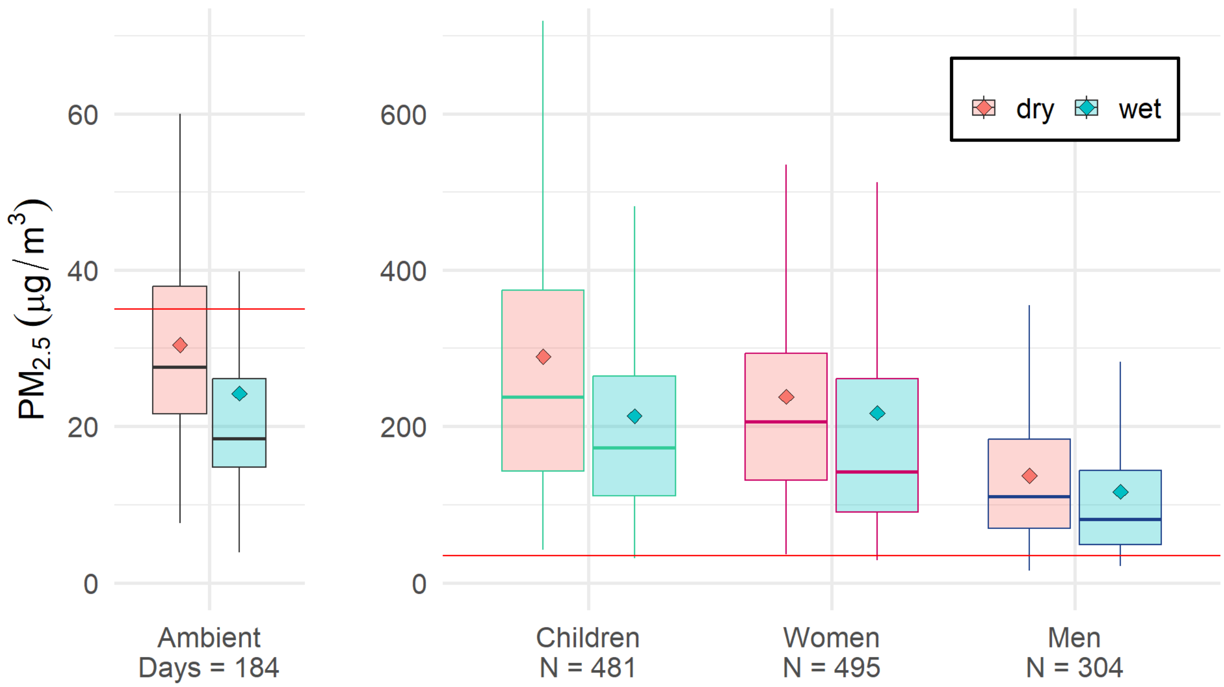

Appendix B11: $PM_{2.5}$ Concentration Distributions for Personal Exposure Samples and Ambient Air, Stratified by Season. The wet seasons are defined as the months between March and May, and September and November. Boxplots represent the average full-sample $PM_{2.5}$ concentration exposure distribution between ambient air, and men, women, and children. The salmon fill color represents the distributions in the dry season and the blue for the wet season. Center lines delineate the median; boxes represent the interquartile range, and whiskers represent the extent of observations within +/- 1.5·IQR. The red line is the WHO interim 1 target of 35 $\mu g/m^3$, and the diamonds represent the means.

Appendix B12: Exponentiated coefficients from linear mixed effect modeling examining associations between the 48-hour sample average $PM_{2.5}$ concentrations (µg·m-3) of children with their schooling vs non-schooling months as the fixed predictor variable.

Term	Estimated Ratio	95% Confidence
Intercept	373.8	(327.0, 427.2)
In-School Months	0.48	(0.40, 0.56)

APPENDIX C

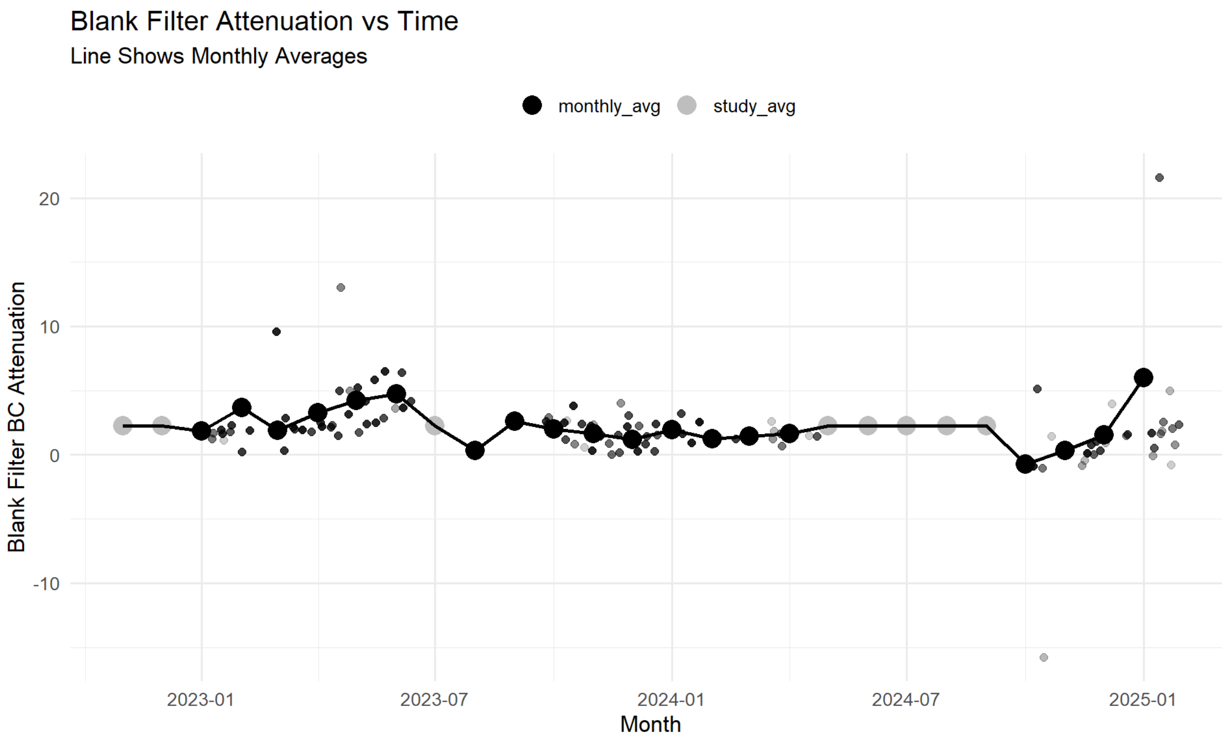

Appendix C1: UPAS Blank Filter Attenuation Loadings. The small points represent each individual blank filter attenuation. The monthly averages are the large points connected by the line (used for filter sample background subtractions). Grey coloring for the monthly average points indicates the study average was used for that month due to a lack of filter attenuation data.

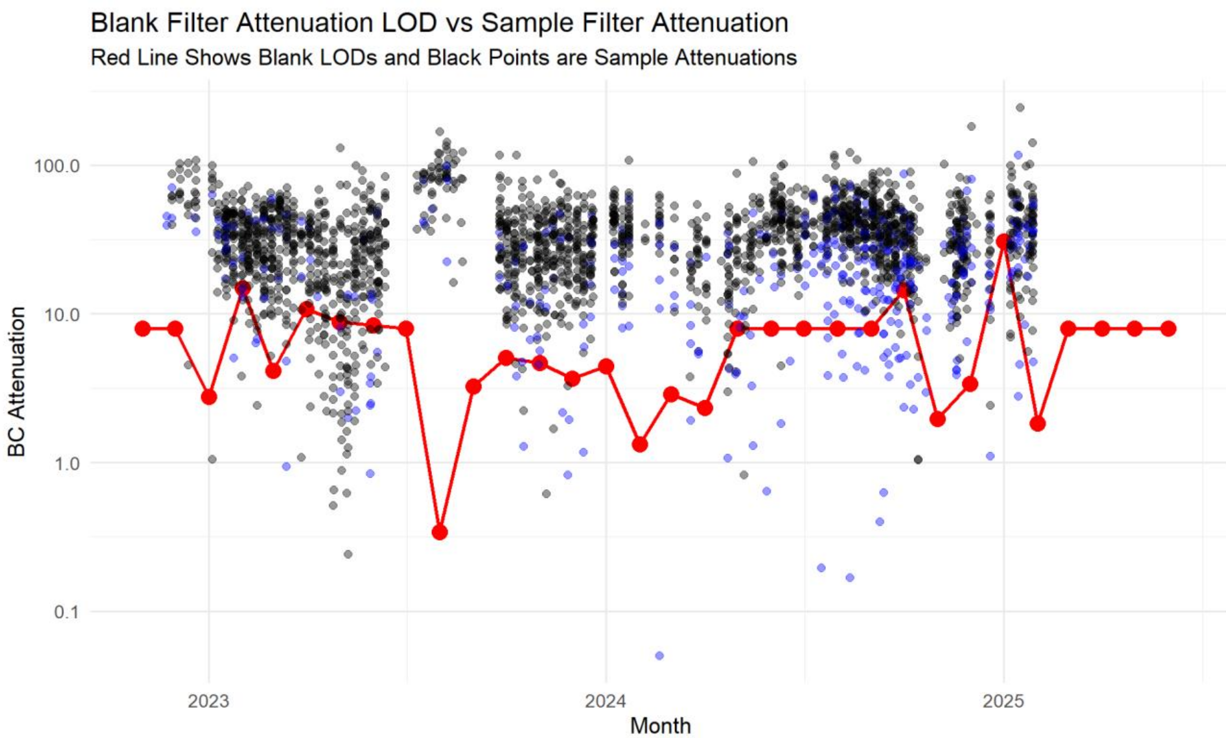

Appendix C2: The monthly calculated blank attenuation limits of detection (Red) compared to sample filter BC attenuation (black) over time. Blue points are samples that were excluded from analysis due to invalid compliance criteria.

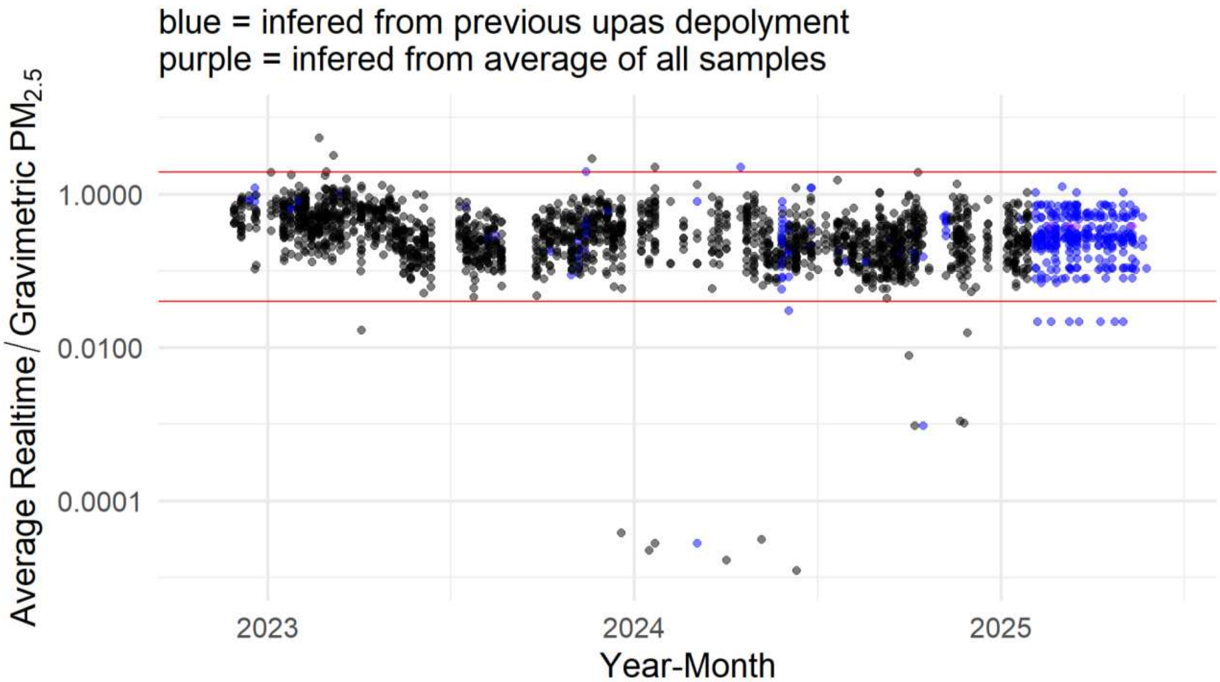

Appendix C3: UPAS Correction Ratios. Each dot represents a participant's time-averaged PM2.5 concentration ratio between the Sensirion (real-time sensor) and the UPAS filter sample (for times when the filter pump was on). The red lines show the correction ratio thresholds, calculated as the geometric mean for the ratios +/- 2 geometric standard deviations (0.04, 1.97). Black dots indicate the correction ratio was calculated using the gravimetric filter loading from the same sample, blue dots indicate the sample used the correction ratio calculated by the most recent sample using the same UPAS (for samples that have not had their filter loadings analyzed yet), and purple dots indicate the sample used the average correction ratio across all samples (for samples that never had a filter measured from the same UPAS).

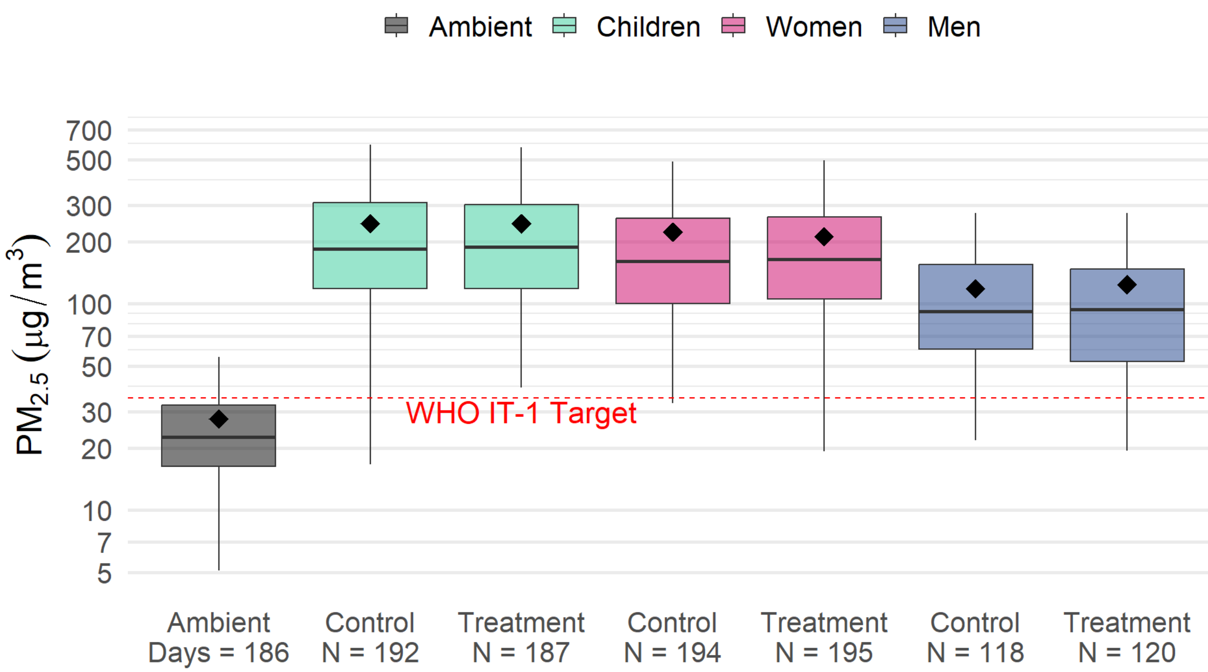

Appendix C4: Boxplots represent the average (~48-hr for personal samples, and 24-hr for ambient) $PM_{2.5}$ concentration distribution among ambient air, and personal exposure samples of men, women, and children from control and intervention groups during the baseline phase of the study. The Y-axis is logscale. The ambient box depicts the distribution of all the daily average $PM_{2.5}$ concentrations recorded across all sampling locations within the same 16-month window when these baseline phase personal exposure samples occurred. Center lines delineate the median; boxes represent the interquartile range, and whiskers represent the extent of observations within +/- 1.5·IQR. The red line is the WHO interim 1 target of 35 of $\mu g{\cdot}m^{-3}$. The black diamonds represent the means.

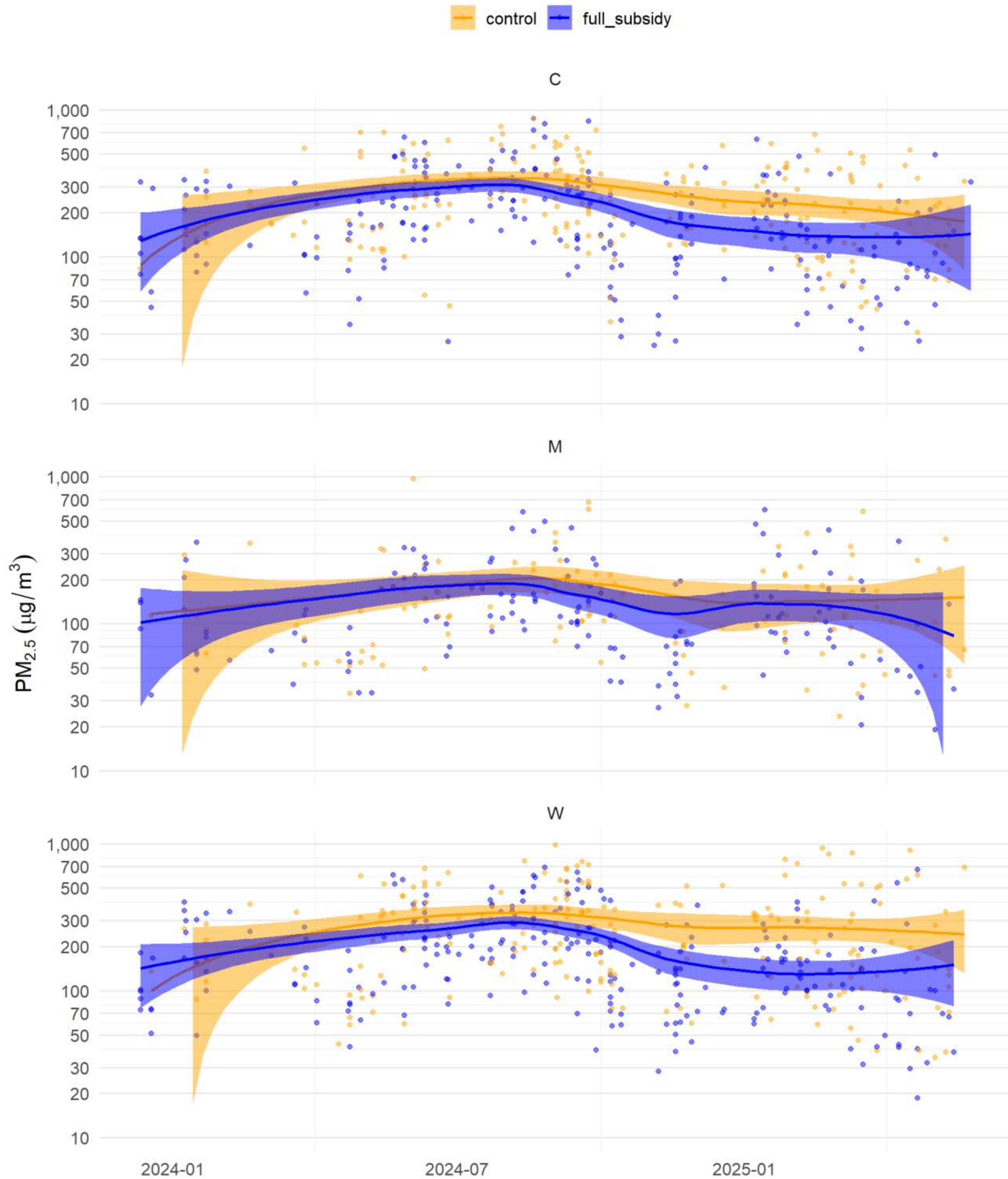

Appendix C5: Temporal Distribution in 48-hour average personal $PM_{2.5}$ exposures between intervention groups (baseline phase excluded) among the demographics.

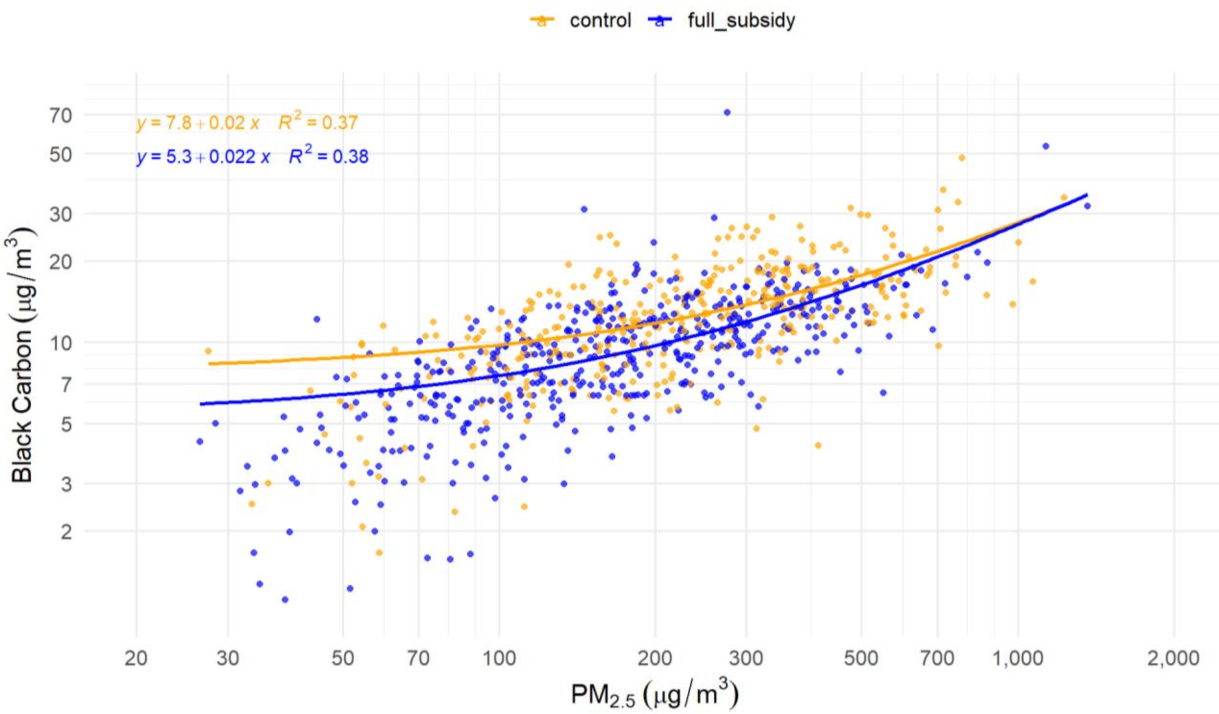

Appendix C6: Scatter plot of intervention sample's (n=819) 48-hour average $PM_{2.5}$ and BC personal exposures. The lines show the linear regression line of best fit and are curved because of the log scale used for the x- and y-axis. The equations for the regression lines along with the R^2 values are shown in the top right.

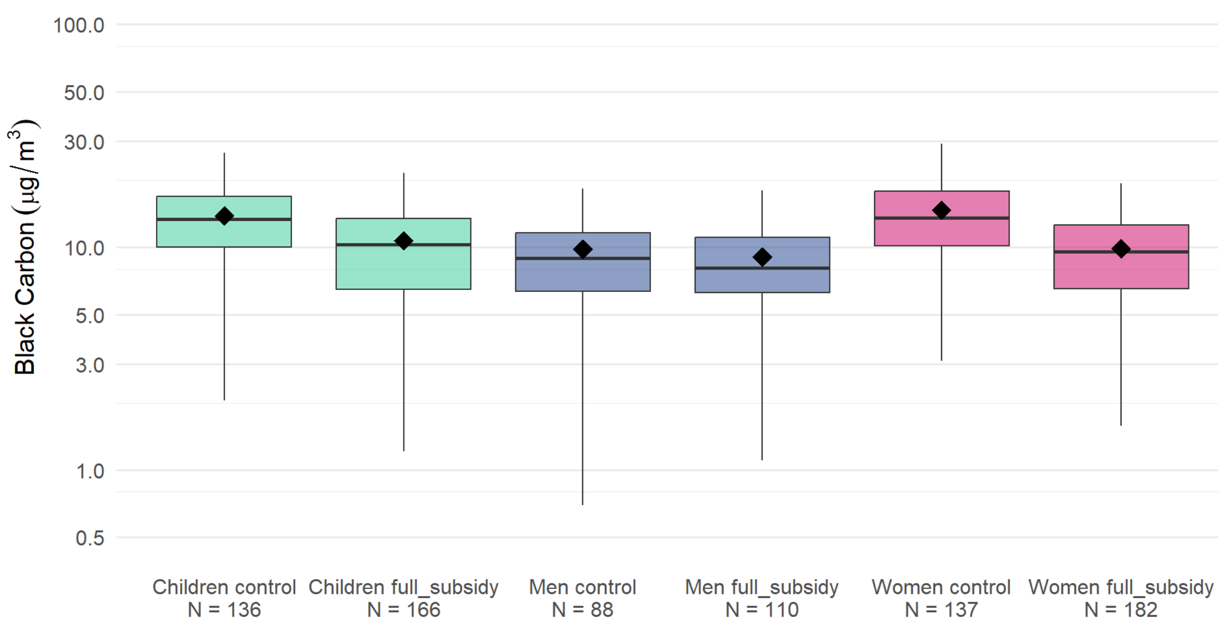

Appendix C7: Boxplots represent the average ~48-hr personal BC concentration distribution among men, women, and children for the control and treatment groups during the intervention phase of the study. The Y-axis is logscale. Center lines delineate the median; boxes represent the interquartile range, and whiskers represent the extent of observations within +/- 1.5·IQR. The black diamonds represent the means.

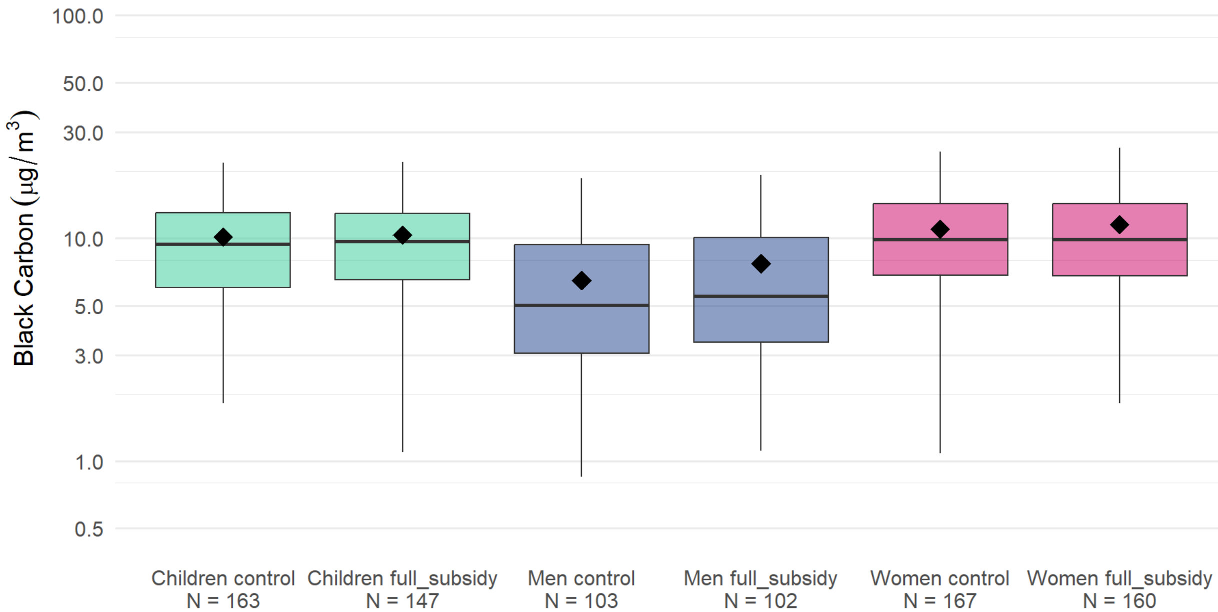

Appendix C8: Boxplots represent the average ~48-hr personal BC concentration distribution among men, women, and children for the control and treatment groups during the baseline phase of the study. The Y-axis is logscale. Center lines delineate the median; boxes represent the interquartile range, and whiskers represent the extent of observations within +/- 1.5·IQR. The black diamonds represent the means.

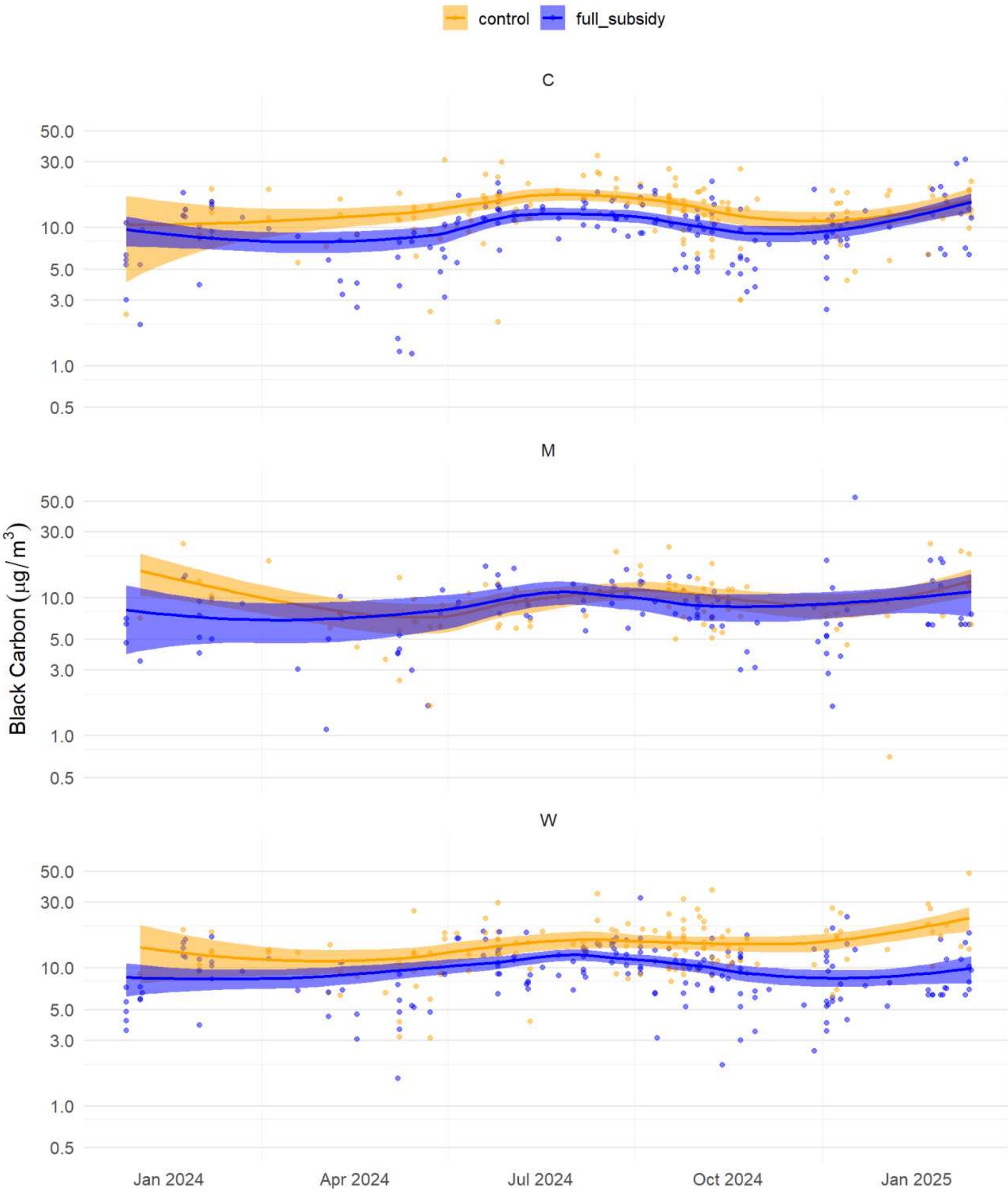

Appendix C9: Temporal Distribution in 48-hour average personal BC exposures between intervention groups (baseline phase excluded) among the demographics.

APPENDIX D: LARGE PARTICLE EMISSIONS FROM HUMAN VOCALIZATION AND PLAYING OF WIND INSTRUMENTS

D.1 Introduction

The COVID-19 pandemic has motivated a growing body of research on human respiratory aerosol generation and disease transmission associated with activities like talking, singing, and playing musical instruments.[1–13] To date, most of this research has focused on smaller particles (aerodynamic particle diameter, $d_p < 10$ μm), which are relatively easy to count and size using conventional instruments like optical particle counters and aerodynamic particle sizers.[14] Smaller particles are important because they can remain airborne for hours, travel distances beyond typical "close-contact" thresholds used in disease control guidance (~2 m), and have been shown to transmit infectious pathogens in air.[7,15]

However, larger particles ($d_p > 10$ μm) are also emitted during the same respiratory aerosol generation processes. Larger particles remain airborne for only seconds to minutes and are emitted at lower rates than their smaller counterparts; however, their mass emissions far outweigh those of smaller particles. Thus, larger particles have the potential to harbor more pathogens, on a per-particle basis, which could result in a more concentrated dose delivered to a given cell/receptor.[16–18] Pathogens transported within large particles may also remain viable for longer periods of time than smaller ones due to their substantially longer evaporation times in typical room air conditions;[6] these characteristics may also allow them to serve as vectors for fomite transmission, after depositing onto a surface that is later contacted by a new host.[7,19] Additionally, some respiratory diseases are more commonly transmitted via larger particles than smaller ones.[18] Therefore, it is important to characterize emissions rates for all particle sizes.

Conventional aerosol counting and sizing instruments are limited in their ability to measure larger particles because such particles have a relatively high inertia in air (i.e., they experience high rates of aspiration and transmission losses during sampling).[20] Open-path laser instruments have been used to size larger airborne particles[9,17], but such measurements are considered semi-quantitative, especially under turbulent flow conditions (e.g., during vocalization). For example, Standnytskyi et al. reported emissions rates of large and small particles emitted from 25 seconds of talking; however, these size-resolved results are considered semi-quantitative because there was no effective way to equate scattered light intensity to particle size, since light intensity varied across the laser sheet. They referred to the top 25% of the brightest light scattering particles as large, and the remainder as small.

This measurement challenge has produced a gap in understanding of large particle emissions from various human activities. Several previous studies have sought to characterize the full spectrum of aerosol sizes,[9,17,21–25] but these experiments were limited by small sample sizes ($n < 12$) and mainly focused on emissions from talking, with little variation in the type of speech and articulation investigated. A recent study by Harrison et al.[5] utilized a larger cohort of participants to investigate large particle emissions from speech ($n = 43$) and singing ($n = 26$), but did not consider emissions from any musical instruments or the effect of face coverings.

The objective of this work was to characterize large respiratory aerosol ($35 < d_p < 100$ μm) and droplet ($d_p > 100$ μm) emissions from a panel of individuals ($n = 70$) of varying age and sex while talking, singing, and playing various wind instruments. A secondary objective was to examine the efficacy of face masks and instrument bell covers (i.e., single layered spandex-like woven fabric covers that fit tightly around the instrument bell) at mitigating these emissions. The cutoff at 35 μm used here is based on the upper size limit of detection for the measurement techniques used in the Good et al. 2021 and Volckens et al. 2022 studies, which characterized small particle emissions ($0.25 < d_p < 35$ μm) from the same set of vocalization and instrument performances, and because particles smaller than 35 μm are difficult to detect using the low-magnification optical methods employed here.

D.2 Methods

D.2.1 Data Collection

Data were collected from a panel of healthy volunteers as part of the CSU Performing Arts Aerosol Study.[26,27] Participants were recruited in equal proportions of minors (aged 12- 17 years at the time of participation) and adults (age 18 years and older at the time of participation); aiming for an equal distribution of participants across types of musical instruments and skill level. For the safety of staff and participants, people were excluded from the study if they were currently experiencing COVID-19 symptoms, had a COVID-19 diagnosis in the past month, or had close contact with an infected person in the previous two weeks (consistent with state and local quarantine protocols at the time). Participants brought in their own musical instruments and face masks which varied in type from homemade cotton and other types of fabric materials, to surgical-style masks. Upon arrival, participants provided written informed consent, or assent if a minor (along with consent from their legal guardian), as detailed by the US regulatory guidelines for research on human subjects (CSU approval #20-10174H). They also provided information on their height, weight, age, and sex. Additional information on the study procedures can be found in previous publications.[26,27]

Participants donned polypropylene disposable coveralls (McMasterCarr, IL) and hair nets to minimize particle emissions from their clothing and hair. Participants then entered a 3.45 m x

2.8 m x 2.45 m clean-room environment, with low background particle ($0.25 < d_p < 35$ μm) concentration (~5 cm^{-3}) and a high, HEPA-filtered, air circulation rate (~8.5 air changes per hour).[26,28] Temperature and humidity were recorded in the clean room using LabVIEW (National Instruments, TX, version 21.0, https://www.ni.com/en-us/shop/labview.html) instrument control and data acquisition software. Over the course of a 2-hr measurement period, participants either sang or played their instrument (using provided sheet music) into an aerosol sampling inlet cone both with and without masks or bell covers, and everyone ended their sessions with a 4-min period of reading out loud (no mask) from a predetermined passage, as previously described.[26,27]

Participants were asked to position their instrument bells or mouths (if talking or singing), right at the entrance plane of the inlet cone (Figure S1 and S2), so that all particle emissions were entrained into the cone's sampled airflow (10 $L \cdot min^{-1}$). However, as noted above, particles larger than ~35 μm in aerodynamic diameter are likely to settle under the force of gravity prior to reaching the aerosol sizing equipment. Therefore, the lower half of the inlet cone was arrayed with seven 5 cm x 7.5 cm water-sensitive paper (WSP) cards (TeeJet Technologies Water Sensitive Paper Spraying Systems Co.). The card array was affixed to a single magnetic tray to streamline the process of setup and takedown, as shown in Figure S3. These cards undergo a permanent change of color when they come into contact with water (see Figure 1A), allowing each liquid particle that lands on the WSP surface to be imaged, sized, and counted under a microscope.

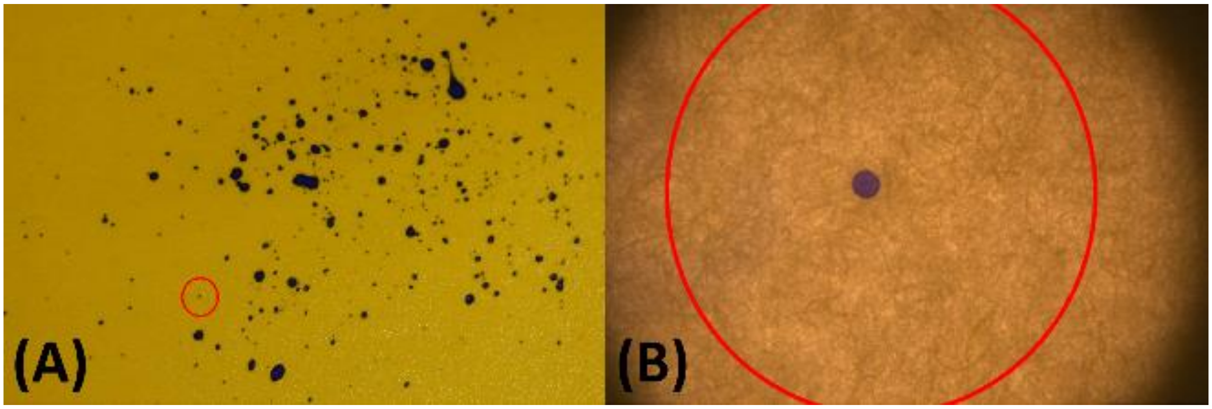

Figure 1. Example of staining on WSP cards (Not from an actual participant performance set). **(A)** Full WSP card with example of staining. **(B)** Microscope image of one salivary spot on a WSP card.

One tray (each tray consists of 7 WSP cards) was collected for each of three different "performance sets" per participant: (1) singing (if vocalist) or playing an instrument (if musician) without a mask/bell cover, (2) singing or playing an instrument with a mask/bell cover, and (3) talking without a mask. For 25 participants, an additional "blank" WSP card set was collected as a negative control. The blank WSP cards were taped to the magnetic inlet cone tray the same way as for the normal performance sets, but these trays were left in an open container placed on a table within the clean room approximately 4 feet away from the inlet cone for the duration of a participant's time in the clean room.

D.2.2 Data Analysis

After each session, WSP cards were air-dried for 20 minutes and then stored in plastic zip-lock bags. Spots on the WSP cards were imaged with a Leitz Orthoplan microscope (85X magnification) fitted with a Progres Gryphax (NAOS 20.0MP CMOS Color, Feasterville, PA) digital camera. Under these settings, the smallest and largest spot sizes that could be resolved were 18 and 1,770 μm in diameter, respectively. Each card was divided into 36 possible grid cells, and a random number generator selected 15 cells for imaging (105 images per set).

Collected images were analyzed with ImageJ software (version 1.51, https://imagej.nih.gov/ij/all-notes.html) to quantify the area of each spot, using methods described in Woolf et al.[29] Briefly, a color thresholding algorithm was developed in ImageJ to detect the edges of the blue spot stains against the yellow WSP card backgrounds. To optimize this algorithm, spot stains for 29 WSP cards were counted manually under a microscope and RGB color thresholds were adjusted to minimize the mean absolute error between the number of spots counted manually and with the color thresholding algorithm. The final iteration of this algorithm produced a mean absolute error of +/- 3% for the test set. No adjustments were made for overlapping spots because the spot density was too low on each card for spot overlap to be a problem. See Figure S4 for an example of the results from this algorithm.

Data on spot count, size, and location were imported into R, version 4.0.2, (https://www.r-project.org/) for further analysis. A spread-factor equation

$$d_p = 1.364e^{-5}d_s + 0.4443d_s - 1.4758 \qquad (1)$$

was used to convert spot diameter (d_s) to aerodynamic particle diameter (d_p) at the time of impact, following the calibration provided by Harrison et al.[5] To estimate the original emitted particle diameters, we modeled the change in diameter between the point of release and WSP contact using a deterministic model (2.5 ms time-steps) based on the rate of particle evaporation

$$\frac{d(d_p)}{dt} = \frac{4DM}{R\rho_p d_p}\left(\frac{P_g}{T_g} - \frac{P_d}{T_d}\right) \qquad (2)$$

and particle settling

$$V_{TS} = \frac{\rho_p d_p^2 g C_c}{18\eta} \qquad (3)$$

where d_p is the particle aerodynamic diameter, D is the molecular diffusivity of water vapor in air at 293K, M is the molecular weight of water, R is the universal gas constant, ρ_p is the density of liquid saliva,[30] P_g is the vapor pressure of water at ambient conditions, T_g is the ambient temperature, P_d is the vapor pressure of water at the particle's surface, T_d is the temperature at the particle's surface, V_{TS} is the particle terminal settling velocity, g is the acceleration due to gravity, C_c is the Cunningham Correction factor, and η is the dynamic viscosity of air.[31]

Ambient RH was measured by an Omega Engineering HX92BC series sensor in the room about 1.5 m from the inlet cone. A 6-cm travel distance between the WSP and the emission point was assumed for all particles. This distance was chosen based on observations of the typical distance between a participant's mouth/instrument bell and the center of the WSP card trey. Participants were reminded to keep their instrument bells or mouths as close to the entrance plane of the inlet cone as possible at the beginning of each performance set (2-3 cm from the center of the WSP trey); however, this distance inevitably fluctuated during performances, and a 6 cm distance was observed as the average across all participant performance sets. Sensitivity analyses (Figures S5) indicated that the a 6-cm (assumed) travel distance had minimal impact on size-resolved results, only producing a maximum error of +/- 4 µm for the smallest, most sensitive, size bin measured when varying the assumed travel distance between 3 – 9 cm. Particle counts were aggregated into log-equivalent size bins based on their aerodynamic diameters at their point of release and summed for each participant and card location. Counts were then blank-corrected, by size, and extrapolated to each card's total surface area.

To estimate the full-plume emission rates, we interpolated the spatial distribution of summed particle counts, grouped by activity and size bin, between the 7 card locations and then extrapolated this pattern across our measurement domain using a bicubic spline extrapolation (R

Akima::interp function; see SI for additional information). The extrapolated area consisted of the lower half of the sampling inlet cone and extended approximately 17 cm downstream into the sampling duct. Figure S9 provides an example of the bicubic spline extrapolation output for the talking performance sets. Each facet in this figure represents a size bin and the number in parenthesis on top of each tile shows the extrapolation coefficient for that size bin. These coefficients were calculated by dividing the average number of particles estimated with the bicubic spline extrapolation by the average number of particles detected experimentally for each size bin and activity type and were then multiplied by the background corrected and surface-area-ratio expanded counts for each individual performance set. Table S1 summarizes average experimentally detected counts vs the average bicubic spline extrapolated counts for each activity. These calculations resulted in estimates for the total count and size distribution of each participant's performance set at the point of release. Particle emission rates are reported as total counts (i.e., total number of particles divided by the event duration, $\#\cdot min^{-1}$), size-resolved counts ($\#\cdot min^{-1}$ per size bin), and total mass (i.e., converting the size-resolved counts to mass, assuming particle density[30] of 1,007 $kg\cdot m^{-3}$ and taking the sum, $\mu g\cdot min^{-1}$).

Linear mixed models were developed to examine associations between large-particle emissions and the following variables: instrument type (brass vs. woodwind), participant age (adult vs. minor), and sex (male vs. female). The estimated variance for the participant-specific random effect was zero, indicating no correlation between an individual's talking and instrument playing (or singing) emissions rates. Models that additionally adjusted for instrument or vocalization class (i.e. brass, woodwind, talking, or singing) were fit to assess pairwise differences between classes with Tukey adjustment. These models were only developed for the instruments (no bell cover), singing (no masks), and the talking performance sets due to small sample sizes in the other performance set types. Emission rates were log-transformed to meet model assumptions. The models took the form:

$$Y_{ij} = \beta_0 + \boldsymbol{\beta}^T \boldsymbol{X}_i + \alpha_i + \epsilon_{ij}$$

where Y_i is the log-transformed emission rate for the *j*th measurement from the *i*th participant, $\mathbf{X}_i$ is the set of fixed predictor variables, $\boldsymbol{\beta}$ is the vector of coefficients for the predictor variables, α_i is a random intercept term for participant *i*, and ϵ_{ij} represents the residual model error (assumed to have a mean of zero, be normally distributed, and have constant error variance).

We additionally assessed the ability of age, sex, CO_2 emissions, and loudnes (dBA) to explain variation in large particle emissions by calculating the coefficient of determination (i.e. R^2) from multiple linear regression models fit separately to the instrument and talking datasets.

D.3 Results and Discussion

Data were collected from 70 participants (37 adults and 33 minors). Of these, 31 (44%) were female (self-reported sex assigned at birth), and 39 were male (56%). A total of 168 performance sets were examined: 52 from talking, 11 from singing without a mask, 48 from instrument playing without a bell cover, 4 from singing with a mask, 28 from instrument playing with a bell cover, and 25 blank sets. A breakdown for all the performance set types is provided in Table S2. Descriptive statistics for count and mass emission rates (for non-mask/bell cover performance sets), as a function of performance set type and participant demographics, are shown in Table 1. Large particle emissions varied substantially among performers and within each type of performance set, consistent with prior studies, as shown in Figure 2.

Table 1. Descriptive Statistics for Count Emission Rates (#·min^{-1}) and Mass Emission Rates (µg·min^{-1}) as a Function of Performance Set Type and Participant Demographics for non-mask/bell cover performance sets.

	Large Particles per Minute (#·Min^{-1})							
	Brass	**Woodwinds**	**Singing**	**Talking**	**Adults**	**Minors**	**Females**	**Males**
Geometric Mean	3.8	5.6	54.3	95.1	26.8	22.5	23.8	25.4
Geometric SD	3.1	2.9	3.3	3.8	6.7	6.6	6.8	6.5
Minimum	1.0	1.0	5.0	1.0	1.2	0.7	0.7	1.2
25%	1.5	2.4	33.3	57.2	6.6	4.2	3.7	6.0
Median	3.4	4.0	93.0	93.0	38.9	26.8	39.1	25.5
75%	7.0	10.9	117.0	231.8	145.1	91.2	91.0	145.4
Maximum	27.6	51.7	162.3	710.6	591.2	710.6	656.8	710.6
	Large Particle Mass per Minute (µg·Min^{-1})							
	Brass	**Woodwinds**	**Singing**	**Talking**	**Adults**	**Minors**	**Females**	**Males**
Geometric Mean	0.2	0.4	31.7	40.1	5.9	3.9	5.4	4.4
Geometric SD	3.2	6.4	6.1	10.3	23.6	21.2	25.0	20.6
Minimum	0	0	0	0	0.1	0	0	0.1
25%	0.1	0.2	26.1	11.3	0.4	0.2	0.2	0.3
Median	0.2	0.3	64.7	41.9	11.2	2.7	12.8	3.7
75%	0.4	0.6	71.0	166.9	79.4	38.3	66.6	51.3
Maximum	1.7	350.6	241.3	7507.2	7507.2	4007.3	7507.2	4007.3

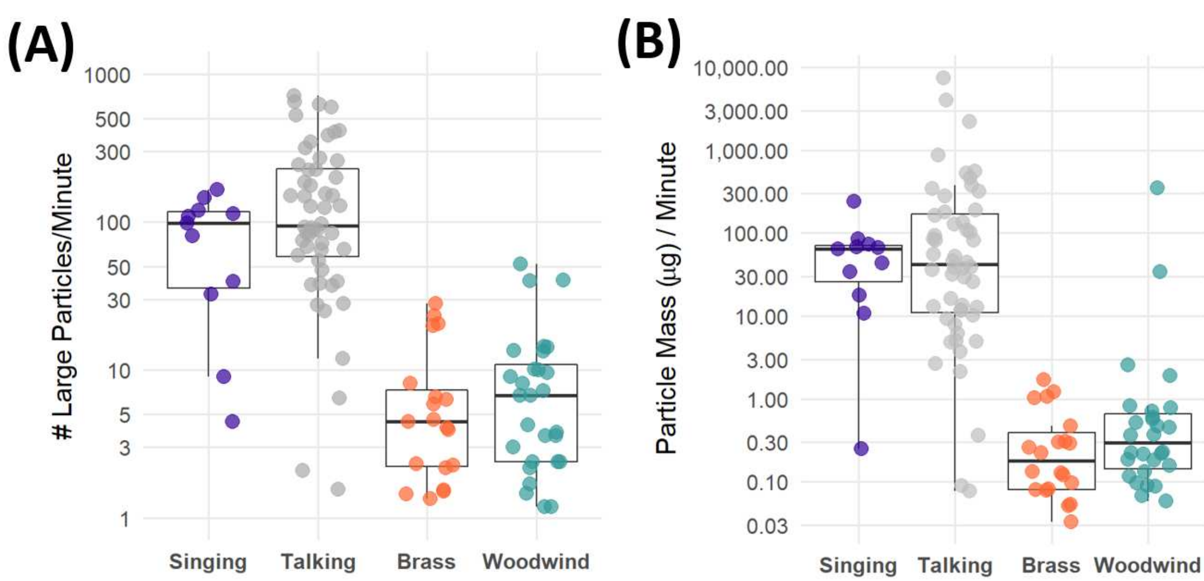

Figure 2. Boxplots of (A) count and (B) mass emission rates for large particles ($d_p > 35$ µm) from singing, talking, and playing wind instruments (for non-mask/bell cover performance sets). Center lines delineate the median, boxes represent the inter-quartile range, and whiskers represent 1.5·IQR or the data minimum. Each dot represents a participant.

For example, count emissions from talking ranged from as low as 1 min^{-1} to as high as 711 min^{-1}. This large variation also provides evidence for the existence of supper-emitters[32] (i.e people with emissions > 1 geometric standard deviation beyond the geometric mean of the data) within the large particle size range (> 35 μm), with the top 5 talking emitters (~10% of participants) accounting for nearly 35% of total talking emissions. No obvious demographic patterns were found among the highest talking emitters, with 3 minors and 2 adults, and 3 females and 2 males, though conclusions are limited with the small sample size (n=5 for the top 10% of emitters).

When examining if supperemitting tendencies for these individuals was consistent across performance activities, the data were inconclusive. Individuals who produced the highest large particle emission rates for talking were not the same individuals who produced the highest rates for their respective musical performance categories. Schlenczek et al. reported similar findings (albeit with a small sample size) in their study where the supperemitters for breathing were not the same as the supperemitters for instrument playing [9]. Future studies should utilize many replicate samples from the same individuals to gather a more statistically robust data set to better understand if superemitting tendencies for individuals are common across activity types and examine the temporal variability among these individuals.

Results show that despite the large interparticipant variability, distinct differences were evident between the emission rates for the vocalization (singing and talking) and instrument playing (brass and woodwind instruments) categories, with vocalization producing on average 19.8 times (95% CI: 12.3, 31.8) higher emission rates than instrument playing (see Table S3 for model output and Figure 2 for graphical results). These results were similar to Schlenczek et al. who reported that wind instruments produce 30-600 times lower concentrations for $d_p > 10$ μm compared with talking and singing.[9] Within the categories of vocalization and instrument playing, pairwise comparison testing indicated nonsignificant differences between taking and singing ($p = 0.57$) and between brass and woodwind instruments ($p = 0.50$), see Table S5 for model results. These non-significant differences run contrary to the previously reported results for smaller particle sizes quantified, using the same participant performance sets,[26,27] where singing had significantly higher emission rates than talking, and brass instruments had significantly higher rates than woodwind instruments.

On the other hand, for large particles, our results align with Schlenczek et al. who reported similar emission rates of $d_p > 50$ μm particles between speaking and singing.[9] We hypothesize that the discrepancy between large and small particles is the result of different generation mechanisms for these different size ranges.[22,33] Smaller respiratory particles ($d_p < 10$ μm), for example, are primarily generated via bronchial fluid film burst and vibration of the vocal folds, while larger particles ($d_p > 35$ μm) likely originate from movement of the lips and tongue during vocalization. We hypothesize two potential modes for large particle ($d_p > 35$ μm) emissions from wind instruments. The first is from saliva at and around the instrument mouthpiece and aerosolized due to "buzzing" by the player. The second is saliva accumulation within the instrument and subsequent droplet release due to vibrations of the instrument walls during playing. However, given the tortuous paths that air must follow to escape most wind instruments; this latter hypothesis seems less likely. These results, when combined with those of Volckens et al. 2022 suggest that while wind instruments produce a lot of small particles, they produce very few large particles.

McCarthy et al.[21] also examined large particle emissions from wind instruments using WSP from a panel of 9 participants. Unlike our results, they found no evidence of large particle emissions from instrument playing. Since McCarthy et al. utilized a smaller sample of participants and were testing for emissions caused only by playing single notes, it is possible that emissions were missed due to the nature of the experimental set up and size of the study. Schelenczek et al. used a holographic setup to detect large particles produced by wind instruments, and although they found no evidence of large particles emitted from the instrument bell, they detected a substantial amount of $d_p > 35$ μm particles emitted from the instrument mouthpiece, suggesting particle filtering by the instrument tubing as a main factor.[9] This filtering of large particles on the inner tubing of the instrument is supported by the Viala et al. (2022) who employed a computational fluid dynamics simulation for a clarinet and reported that particles > 50 μm will deposit inside the instrument before being emitted from the bell.[10]

From a mass standpoint, the differences in emission rates found in this study between performance set types within the categories (i.e., talking vs. singing in the vocalization category) was also insignificant. However, the difference in emission rates between the vocalization and instrument playing categories was even larger than from a particle count basis, with vocalization mass emission rates on average exceeding those for playing instruments by a factor of 132 (95% CI: 60.5, 289) (Figure 2B and Table S4), while from a count basis vocalization only exceeds emissions from instrument play by a factor of 19.8 (95% CI: 12.3, 31.8). This large difference between particle mass emission rates and particle count emission rates elucidates how vocalization performance sets produced a higher proportion of particles on the larger side of their size distribution compared to the instrument performance sets. Count emission rates as a function of particle size and performance activity are provided in Figure 3.

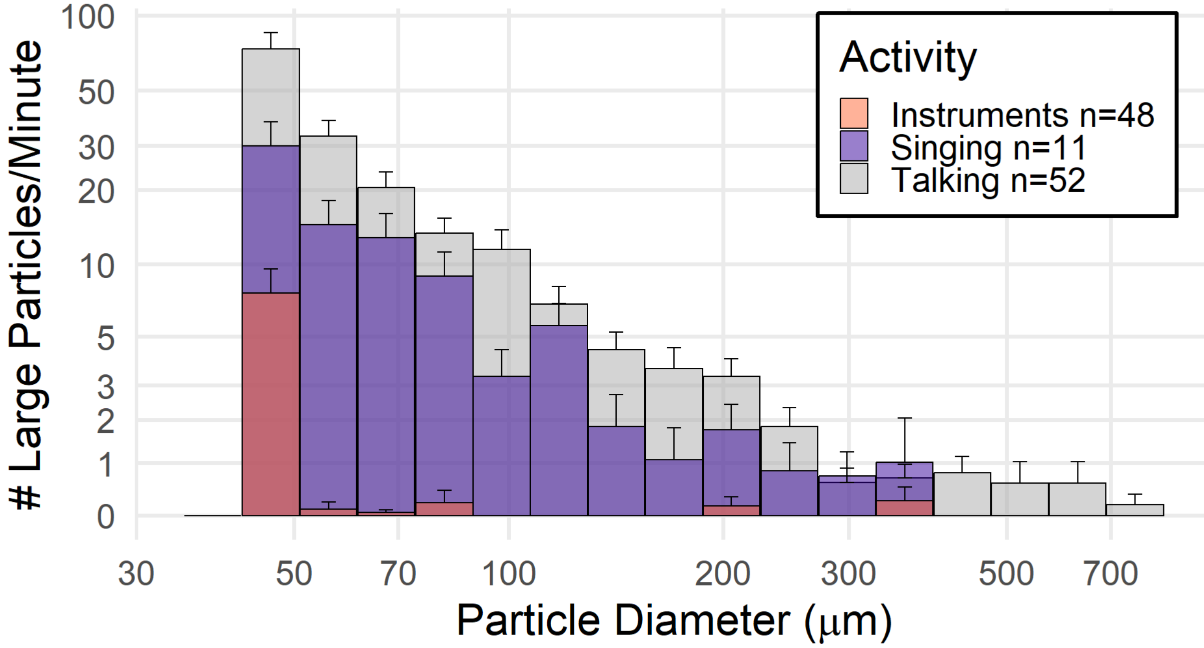

Figure 3. Large particle emission rate size distribution plot. The error bars for each size bin represent the standard error across all participants for the respective activity type.

Vocalization produced higher emission rates for every size bin, but especially towards the larger side of the size spectrum. Xie et al. measured large particle emissions produced by talking from a panel of 7 participants, using WSP cards and glass slides[23]. They determined that about 14% of count emissions came from the 40-50 μm size bin and about 28% from the 50-75 μm size bin. Our study produced about 42% of count emissions coming from the 42-51 μm size bin and about 30% from the 51-74 μm bin. Johnson et al.[22] conducted similar large particle emission quantification experiments for talking with 8 participants, but produced quite different results, finding a substantial mode for large particle emissions at 145 μm, which we did not find in this study. Similarly, Harrison et al.[5] also found no evidence for a secondary mode of large particle emissions around 145 μm. They also reported insignificant differences for count emissions between their talking and singing groups and showed large interparticipant variability between these groups. However, they reported emission rates over twice as high (median values of spanning 227 – 276 particles per minute among their taking, singing, and child adult cohorts) than we found. This discrepancy may be due to differences in experimental set up and natural variation between study populations.

Because this study on large particle emissions was run concurrently to the Good et al.[26] study that focused on small particle emissions from vocalization ($0.25 < d_p < 35$ µm), there were 42 participants who provided talking data for both small and large particle emissions (spanning a size range from 0.25 to 1000 µm). Differences between the count and mass emission rates for these participants are shown in Figure 4.

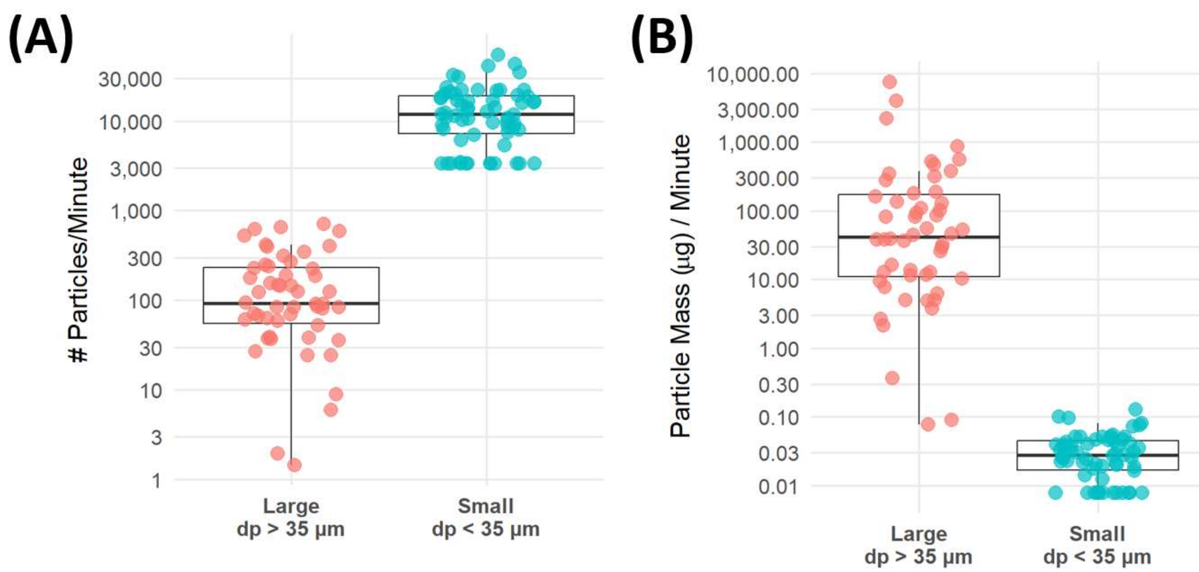

Figure 4. Comparison of particle emission rates between "Large" particles ($d_p > 35$ µm) and "Small" particles ($d_p < 35$ µm) for talking performance sets. **(A)** Count emission rates. **(B)** Mass emission rates.

While participants' large particle count emission rates were much lower than those for their small particles (Figure 4A), their large particle mass emission rates were substantially higher than their small particle mass emission rates (Figure 4B). This difference is due to the cubic relationship between particle diameter and particle mass and is an important point to understand with relation to the spreading of communicable respiratory diseases, where fomite transmission can be a principal route for disease transmission. Like Harrison et al.,[5] we found little correlation ($r^2 = 0.072$) between the large and small particle category count emission rate among the 42 participants who had talking data spanning this full size range, as shown in Figure S10.

An interesting finding from this work came from looking at how large particle emissions changed with increased participant loudness and carbon dioxide (CO_2) output. Previous work[26,27,32] suggests CO_2 output and sound pressure level are correlated with increasing particle emissions for the smaller aerosolized size range (0.25 – 35 μm), and since larger particles are produced via similar physiological pathways, we hypothesized large particles would also have strong correlations with CO_2 and sound volume. However, we found no relationship between these predictors when assessing the strength of these correlations for the large particle emissions. When isolating for only the effect of sound pressure level (voice/instrument volume), no meaningful correlation was found with large particle emissions for any of the performance set types tested, with an R^2 ranging from 0.055 for talking to 0.067 for brass instruments. This is different from our prior work on the smaller particles sizes (0.25 – 35 μm) that suggested a statistically significant correlation between aerosol emission rates and sound pressure for brass instruments (R^2=0.357) and for vocalization (R^2=0.370).[26,27]

In similar fashion, we observed a very low correlation between large particle emission rates and average CO_2 concentrations in sampled air. The factors we measured did not well explain variation in emissions rates, with only 16.1% of variation in large particle emissions from instruments and 8.5% of variation from talking explained by age, sex, loudness, and CO_2. This suggests that variation in large particle emissions is dependent on variables we did not record for this study (i.e., variables beyond age, sex, instrument type, average CO_2, and average dBA). Variables of interest for future investigation include characterizing differences in individuals' saliva production or variances in tongue and lip articulation.[25,34]

The effect of bell covers on mitigating large particle emission rates from instruments is shown in Figure 5A; a similar relationship for the effects of masks on singing is shown in Figure 5B.

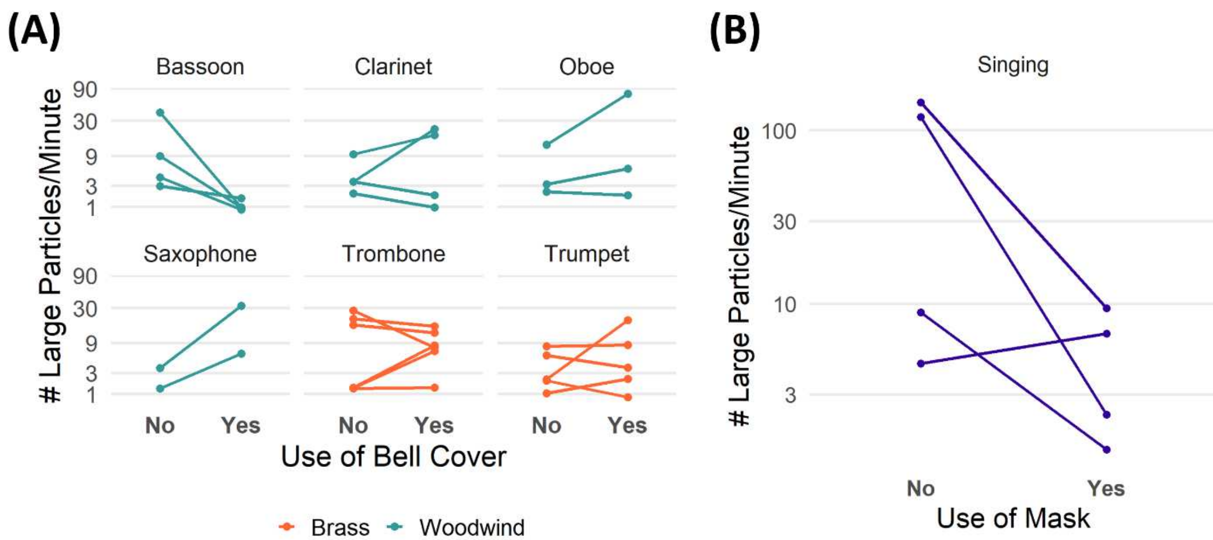

Figure 5. Emission rates with and without mitigation. Points represent individuals' performance set emission rates, and lines connecting two points indicate that the same individual produced both sets. **(A)** Showing 6 instruments count emission rates with and without a bell cover. **(B)** Showing Singing count emission rates with and without a mask.

These plots show the change in measured emission rate, on a per-participant basis; the left side of each panel shows an individuals' count emission rate without a bell cover/mask, and the right side shows their emissions with a bell cover/mask. Lines connecting two dots indicate these two performance sets were conducted by the same person. Most of the instruments tested had some people whose emission rates increased and some people whose rates decreased when using a bell cover.

These results provide little evidence to suggest that bell covers either mitigate or enhance large particle emission rates for wind instruments (which are very low to begin with), counter to what was seen for the smaller aerosols[27] where the use of bell covers produced a statistically significant effect for brass instruments. The counter-intuitive effect of the bell cover (Figure 5) could be due to the flow resistance imparted by the bell cover, which produced unintended consequences during playing. In other words, the additional pressure drop from the bell cover may require that participants blow harder into their mouthpiece, resulting in more particles being expelled from the instruments' keyholes or from around participants' mouths (i.e., increased "buzzing"); such an effect would likely vary from instrument to instrument, but the hypothesis remains untested. On the other hand, for the vocalization sets, wearing a mask proved to decrease large particle emissions substantially with an average decrease of 92.5% (95% CI: 97.9%, 73.7%). As shown in Figure 5B, all but one participant had dramatic reductions in large particle emissions (the one participant already had a low emission rate without a mask). This reduction in large particle emissions for singing while wearing a mask is further illustrated by the emission rate size distribution graph shown in Figure 6.

Here, it is evident that wearing a mask eliminates all the largest size bins of particle emissions for singing and significantly reduced the emission rate for the smallest size bin we tested (42 – 51μm). The substantial reduction in large particle emissions for singing while wearing a mask is consistent with the mask efficiency findings from previous studys investigating smaller aerosols.[27,35,36] It should be noted that most of the particles considered in this study ($d_p > 35$ μm) would have sufficient inertia (whether by settling or being present in the jet of exhaled air) to be filtered out by masks via impaction[31]. Although we did not evaluate the

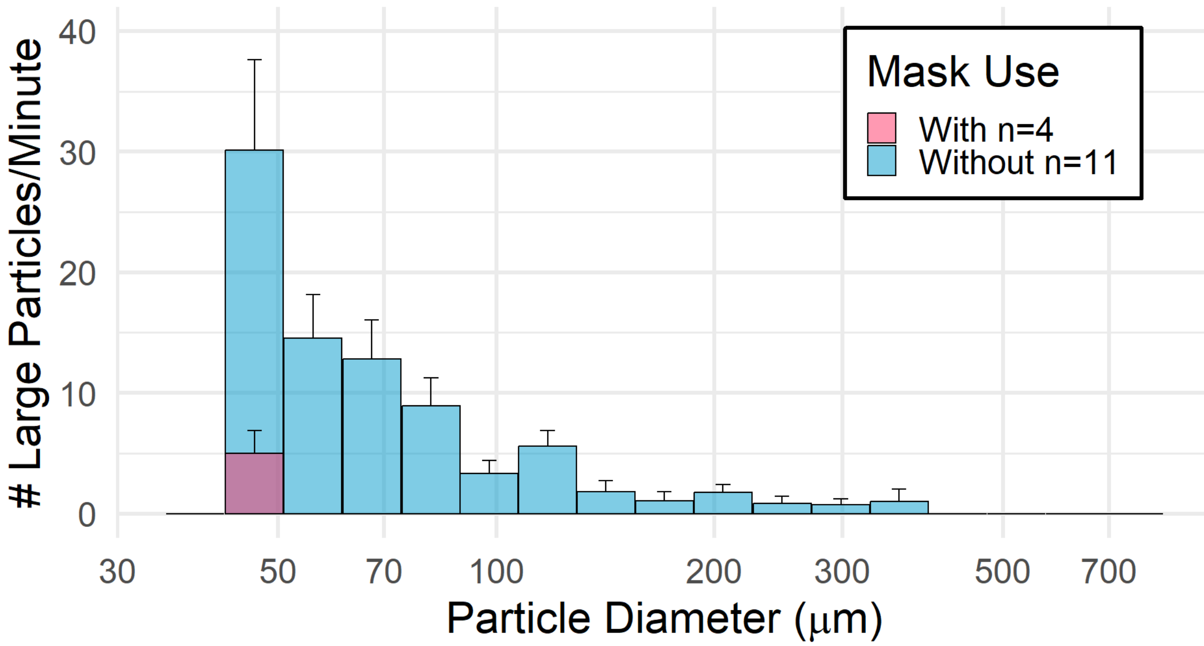

Figure 6. Large particle emission rate size distribution plot for singing with and without a mask.

effects of masking on large particle emissions from talking, we cannot think of a credible reason why wearing one would not also decrease this emission rate, given its similarity in mode of production, particle size distribution, and emission rate, to that of singing.

Overall, humans emit fewer large salivary particles (35 – 1,000μm) than smaller respiratory particles (0.25 – 35 μm), an average of 415 (standard deviation of 1,090) times less for talking. However, the mass of the larger particles far outweighs that of the smaller particles by an average factor of 30,300 (standard deviation of 147,350) when talking. Although these larger particles do not stay suspended in the air for as long as smaller particles, their increased volume implies that, on a per-particle basis, they may contain higher amounts of potentially pathogen-laden biological material and therefore, pose a considerable risk for disease transmission, especially for respiratory diseases where large particles are the primary vector for transmission.

Human vocalization (talking and singing) produces about 19.8 times more large particle emissions on a count basis, and about 132 times more emissions on a mass basis than instrument playing (brass and woodwind). However, within these two categories there is no statistically significant difference between the emissions rates for either talking vs. singing or brass vs. woodwind instrument playing. We also found through multiple linear regression modeling that age, sex, instrument type, CO_2 production, and sound pressure level do not explain a meaningful amount of variation for large particle emission rates for any performance category. Lastly, we determined that using a bell cover had negligible effects on large particle emission rates from the already low emissions detected for brass and woodwind instrument playing, but that wearing a mask dramatically reduces large particle emission rates for singing.

D.4 Acknowledgments

This work was funded by unrestricted philanthropic donations to the School of Music, Theatre, and Dance at Colorado State University. The authors wish to acknowledge input into the experimental design from members of the study scientific advisory board, including Allen Henderson (Georgia Southern University), Charles Henry (Colorado State University), Emily Morgan (Colorado State University), Heather Pidcoke (Colorado State University), and Timothy Rhea (Texas A&M University).

D.5 References

(1) Samet, J. M.; Burke, T. A.; Lakdawala, S. S.; Lowe, J. J.; Marr, L. C.; Prather, K. A.; Shelton-Davenport, M.; Volckens, J. SARS-CoV-2 Indoor Air Transmission Is a Threat That Can Be Addressed with Science. *Proc. Natl. Acad. Sci. U. S. A.* **2021**, *118* (45), e2116155118. https://doi.org/10.1073/pnas.2116155118.

(2) Samet, J. M.; Prather, K.; Benjamin, G.; Lakdawala, S.; Lowe, J.-M.; Reingold, A.; Volckens, J.; Marr, L. C. Airborne Transmission of Severe Acute Respiratory Syndrome Coronavirus 2 (SARS-CoV-2): What We Know. *Clin. Infect. Dis.* **2021**, *73* (10), 1924–1926. https://doi.org/10.1093/cid/ciab039.

(3) Lipinski, T.; Ahmad, D.; Serey, N.; Jouhara, H. Review of Ventilation Strategies to Reduce the Risk of Disease Transmission in High Occupancy Buildings. *Int. J. Thermofluids* **2020**, *7–8*, 100045. https://doi.org/10.1016/j.ijft.2020.100045.

(4) Morawska, L.; Milton, D. K. It Is Time to Address Airborne Transmission of Coronavirus Disease 2019 (COVID-19). *Clin. Infect. Dis.* **2020**, *71* (9), 2311–2313. https://doi.org/10.1093/cid/ciaa939.

(5) Harrison, J.; Saccente-Kennedy, B.; Orton, C. M.; McCarthy, L. P.; Archer, J.; Symons, H. E.; Szczepanska, A.; Watson, N. A.; Browne, W. J.; Moseley, B.; Philip, K. E. J.; Hull, J. H.; Calder, J. D.; Costello, D.; Shah, P. L.; Epstein, R.; Reid, J. P.; Bzdek, B. R. Emission Rates, Size Distributions, and Generation Mechanism of Oral Respiratory Droplets. *Aerosol Sci. Technol.* **2023**, 1–13. https://doi.org/10.1080/02786826.2022.2158778.

(6) Oswin, H. P.; Haddrell, A. E.; Otero-Fernandez, M.; Mann, J. F. S.; Cogan, T. A.; Hilditch, T. G.; Tian, J.; Hardy, D. A.; Hill, D. J.; Finn, A.; Davidson, A. D.; Reid, J. P. The Dynamics of SARS-CoV-2 Infectivity with Changes in Aerosol Microenvironment. *Proc. Natl. Acad. Sci.* **2022**, *119* (27), e2200109119. https://doi.org/10.1073/pnas.2200109119.

(7) Wang, C. C.; Prather, K. A.; Sznitman, J.; Jimenez, J. L.; Lakdawala, S. S.; Tufekci, Z.; Marr, L. C. Airborne Transmission of Respiratory Viruses. *Science* **2021**, *373* (6558), eabd9149. https://doi.org/10.1126/science.abd9149.

(8) Gregson, F. K. A.; Watson, N. A.; Orton, C. M.; Haddrell, A. E.; McCarthy, L. P.; Finnie, T. J. R.; Gent, N.; Donaldson, Gavin. C.; Shah, P. L.; Calder, J. D.; Bzdek, B. R.; Costello, D.; Reid, J. P. Comparing Aerosol Concentrations and Particle Size Distributions Generated by Singing, Speaking and Breathing. *Aerosol Sci. Technol.* **2021**, *55* (6), 681–691. https://doi.org/10.1080/02786826.2021.1883544.

(9) Schlenczek, O.; Thiede, B.; Turco, L.; Stieger, K.; Kosub, J. M.; Müller, R.; Scheithauer, S.; Bodenschatz, E.; Bagheri, G. Experimental Measurement of Respiratory Particles Dispersed by Wind Instruments and Analysis of the Associated Risk of Infection Transmission. *J. Aerosol Sci.* **2023**, *167*, 106070. https://doi.org/10.1016/j.jaerosci.2022.106070.

(10) Viala, R.; Creton, M.; Jousserand, M.; Soubrié, T.; Néchab, J.; Crenn, V.; Léglise, J. Experimental and Numerical Investigation on Aerosols Emission in Musical Practice and Efficiency of Reduction Means. *J. Aerosol Sci.* **2022**, *166*, 106051. https://doi.org/10.1016/j.jaerosci.2022.106051.

(11) He, R.; Gao, L.; Trifonov, M.; Hong, J. Aerosol Generation from Different Wind Instruments. *J. Aerosol Sci.* **2021**, *151*, 105669. https://doi.org/10.1016/j.jaerosci.2020.105669.

(12) Stockman, T.; Zhu, S.; Kumar, A.; Wang, L.; Patel, S.; Weaver, J.; Spede, M.; Milton, D. K.; Hertzberg, J.; Toohey, D.; Vance, M.; Srebric, J.; Miller, S. L. Measurements and Simulations of Aerosol Released While Singing and Playing Wind Instruments. *ACS Environ. Au* **2021**, *1* (1), 71–84. https://doi.org/10.1021/acsenvironau.1c00007.

(13) Wang, L.; Lin, T.; Da Costa, H.; Zhu, S.; Stockman, T.; Kumar, A.; Weaver, J.; Spede, M.; Milton, D. K.; Hertzberg, J.; Toohey, D. W.; Vance, M. E.; Miller, S. L.; Srebric, J. Characterization of Aerosol Plumes from Singing and Playing Wind Instruments Associated with the Risk of Airborne Virus Transmission. *Indoor Air* **2022**, *32* (6), e13064. https://doi.org/10.1111/ina.13064.

(14) Mahjoub Mohammed Merghani, K.; Sagot, B.; Gehin, E.; Da, G.; Motzkus, C. A Review on the Applied Techniques of Exhaled Airflow and Droplets Characterization. *Indoor Air* **2021**, *31* (1), 7–25. https://doi.org/10.1111/ina.12770.
(15) Nazaroff, W. W. Indoor Bioaerosol Dynamics. *Indoor Air* **2016**, *26* (1), 61–78. https://doi.org/10.1111/ina.12174.
(16) Thomas, R. J. Particle Size and Pathogenicity in the Respiratory Tract. *Virulence* **2013**, *4* (8), 847–858. https://doi.org/10.4161/viru.27172.
(17) Stadnytskyi, V.; Bax, C. E.; Bax, A.; Anfinrud, P. The Airborne Lifetime of Small Speech Droplets and Their Potential Importance in SARS-CoV-2 Transmission. *Proc. Natl. Acad. Sci.* **2020**, *117* (22), 11875–11877. https://doi.org/10.1073/pnas.2006874117.
(18) Alonso, C.; Raynor, P. C.; Davies, P. R.; Torremorell, M. Concentration, Size Distribution, and Infectivity of Airborne Particles Carrying Swine Viruses. *PLOS ONE* **2015**, *10* (8), e0135675. https://doi.org/10.1371/journal.pone.0135675.
(19) Tellier, R. Review of Aerosol Transmission of Influenza A Virus. *Emerg. Infect. Dis.* **2006**, *12* (11), 1657–1662. https://doi.org/10.3201/eid1211.060426.
(20) Volckens, J.; Peters, T. M. Counting and Particle Transmission Efficiency of the Aerodynamic Particle Sizer. *J. Aerosol Sci.* **2005**, *36* (12), 1400–1408. https://doi.org/10.1016/j.jaerosci.2005.03.009.
(21) McCarthy, L. P.; Orton, C. M.; Watson, N. A.; Gregson, F. K. A.; Haddrell, A. E.; Browne, W. J.; Calder, J. D.; Costello, D.; Reid, J. P.; Shah, P. L.; Bzdek, B. R. Aerosol and Droplet Generation from Performing with Woodwind and Brass Instruments. *Aerosol Sci. Technol.* **2021**, *55* (11), 1277–1287. https://doi.org/10.1080/02786826.2021.1947470.
(22) Johnson, G. R.; Morawska, L.; Ristovski, Z. D.; Hargreaves, M.; Mengersen, K.; Chao, C. Y. H.; Wan, M. P.; Li, Y.; Xie, X.; Katoshevski, D.; Corbett, S. Modality of Human Expired Aerosol Size Distributions. *J. Aerosol Sci.* **2011**, *42* (12), 839–851. https://doi.org/10.1016/j.jaerosci.2011.07.009.
(23) Xie, X.; Li, Y.; Sun, H.; Liu, L. Exhaled Droplets Due to Talking and Coughing. *J. R. Soc. Interface* **2009**, *6 Suppl 6*, S703-714. https://doi.org/10.1098/rsif.2009.0388.focus.
(24) Chao, C. Y. H.; Wan, M. P.; Morawska, L.; Johnson, G. R.; Ristovski, Z. D.; Hargreaves, M.; Mengersen, K.; Corbett, S.; Li, Y.; Xie, X.; Katoshevski, D. Characterization of Expiration Air Jets and Droplet Size Distributions Immediately at the Mouth Opening. *J. Aerosol Sci.* **2009**, *40* (2), 122–133. https://doi.org/10.1016/j.jaerosci.2008.10.003.
(25) Shen, Y.; Courtney, J. M.; Anfinrud, P.; Bax, A. Hybrid Measurement of Respiratory Aerosol Reveals a Dominant Coarse Fraction Resulting from Speech That Remains Airborne for Minutes. *Proc. Natl. Acad. Sci.* **2022**, *119* (26), e2203086119. https://doi.org/10.1073/pnas.2203086119.
(26) Good, N.; Fedak, K. M.; Goble, D.; Keisling, A.; L'Orange, C.; Morton, E.; Phillips, R.; Tanner, K.; Volckens, J. Respiratory Aerosol Emissions from Vocalization: Age and Sex Differences Are Explained by Volume and Exhaled CO_2. *Environ. Sci. Technol. Lett.* **2021**, *8* (12), 1071–1076. https://doi.org/10.1021/acs.estlett.1c00760.
(27) Volckens, J.; Good, K. M.; Goble, D.; Good, N.; Keller, J. P.; Keisling, A.; L'Orange, C.; Morton, E.; Phillips, R.; Tanner, K. Aerosol Emissions from Wind Instruments: Effects of Performer Age, Sex, Sound Pressure Level, and Bell Covers. *Sci. Rep.* **2022**, *12* (1), 11303. https://doi.org/10.1038/s41598-022-15530-x.
(28) Fedak, K. M.; Good, N.; Walker, E. S.; Balmes, J.; Brook, R. D.; Clark, M. L.; Cole-Hunter, T.; Devlin, R.; L'Orange, C.; Luckasen, G.; Mehaffy, J.; Shelton, R.; Wilson, A.; Volckens, J.; Peel, J. L. Acute Changes in Lung Function Following Controlled Exposure to Cookstove Air Pollution in the Subclinical Tests of Volunteers Exposed to Smoke (STOVES) Study. *Inhal. Toxicol.* **2020**, *32* (3), 115–123. https://doi.org/10.1080/08958378.2020.1751750.
(29) Woolf, M. S.; Dignan, L. M.; Scott, A. T.; Landers, J. P. Digital Postprocessing and Image Segmentation for Objective Analysis of Colorimetric Reactions. *Nat. Protoc.* **2021**, *16* (1), 218–238. https://doi.org/10.1038/s41596-020-00413-0.

(30) Kubala, E.; Strzelecka, P.; Grzegocka, M.; Lietz-Kijak, D.; Gronwald, H.; Skomro, P.; Kijak, E. A Review of Selected Studies That Determine the Physical and Chemical Properties of Saliva in the Field of Dental Treatment. *BioMed Res. Int.* **2018**, *2018*, e6572381. https://doi.org/10.1155/2018/6572381.
(31) Hinds, W. C. *Aerosol Technology: Properties, Behavior, and Measurement of Airborne Particles*, 2nd ed.; Wiley: New York, 1999.
(32) Asadi, S.; Wexler, A. S.; Cappa, C. D.; Barreda, S.; Bouvier, N. M.; Ristenpart, W. D. Aerosol Emission and Superemission during Human Speech Increase with Voice Loudness. *Sci. Rep.* **2019**, *9* (1), 2348. https://doi.org/10.1038/s41598-019-38808-z.
(33) Morawska, L.; Johnson, G. R.; Ristovski, Z. D.; Hargreaves, M.; Mengersen, K.; Corbett, S.; Chao, C. Y. H.; Li, Y.; Katoshevski, D. Size Distribution and Sites of Origin of Droplets Expelled from the Human Respiratory Tract during Expiratory Activities. *J. Aerosol Sci.* **2009**, *40*, 256–269. https://doi.org/10.1016/j.jaerosci.2008.11.002.
(34) Abkarian, M.; Stone, H. A. Stretching and Break-up of Saliva Filaments during Speech: A Route for Pathogen Aerosolization and Its Potential Mitigation. *Phys. Rev. Fluids* **2020**, *5* (10), 102301. https://doi.org/10.1103/PhysRevFluids.5.102301.
(35) Leung, N. H. L.; Chu, D. K. W.; Shiu, E. Y. C.; Chan, K.-H.; McDevitt, J. J.; Hau, B. J. P.; Yen, H.-L.; Li, Y.; Ip, D. K. M.; Peiris, J. S. M.; Seto, W.-H.; Leung, G. M.; Milton, D. K.; Cowling, B. J. Respiratory Virus Shedding in Exhaled Breath and Efficacy of Face Masks. *Nat. Med.* **2020**, *26* (5), 676–680. https://doi.org/10.1038/s41591-020-0843-2.
(36) Anfinrud, P.; Stadnytskyi, V.; Bax, C. E.; Bax, A. Visualizing Speech-Generated Oral Fluid Droplets with Laser Light Scattering. *N. Engl. J. Med.* **2020**, *382* (21), 2061–2063. https://doi.org/10.1056/NEJMc2007800.